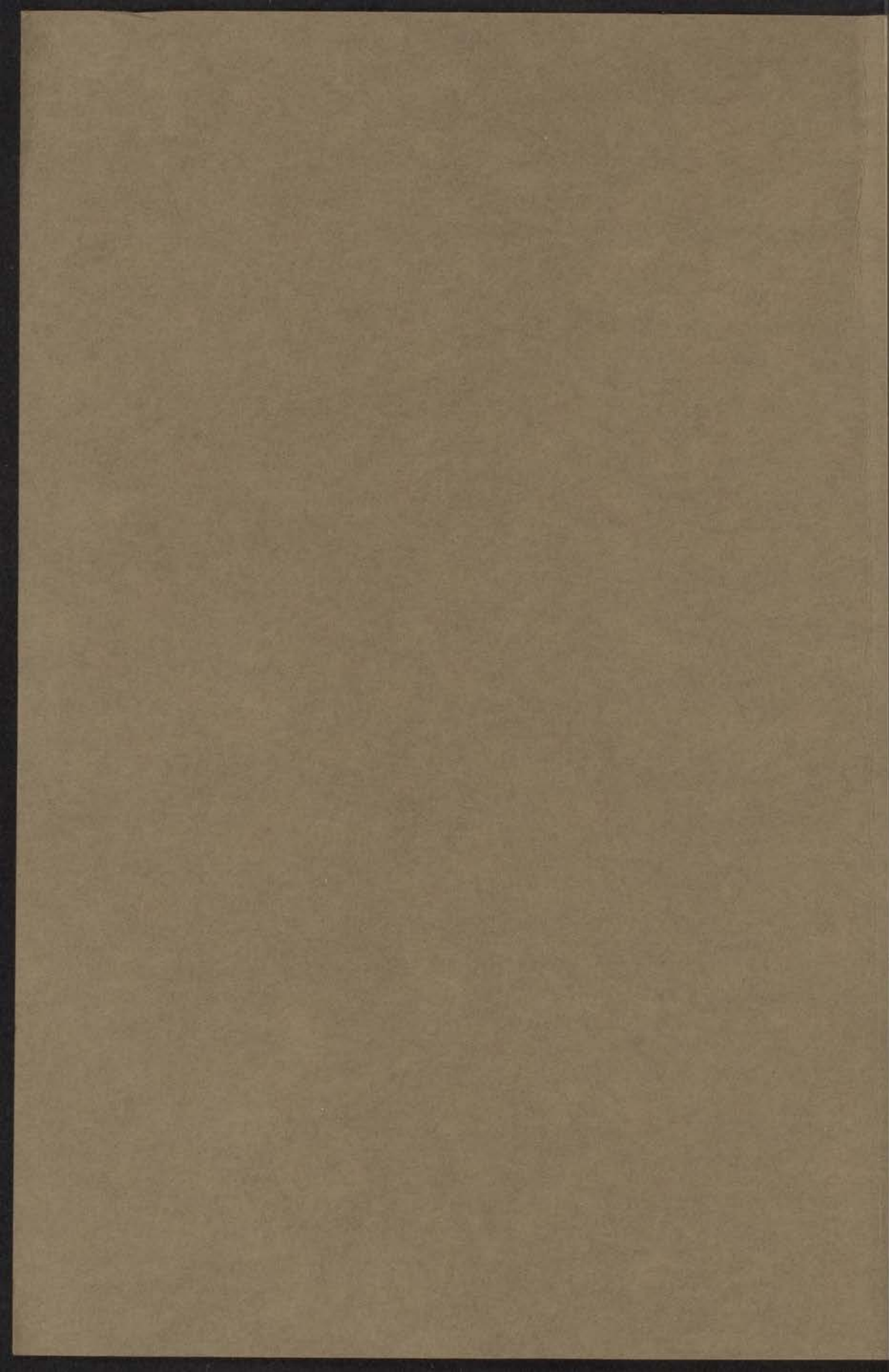


EXPERIMENTS ON NON-RADIATIVE PROCESSES  
IN PHOSPHORESCENT MOLECULES

SPIN-FORBIDDEN TRANSITIONS and  
SPIN-LATTICE RELAXATION

D. ANTHEUNIS



# EXPERIMENTS ON NON-RADIATIVE PROCESSES IN PHOSPHORESCENT MOLECULES

## SPIN-FORBIDDEN TRANSITIONS and SPIN-LATTICE RELAXATION

Abstract: The spin-forbidden transitions and spin-lattice relaxation processes in phosphorescent molecules are investigated. The results show that the spin-lattice relaxation is the dominant process in the non-radiative decay of the phosphorescent state.

1. Introduction: The spin-forbidden transitions and spin-lattice relaxation processes in phosphorescent molecules are investigated. The results show that the spin-lattice relaxation is the dominant process in the non-radiative decay of the phosphorescent state.

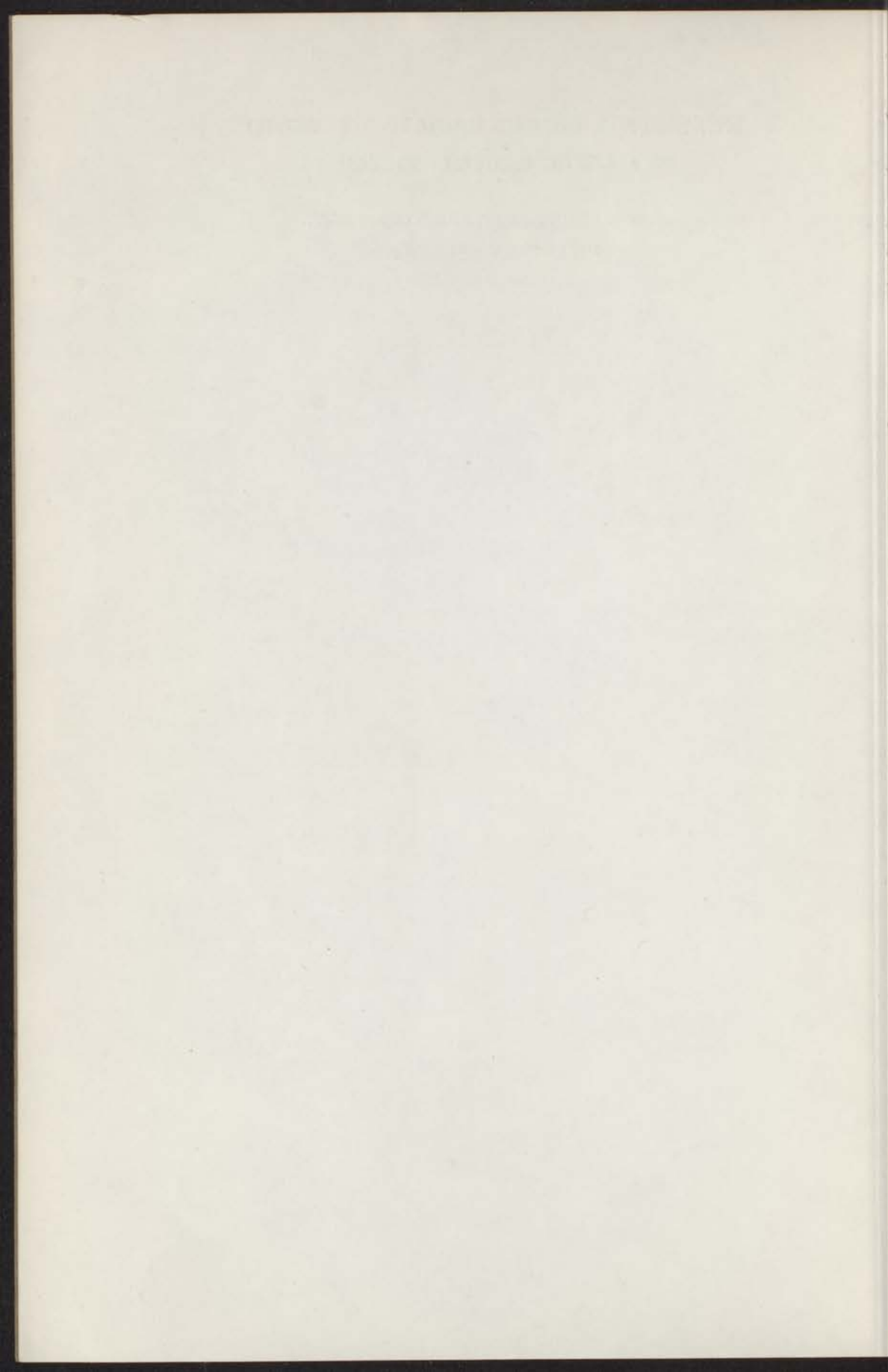
2. Experimental: The spin-forbidden transitions and spin-lattice relaxation processes in phosphorescent molecules are investigated. The results show that the spin-lattice relaxation is the dominant process in the non-radiative decay of the phosphorescent state.

3. Discussion: The spin-forbidden transitions and spin-lattice relaxation processes in phosphorescent molecules are investigated. The results show that the spin-lattice relaxation is the dominant process in the non-radiative decay of the phosphorescent state.

4. Conclusion: The spin-forbidden transitions and spin-lattice relaxation processes in phosphorescent molecules are investigated. The results show that the spin-lattice relaxation is the dominant process in the non-radiative decay of the phosphorescent state.

References: 1. J. K. Stille, *Phys. Rev.*, **50**, 103 (1941).  
2. J. K. Stille, *Phys. Rev.*, **50**, 103 (1941).  
3. J. K. Stille, *Phys. Rev.*, **50**, 103 (1941).

5. Acknowledgments: The author wishes to thank the National Science Foundation for their generous support of this work.



1. Eén-elektron één-centrum integralen van de spin-baan koppeling spelen een wezenlijke rol bij de beschrijving van het effect van aza-substitutie in een aromatisch molecuul op de relatieve kansen voor het bevolken en het stralingsloos verval van de afzonderlijke spinniveaus van de fosforescerende triplettoestand.

Hoofdstuk V van dit proefschrift.

2. In proeven, die tot doel hebben kinetische parameters van de fosforescerende triplettoestand van aromatische molekulen in vaste oplossing te bepalen, dient men bedacht te zijn op ernstige systematische fouten in de experimentele resultaten als gevolg van opwarmingseffekten door intense bestraling.

Hoofdstuk IV, VI en VII van dit proefschrift.

3. Het wekt verwondering dat Tyshchenko c.s. de polarisatie effecten in het kernresonantie spectrum, dat zij opnamen tijdens de thermische ontleding van benzoylperoxide in een oplossing van cyclohexanon met lupinine, trachten te beschrijven met de theorie van Bargon en Fischer.

Tyshchenko, A.A., Abduvakhobov, A.A., Leont'ev, V.B., Aslanov, Kh.A., and Sadykov, A.S., 1972, Doklady Akademii Nauk SSSR, 204 (5), 1178; translated in 1972, Doklady Phys. Chem., 202-207, 510.

Bargon, J., and Fischer, H.Z., 1968, Z. Naturf., 23a, 2109.

4. Het temperatuurgedrag van de spin-roosterrelaxatie in de fosforescerende triplettoestand van een isotopisch mengkristal van naftaleen, zoals dat door Schwoerer c.s. is waargenomen, vertoont opmerkelijke overeenkomst met de relaxatie in de laagst aangeslagen doublettoestand van  $\text{Cr}^{3+}$  in  $\text{Al}_2\text{O}_3$ .

Schwoerer, M., Konzelmann, U., and Kilpper, D., 1972, Chem. Phys. Lett., 13, 272.

Geschwind, S., Devlin, G.E., Cohen, R.L., and Chinn, S.R., 1965, Phys. Rev., 137 A, 1087.

5. Met de huidige kennis van zaken kan niet worden uitgesloten dat singuletoestanden een overheersende rol kunnen spelen bij "het zien" en de foto-

chemie van retinal.

Kropf, A., and Hubbard, R., 1970, Photochem. Photobiol., 12, 249.

Bensasson, R., Land, E.J., and Truscott, T.G., 1973, Photochem. Photobiol., 17, 53.

Rosenfeld, T., Alchalel, A., and Ottolenghi, M., 1974, J. phys. Chem., 78, 336.

6. Het is belangrijk om na te gaan of de fasegeheugentijd  $T_2$  van gelocaliseerde triplet elektronspins in molekuulkristallen, die bij temperaturen in het vloeibare helium gebied zonder uitwendig veld een waarde heeft in de orde van  $10^{-5}$  s, niet aanzienlijk wordt verkort in een sterk magnetisch veld.
7. Het verdient aanbeveling lengtemetingen, zoals die worden toegepast bij de beschrijving van soorten in de systematische biologie, te noteren op een wijze die in de fysica bij de presentatie van meetgegevens gebruikelijk is.
8. Er bestaan minstens twee zinvolle alternatieven voor de bevestiging van het binnenste venster in optische cryostatens.
9. De wijze waarop Schwoerer c.s. en Wolfe één enkele parameter gebruiken om spin-roosterrelaxatie in de fosforescerende triplettoestand van aromatische molekulen te beschrijven is aanvechtbaar.

Schwoerer, M., Konzelmann, U., and Kilpper, D., 1972, Chem. Phys. Lett., 13, 272 .

Konzelmann, U., and Schwoerer, M., 1973, Chem. Phys. Lett., 18, 143.

Wolfe, J.P., 1971, Chem. Phys. Lett., 10, 212.
10. Op grond van enthalpie overwegingen kan men besluiten dat de verdamer in een traditionele  $^3\text{He} - ^4\text{He}$  mengsel koelmachine niet de meest geschikte plaats is om als thermische verankering van een scherm te dienen.

EXPERIMENTS ON NON-RADIATIVE PROCESSES  
IN PHOSPHORESCENT MOLECULES

SPIN-FORBIDDEN TRANSITIONS and  
SPIN-LATTICE RELAXATION

PROEFSCHRIFT

TER VERKRIJGING VAN DE GRAAD VAN DOCTOR IN DE  
WISKUNDE EN NATUURWETENSCHAPPEN AAN DE RIJKS-  
UNIVERSITEIT TE LEIDEN, OP GEZAG VAN DE RECTOR  
MAGNIFICUS DR. A. E. COHEN, HOOGLERAAR IN DE FACUL-  
TEIT DER LETTEREN, VOLGENS BESLUIT VAN HET COLLEGE  
VAN DEKANEN TE VERDEDIGEN OP DONDERDAG 20 JUNI  
1974 TE KLOKKE 16.15 UUR

door

DAN ANTHEUNIS  
geboren te Terneuzen in 1946

EXPERIMENTS ON NON-RADIATIVE PROCESSES

IN PHOSPHORESCENT MOLECULES

PROMOTOR: PROF. DR. J. H. VAN DER WAALS



Aan de nagedachtenis van mijn vader  
aan mijn broeder  
aan Majda, Marjolien en Eorien

## CONTENTS

page

Chapter I	INTRODUCTION AND SURVEY	9
	References	13
Chapter II	PHOSPHORESCENT MOLECULES	14
	1. The energy level diagram	14
	2. Zero-field splitting	16
	3. Spin-orbit coupling and phosphorescence	18
	4. Intersystem crossing	24
	5. Spin alignment on optical pumping	25
	References	27
Chapter III	EXPERIMENTAL	29
	1. The microwave induced phosphorescence experiment	29
	2. The equipment	31
	2.1 Cryogenics	31
	2.2 Microwaves	33
	2.3 Optics	34
	3. The systems studied	34
	References	
Chapter IV	SPIN-FORBIDDEN RADIATIONLESS PROCESSES IN ISOELECTRONIC MOLECULES: ANTHRACENE, ACRIDINE AND PHENAZINE. A STUDY BY MICROWAVE INDUCED DELAYED PHOSPHORESCENCE.	37
	1. Introduction	38
	2. Samples and equipment	40
	2.1 The crystals	40
	2.2 The equipment	41
	3. The experiments and their analysis	41
	3.1 The absolute decay rates and relative radiative rates	43
	3.2 Steady-state populations and populating rates	46
	3.3 The temperature effect	48
	4. Results	51
	4.1 The dominance of radiationless $T_0 \rightarrow S_0$ decay over the phosphorescence emission	51

	4.2 Comparison with predictions from theory	52
	4.3 Comparison with other experiments	55
	4.4 The effect of aza-substitution on $k_y$ and $k_z$	57
	5. Conclusion	58
	Notes	62
	References	63
Chapter V	THE DEPENDENCE ON SPIN STATE OF THE RATES NON-RADIATIVE TRANSITIONS	65
	1. The Model	
	2. The populating and decay for aza-aromatic molecules	71
	Appendix	76
	References	80
Chapter VI	KINETICS OF POPULATING AND DECAY OF THE PHOSPHORESCENT STATE OF TETRAMETHYLPYRAZINE IN DURENE, A SYSTEM WITH SKEW SPIN AXES	81
	1. Introduction	81
	2. Experimental and results	83
	2.1 Equipment and principle of the experiments	83
	2.2 Decay rates	84
	2.3 Assignment of the decay rates	86
	2.4 Isolation between the spin states	87
	2.5 Populating rates	91
	3. Discussion	93
	References	95
Chapter VII	SPIN-LATTICE RELAXATION IN PHOSPHORESCENT TRIPLET STATES	96
	1. Introduction	96
	2. Samples and equipment	97
	3. The kinetics of the triplet state	97
	3.1 The low temperature region of isolation	98
	3.2 The intermediate region	99
	3.3 The high temperature region of dominant relaxation	101
	4. The measurement of spin-lattice relaxation rates	102
	4.1 Acridine in biphenyl	102
	4.2 Quinoxaline in durene and perdeutero naphthalene	105

	page
4.3 Phenanthrene in biphenyl and fluorene	108
4.4 Tetramethylpyrazine in durene	111
References	114
SAMENVATTING	116
STUDIEOVERZICHT	119
NAWOORD	120

The present work is part of the research program of the *Stichting voor Fundamenteel Onderzoek der Materie (FOM)*, which is financially supported by the *Nederlandse Organisatie voor zuiver-wetenschappelijk onderzoek (ZWO)*.

## CHAPTER I

### INTRODUCTION AND SURVEY

In this thesis we present an experimental investigation of the radiationless processes that follow on optical excitation of an aromatic molecule. These processes are of two different kinds:

- (a) *Intersystem crossing (ISC)* between singlet and triplet electronic states, and vice versa;
- (b) *Spin-lattice relaxation* between the three spin components of the lowest triplet state  $T_0$ .

To see what is meant let us turn to the simple diagram of fig. 1.

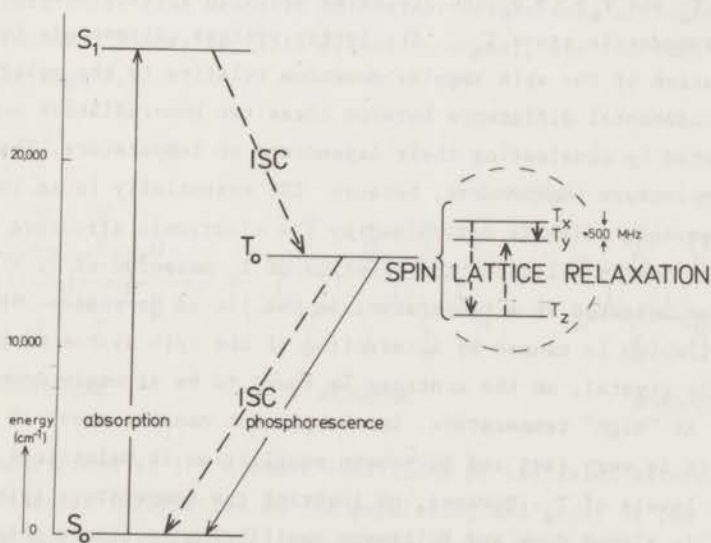


Fig. 1.

Suppose an aromatic molecule is excited by the absorption of UV light in

its first singlet-singlet absorption band  $S_1 \leftarrow S_0$ , then in addition to any  $S_1 \rightarrow S_0$  fluorescence that may result, one usually observes a long lived afterglow in the visible if the molecule is incorporated in a rigid matrix at low temperature. This "phosphorescence", a common feature of polyatomic molecules with chains of double bonds, was first explained by G.N. Lewis and his school [1]. Part, or in some instances nearly all of the molecules excited into  $S_1$  convert a substantial fraction of their electronic energy into vibrational energy and cross over into the lowest triplet state  $T_0$ . From this metastable state the molecules return to the ground state, either by the emission of phosphorescence, or again by a non-radiative process.

Contrary to the situation in atoms which is governed by spherical symmetry, the three spin components of the state  $T_0$  in a polyatomic molecule do not have to be degenerate. In the insert of fig. 1 we show the zero-field splitting of anthracene as an example. As we shall see later each of the components corresponds to a situation in which the spin angular momentum lies in one of the principal planes of the molecule. For instance component  $T_x$  has the spin lying in the plane  $x = 0$ .

In the present thesis we are primarily concerned with the non-radiative processes that arise in the optical pumping cycle  $S_0 \xrightarrow{h\nu} S_1 \xrightarrow{-} T_0 \xrightarrow{-} S_0$ : the  $S_1 \xrightarrow{-} T_0$  and  $T_0 \xrightarrow{-} S_0$  ISC processes and spin-lattice relaxation in the excited paramagnetic state  $T_0$ . The latter process corresponds to jumps in the orientation of the spin angular momentum relative to the molecular frame.

The fundamental difference between these two non-radiative processes can be illustrated by considering their dependence on temperature. The rates for ISC are *temperature independent*, because ISC essentially is an intramolecular process which is determined by the electronic structure of the molecule. In nearly all cases the lifetime of  $T_0$  measured at 77 K thus equals its lifetime measured at a temperature in the liquid He region. Spin-lattice relaxation, which is caused by interaction of the spin system with the phonon field of the crystal, on the contrary is found to be strongly *temperature dependent*. At "high" temperature, in the present context above 10 K for instance, it is very fast and Boltzmann equilibrium is maintained over the three spin levels of  $T_0$ . However, on lowering the temperature spin-lattice relaxation is slowed down and Boltzmann equilibrium no longer obtains.

For most of the molecules of the present study we finally reach a situation, below 1.5 K for instance, where spin-lattice relaxation becomes an improbable event relative to the decay of  $T_0$ . The three spin levels then are

isolated from one another and the relative populations of the levels are determined by the populating and decay processes. Since these processes turn out to be very anisotropic with respect to the orientation of the triplet spin, such isolation usually leads to a marked "spin alignment" where one or two of the levels carry most of the population.

Before coming to the experimental material gathered on the various radiationless processes we first present in chapter II a brief commentary on the energy level diagram and optical pumping cycle of fig. 1 in relation to the molecular structure.

Then in chapter III we give an outline of the equipment used in what essentially are microwave induced phosphorescence experiments. By irradiation of the system with microwaves resonant with one of the zero-field transitions one perturbs the population distribution over the spin levels, and this perturbation is monitored via the change in phosphorescence emission it produces. Such experiments may be done either under continuous illumination or during the decay that follows a period of UV excitation. At the end of the chapter we present a quick reference list of all systems studied in this thesis.

In chapter IV we discuss experiments carried out on a series of seven iso-electronic three-ring aromatic molecules: anthracene, acridine (9-azaanthracene), phenazine (9,10-diazaanthracene), and four deuterated isomers; see fig. 2.

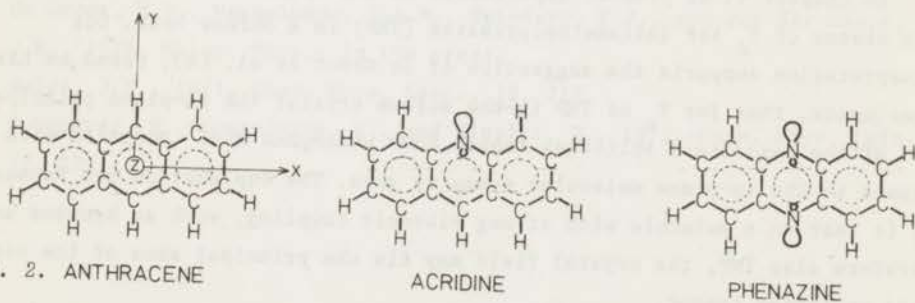


Fig. 2. ANTHRACENE

ACRIDINE

PHENAZINE

The experiments, done at 1.2 K under conditions of isolation between the levels, yield quantitative information on the populating and decay of the triplet state and on how these properties are affected by nitrogen substitution and replacement of H by D.

These particular three-ring compounds not only have been chosen because they have a well-understood electronic structure with a triplet state that is

at almost exactly the same energy and has the same spin distribution for all seven molecules, but also for the following reason. For the three-ring aromatics  $T_0$  lies very low and radiationless decay is so dominant that when measuring the absolute total decay rates of the three spin levels one may equate the results with the absolute rates for the *non-radiative part* of this decay. Although the phosphorescence emission is used as a monitor to follow the fate of the population in the  $T_0$  manifold in our experiments, it does not contribute significantly to the decay! In previous studies phosphorescence constituted a major decay channel and, in the absence of quantum yield measurements, one could not extract the radiationless decay rates from the experiments. Such information is important because it permits one to make a quantitative test of recent theories on radiationless transitions [2,3] and in particular of the predictions about the selectivity of the ISC processes of populating and decay with respect to the different spin states and also about the "deuterium effect" [2].

Chapter IV is a published paper [4]. At the time it was submitted, a paper appeared by Metz with calculations on  $T_0 \rightarrow S_0$  ISC in aromatic hydrocarbons [5]. Subsequently it was realized that Metz's ideas may be generalized to include the populating processes and also to ISC in the nitrogen heterocyclics. The qualitative aspects of this generalization are presented in chapter V, which thus forms an extension of the discussion of chapter IV.

In chapter VI we present experiments on the dynamic behaviour of the spin states of  $T_0$  for tetramethylpyrazine (TMP) in a durene host. Our interpretation supports the suggestion of de Groot et al. [6], based on ESR experiments, that for  $T_0$  of TMP in the durene crystal the in-plane principal axes of the zero-field splitting tensor *have undergone a 45° rotation* with respect to the in-plane molecular symmetry axes. The explanation put forward [6] is that in a molecule with strong vibronic coupling, such as benzene and therefore also TMP, the crystal field may fix the principal axes of the zero-field splitting tensor.

The final chapter (VII) is a survey of various methods for the experimental investigation of spin-lattice relaxation in localized excited triplet states in organic molecular crystals in zero-field. Only in the recent past a first few experimental data became available on this subject [7,8]. For the systems of present interest it is an open question how the phonon field of the lattice is coupled to the triplet electron spin. The



success of microwave induced phosphorescence experiments in the investigation of the feeding and emptying processes of  $T_0$  raised the idea to try out in how far one can extend these experiments and apply them to situations where the spin levels of  $T_0$  become effectively coupled by spin-lattice relaxation. We have been able to measure relaxation rates and their temperature dependence from about 1.2 K up to about 15 K.

#### REFERENCES

- [1] Lewis, G.N., and Kasha, M., 1944, J. Am. Chem. Soc., 66, 2100.  
Lewis, G.N., and Kasha, M., 1945, J. Am. Chem. Soc., 67, 994.
- [2] Henry, B.R., and Siebrand, W., 1971, J. chem. Phys., 54, 1072.
- [3] Metz, F., Friedrich, S., and Hohlneicher, G., 1972, Chem. Phys. Lett., 16, 353.
- [4] Antheunis, D., Botter, B.J., Schmidt, J., and van der Waals, J.H., 1974, Molec. Phys., in the press.
- [5] Metz, F., 1973, Chem. Phys. Lett., 22, 186.
- [6] De Groot, M.S., Hesselmann, I.A.M., Reinders, F.J., and van der Waals, J.H., 1974, Molec. Phys., in the press.
- [7] Wolfe, J.P., 1971, Chem. Phys. Lett., 10, 212.
- [8] Schwoerer, M., Konzelmann, U., and Kippler, D., 1972, Chem. Phys. Lett., 13, 272.

## CHAPTER II

### PHOSPHORESCENT MOLECULES

#### 1. THE ENERGY LEVEL DIAGRAM

In a polyatomic molecule the valence electrons contributed by the individual atoms can be thought to move in orbits described by molecular orbitals (M.O.'s). In planar molecules with a series of double bonds, such as (aza) aromatic compounds, these electrons, or rather the M.O.'s in which they move, can be classified as the *delocalized*  $\pi$  electrons and the more *localized*  $\sigma$  and  $n$  electrons. Whereas the probability density of the  $\sigma$  and  $n$ -orbitals has a maximum in the molecular plane, the  $\pi$ -orbitals have a node in this plane.

One distinguishes bonding ( $\sigma, \pi$ ) and antibonding ( $\sigma^*, \pi^*$ ) M.O.'s. In the ground state the bonding orbitals and also the  $n$ -orbitals are each filled with two electrons with their spins paired ( $S = 0$ ; singlet state); the localization of the  $\sigma$ -electrons then is pair wise in the  $\sigma$ -orbitals between each pair of chemically bonded atoms.

A special type of  $\sigma$ -orbital is provided by the  $n$ -orbital(s) which may occur in molecules containing hetero atoms, such as the two nitrogen atoms in phenazine. The valency of N (5) is one higher than that of carbon; each N atom in phenazine or acridine may be thought of as contributing two electrons to the C-N  $\sigma$ -bonds, two electrons are housed in the "non-bonding"  $n$ -orbital, and the fifth is a delocalized  $2p_z$   $\pi$ -electron similar to that of an aromatic carbon atom. Although this is not strictly true [1], in first instance one may think of these  $n$ -orbitals as relatively pure atomic wave functions ( $(sp)^2$  trigonal hybrids).

In an aromatic hydrocarbon, like anthracene, the lowest energy transition in the molecule occurs when by the absorption of near UV light an electron is

promoted from the highest filled  $\pi$ -orbital to the lowest empty  $\pi^*$  orbital, giving rise to an excited singlet state of so-called  $\pi \rightarrow \pi^*$  orbital type; since  $\pi \rightarrow \pi^*$  excitations are of parity + with respect to reflection in the molecular plane, the "allowed"  $\pi \rightarrow \pi^*$  transitions of aromatic molecules are polarized in the plane of the molecule.

The lowest excited  ${}^1\pi\pi^*$  state of anthracene and that of phenazine are at almost equal energy since they arise from the same system of 14  $\pi$ -electrons; they correspond to an x-polarized transition from the ground state. However, in phenazine an additional possibility arises. Here a lone pair electron from an n-orbital can be promoted to the lowest empty  $\pi^*$  MO and now the lowest singlet state is  ${}^1n\pi^*$ . The  $n \rightarrow \pi^*$  excitation has negative parity for reflection in the molecular plane. Hence  $S_1 \leftrightarrow S_0 ({}^1n\pi^*)$  is out-of-plane (z) polarized; see the two diagrams of fig.1.

When the molecule is excited two orbitals are occupied by a single electron and then it is also possible that these two electrons have their spin angular momentum parallel thus giving rise to a triplet state. This state has a lower energy than the corresponding singlet state because the interelectronic repulsion is reduced for a triplet state. Since this reduction in general is smaller for  $n\pi^*$  than for  $\pi\pi^*$  states [2] phenazine still has a lowest triplet state  $T_0$  which is  ${}^3\pi\pi^*$  and, again, quite similar to the corresponding state of anthracene, see fig.1.

Next consider what happens when phenazine, for instance, by absorption of a quantum of near UV light has been excited into the singlet state  $S_1$ . Subsequently, no  $S_1 \rightarrow S_0$  fluorescence emission is seen, but instead one observes a red ( $\lambda > 6500 \text{ \AA}$ ) long lived ( $\approx 14 \text{ ms}$ ) phosphorescence from the lowest triplet state  $T_0$ . Apparently, once phenazine is in  $S_1$  its spin state and electronic configuration are converted into those of the lowest triplet state at a rate which is thought to be of the order  $10^8 \text{ s}^{-1}$ . Actually  $S_1 \rightarrow T_0$  crossing competes with  $S_1 \rightarrow S_0$  emission. In phenazine  $S_1 \rightarrow T_0$  ISC wins, but in anthracene  $S_1 \rightarrow T_0$  ISC and  $S_1 \rightarrow S_0$  fluorescence have comparable rates. Once in  $T_0$ , the molecule returns to the ground state either by emission of a photon, i.e. it phosphoresces, or by a radiationless process, again called ISC.

Anthracene and its aza-derivatives have as a special feature that radiative decay is almost negligible relative to the non-radiative  $T_0 \rightarrow S_0$  crossing.

## 2. ZERO-FIELD SPLITTING

Thus far neither the symmetry of the molecule, nor magnetic interactions have entered the discussion. In a polyatomic molecule the three triplet spin levels, in general, are distinguishable since the magnetic dipolar interaction between the parallel electron spins causes a zero-field splitting. In the present instance this splitting is of the order of 3000 MHz = 0.1 cm<sup>-1</sup>.

The magnetic substates T<sub>x</sub>, T<sub>y</sub> and T<sub>z</sub> of T<sub>0</sub>, see fig. 1 or I.1, are eigenfunctions of the spin hamiltonian

$$^* \mathcal{H}_{SS} = \vec{S} \cdot \vec{T} \cdot \vec{S} \quad (1a)$$

$$= -XS_x^2 - YS_y^2 - ZS_z^2. \quad (1b)$$

$\vec{S}$  stands for the operator for the total spin angular momentum  $\sum \vec{S}(i)$ , where  $i$  labels the electrons.  $\vec{T}$  is the zero-field splitting tensor, which when written in principal axes form results in (1b) for  $\mathcal{H}_{SS}$ . For symmetrical molecules the principal axes of the zero-field splitting tensor generally coincide with the symmetry axes of the molecule. Tetramethylpyrazine in a durene crystal (chapter VI) provides an intriguing exception. X, Y and Z are the energies of the zero-field components; X + Y + Z = 0.

Let  $|1\rangle$ ,  $|0\rangle$  and  $|-1\rangle$  be the eigenfunctions of S<sub>z</sub>, for instance for T<sub>0</sub> of anthracene. When thinking of T<sub>0</sub> in terms of a single configuration of closed shells and two singly occupied orbitals, these functions could be written in terms of Slater determinants as follows:

$$\left. \begin{aligned} |1\rangle &= |a_1 \bar{a}_1 \dots a_{32} \bar{a}_{32} \pi \pi^*| \\ |0\rangle &= \frac{1}{\sqrt{2}} (|a_1 \bar{a}_1 \dots a_{32} \bar{a}_{32} \pi \pi^*| + |a_1 \bar{a}_1 \dots a_{32} \bar{a}_{32} \bar{\pi} \bar{\pi}^*|) \\ |-1\rangle &= |a_1 \bar{a}_1 \dots a_{32} \bar{a}_{32} \bar{\pi} \bar{\pi}^*| \end{aligned} \right\} (2)$$

A bar denotes the single particle  $|\beta\rangle$  spin, no bar stands for an  $|\alpha\rangle$  spin function. The 66 H- and C-valence electrons in anthracene are distributed over the 32  $a_1 \dots a_{32}$  doubly filled MO's and the two single occupied highest bonding and lowest antibonding  $\pi$  orbitals denoted by  $\pi$  and  $\pi^*$ .

The states T<sub>x</sub>, T<sub>y</sub> and T<sub>z</sub> are related to the eigenfunctions of S<sub>z</sub>, (2), by

the following linear combinations:

$$\begin{aligned} T_x &= \frac{1}{\sqrt{2}} (|- \rightarrow - | + \rightarrow) \\ T_y &= \frac{i}{\sqrt{2}} (|- 1 \rangle + | + \rangle) \\ T_z &= |0 \rangle \end{aligned} \quad (3)$$

It is easily verified that the product  $S_u T_v$ , where  $u, v = x, y, z$ , satisfies the properties [3]:

$$\text{for } u = v \quad S_u T_u = 0 \quad (4a)$$

$$\text{and for } u \neq v \quad S_x T_y = -S_y T_x = i T_z; \text{ etc.} \quad (4b)$$

Physically (4a) means that when the molecule is in the eigenstate  $T_u$  the component of the spin angular momentum along the  $u$ -axis has a zero expectation value and hence the spin lies in the plane  $u = 0$ . As follows from (4b) magnetic dipolar transitions are allowed between any pair of zero-field levels with linearly polarized  $H_1$ -fields. For instance, if anthracene is excited into  $T_z$ , the spin is oriented in the molecular plane. A  $y$ -polarized microwave field  $\vec{H}_1(t) = H_1 \sin \omega t \vec{e}_y$  at the frequency  $\omega = |X-Z|/\hbar$ , i.e.  $\omega/2\pi = 2396$  MHz, then stimulates the  $T_z \rightarrow T_x$  transition.

From (4a) and (4b) it further follows that

$$\langle T_u | \vec{S} | T_u \rangle = 0 \quad u = x, y, z \quad (5)$$

There is no magnetic moment for a molecular triplet state in zero-field. Therefore it is appropriate to use the concept *spin alignment* for a preferential spin orientation in our case, opposite to spin polarization whenever a net magnetic moment results [4]. Finally we note that although our discussion started from the simple MO configuration (2), the results (3) - (5) are perfectly general since they depend on symmetry properties only.

We end by considering the behaviour of a singlet spin function under the action of a spin angular momentum operator. Let us take the two electron spin function

$$|s\rangle = (\alpha(1)\beta(2) - \alpha(2)\beta(1))/\sqrt{2}$$

as an example. We know  $|s\rangle$  to be an eigenfunction of the *total* spin angular momentum operator  $\vec{S}$  with eigenvalue zero,

$$\vec{S} |s\rangle = 0.$$

However, relative to the components of the spin angular momentum operator for a *single* electron one has

$$\begin{aligned} S_x(1) |s\rangle &= \frac{1}{2}(\beta(1)\beta(2) - \alpha(1)\alpha(2)) \\ &= \frac{1}{2} |t_x\rangle, \end{aligned} \tag{6}$$

and by the same reasoning

$$S_x(2) |s\rangle = -\frac{1}{2} |t_x\rangle.$$

Here  $|t_x\rangle$  is the two-electron triplet spin function which satisfies  $S_x(1,2)|t_x\rangle = 0$  and  $S_x(1,2)|t_y\rangle = -S_y(1,2)t_x = i|t_z\rangle$ , etc., cf. (4). Therefore singlet  $\leftrightarrow$  triplet mixing occurs through a spin operator which is antisymmetric for the interchange of the spins. In the present example of two electrons it equals  $S_x(1) - S_x(2)$ . The result is equally applicable to many electron systems [3].

### 3. SPIN-ORBIT COUPLING AND PHOSPHORESCENCE

Here we briefly outline how the anisotropy of the spin-orbit interaction with respect to the orientation of the triplet electron spin leads to selective radiative decay of the separate zero-field levels of  $T_0$ .

SOC is a complicated interaction even in a system as "simple" as the He-atom [5]. In actual practice, when thinking about molecules such as anthracene and phenazine, it can only be discussed by first introducing drastic approximations into the hamiltonian. Our intention is to present a brief outline of the present view on SOC in aromatic molecules. We avoid the historical course of things which might be confusing, but instead, summarize a few outstanding features:

I-(a) For aromatic hydrocarbons, and also for aza-derivatives with a lowest  $\pi\pi^*$  triplet state, it is found experimentally that phosphorescence always is strongly *polarized out-of-plane* [6].

(b) In a pure  $\pi$ -electron description of the optical spectrum of an aromatic compound only in-plane polarizations of the transitions can occur, because as we have noted, all states are of the same parity with respect to reflection in the molecular plane.

The combination of these two facts suggests that for a proper description of phosphorescence one must go beyond the pure  $\pi$ -electron model of the aromatic molecule. One thus is led to expect that in an aromatic hydrocarbon phosphorescence derives its intensity from coupling of  $T_0$  to highly excited singlet states involving the  $\sigma$  core ( $\sigma \rightarrow \pi^*$  or  $\pi \rightarrow \sigma^*$  promotions) [7].

II - In order to shed some light on the above conclusion we note what various authors have found on expanding the matrix elements of the hamiltonian for SOC,  $\mathcal{H}_{SO}$ , as a sum of integrals over atomic orbitals:

(a) *in the  $\pi$ -electron model*. McClure has shown that in the  $\pi$ -electron description SOC is extremely weak [8]. This results from the vanishing of all one- and two-center integrals for reasons of symmetry.

(b) *in the extended description* where also  $\pi\sigma^*$ ,  $\sigma\pi^*$  and/or  $n\pi^*$  states are taken into account:

(i) Aromatic hydrocarbons.

Coupling of  $T_0$  ( $^3\pi\pi^*$ ) with  $^1\sigma\pi^*$  or  $^1\pi\sigma^*$  states gives rise to one-center integrals, as we shall see later on.

The effectiveness of the latter coupling, as opposed to that within a pure  $\pi$ -electron model, is illustrated in the first part of table 1, where we give the results of two representative calculations on the radiative lifetime of the phosphorescent state of benzene: Hamerka and Oosterhoff's estimate obtained within a pure  $\pi$ -electron model and that obtained by Veeman and van der Waals who considered interaction of  $\pi\pi^*$  with  $\sigma\pi^*$  and  $\pi\sigma^*$  states. Tabulated are the mean radiative rates  $k^r = 1/3 \sum_u k_u^r$  and the table also contains a brief reference to the model applied in the calculations.

For a crude order of magnitude calculation we may assume the rates to be proportional to the absolute squares given in the last column of table 1. We use  $E_{^1\sigma\pi^*} - E_{T_0} \approx 10(E_{^1\pi\pi^*} - E_{T_0})$  [10]. Then we obtain the following estimate:

$$\langle ^1\sigma\pi^* | \mathcal{H}_{SO} | ^3\pi\pi^* \rangle \approx 300 \langle ^1\pi\pi^* | \mathcal{H}_{SO} | ^3\pi\pi^* \rangle \quad (7)$$


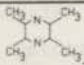
	$k^r$ in $s^{-1}$	model used	typical dependence on $H_{SO}$ , cf. (10)
 benzene	Hameka and Oosterhoff [9] $26 \cdot 10^{-5} - 42 \cdot 10^{-5}$	McClure's description in a $\pi$ -electron model [8]	$\left  \frac{\langle {}^1_{\pi\pi^*}   \mathcal{H}_{SO}   {}^3_{\pi\pi^*} \rangle}{E_{1_{\pi\pi^*}} - E_{T_0}} \right ^2$
benzene	Veeman and van der Waals [10] $4 \cdot 10^{-2}$	coupling to highly excited states involving $\sigma\pi^*$ - and $\pi\sigma^*$ -promotions	$\left  \frac{\langle {}^1_{\sigma\pi^*}   \mathcal{H}_{SO}   {}^3_{\pi\pi^*} \rangle}{E_{1_{\sigma\pi^*}} - E_{T_0}} \right ^2$
experimental [11]	$3.5 \cdot 10^{-2*})$		
 tetramethyl pyrazine	experimental value chapter VI $\approx 5^*)$		$\left  \frac{\langle {}^1_{n\pi^*}   \mathcal{H}_{SO}   {}^3_{\pi\pi^*} \rangle}{E_{1_{n\pi^*}} - E_{T_0}} \right ^2$

Table 1.

This evaluation agrees well with a recent statement of Metz et al. [12], who claimed, without further explanation, that multicenter integrals of spin-orbit coupling do not exceed 1% of the one-center SOC integrals.

(ii) Aza-aromatic compounds with a  $\pi\pi^*$  phosphorescent state.

We have seen in section I that an aza-aromatic molecule contains the non bonding n orbital(s) localized on the N atom(s) in addition to the  $\sigma$ - and  $\pi$ -orbitals of the parent hydrocarbon. With regard to the symmetry n- and  $\sigma$ -orbitals are fully similar. Although the matrix element of the SOC between a  $\pi\pi^*$  and an  $n\pi^*$  state will hardly be different relative to that between a  $\pi\pi^*$  and a  $\sigma\pi^*$  state, SOC between  $T_0$  ( ${}^3_{\pi\pi^*}$ ) and a  ${}^1_{n\pi^*}$  is much more effective. This is caused by the fact that  ${}^1_{n\pi^*}$  lies very close in energy to the lowest triplet state (see the SOC pathways in fig. 1). For an order of magnitude estimate we may write  $E_{1_{n\pi^*}} - E_{T_0} \approx 0.1 (E_{1_{\sigma\pi^*}} - E_{T_0})$ . Thus the denominator of the expression for  ${}^{n\pi^*} k^r$  in the column of table 1 becomes very small for an aza-aromatic molecule, so that after squaring the term which contains the coupling to the  ${}^1_{n\pi^*}$  state entirely dominates.

\*) These values are for the total decay rates  $k_u$ , which here are thought to be mainly radiative.



To illustrate this effect we have also listed the decay rate of  $T_0$  for tetramethylpyrazine (TMP) in table 1. The electronic structure of the lowest triplet states of benzene and TMP are very similar [13]. The considerable shortening of the triplet state lifetime for TMP reflects the effectiveness of the SOC route in molecules with lone-pair orbitals.

To see how the various statements we have made fit together let us consider spin-orbit coupling in some detail. Physically SOC represents the coupling of the electron spin to the local magnetic fields that result from the relative motion of the electrons and nuclei and which may be expressed by the hamiltonian

$$\mathcal{H}_{SO} = g\beta\sum_i \vec{h}(i) \cdot \{\vec{r}, \vec{p}\} \cdot \vec{S}(i) \quad (8)$$

Here  $\vec{h}(i)$  is the internal magnetic field acting on electron  $i$  and  $\{\vec{r}, \vec{p}\}$  symbolizes the aggregate of the positions and momenta of all the electrons relative to a fixed nuclear frame. To reduce (8) to a more manageable form, one customarily follows a similar procedure as used in the qualitative discussion of atomic spectra (see e.g. [14], section 24-2). That is, by neglecting the explicit contributions of the motions of the electrons relative to each other, one may consider the interactions of the spins  $\vec{S}(i)$  with an average field which depends on the position and velocity of electron  $i$  only. In this way (8) may be reduced to [10].

$$\mathcal{H}_{SO} = \sum_K \gamma_K \sum_i \vec{l}_K(i) \cdot \vec{S}(i) \quad (9)$$

In (9)  $\vec{l}_K(i)$  is the orbital angular momentum of electron  $i$  about nucleus  $K$ . The idea behind the approximation leading to (9) is the fact that the effective magnetic field felt by the spin on electron  $i$  due to its motion in the vicinity of the nucleus  $K$  depends strongly on the electron-nucleus distance  $|\vec{r}_{iK}|$ ; for small distances it varies roughly as  $|\vec{r}_{iK}|^{-4}$  [14]. In other words only those regions very close to the nuclei will effectively contribute to SOC. Then the separate contributions of all nuclei may be summed to give (9), where  $\gamma_K$  is approximated by the atomic spin-orbit coupling constant for nucleus  $K$ .

With the aid of fig. 1 we shall now try to understand the principal

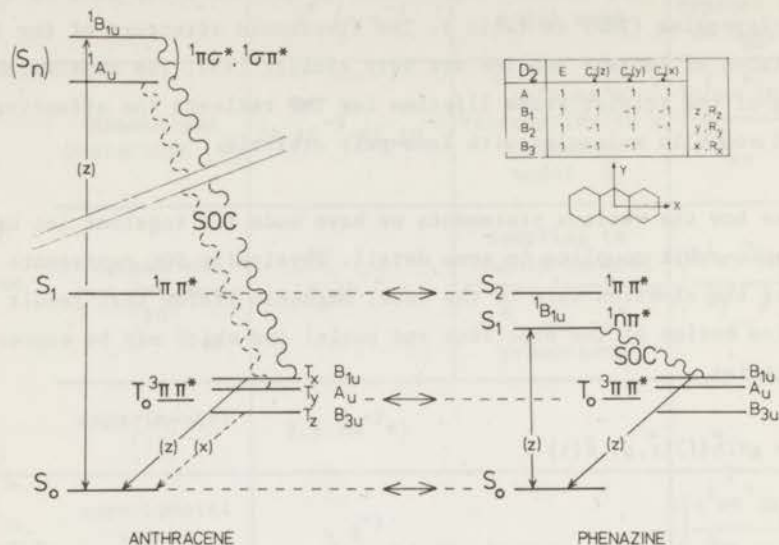


Fig. 1.

features outlined at the beginning of this section, using anthracene and phenazine as examples. These two iso-electronic molecules have a very similar electronic structure on excitation into the state  $T_0$  [15], which is of orbital symmetry  $B_{2u}$  in  $D_{4h}$ . The irreducible representations according to which the zero-field components of  $T_0$  transform are indicated in fig. 1. We apply the symmetry rules for matrix elements in quantum mechanics and remember that the ground state is totally symmetrical. Then by inspection of the character table, it is seen that only  $T_x \rightarrow S_0$  and  $T_z \rightarrow S_0$  are electric dipole allowed transitions with the polarizations  $z$  and  $x$  respectively;  $T_y \rightarrow S_0$  is symmetry forbidden. As we have noted one finds experimentally that the out-of-plane polarization ( $z$ ) strongly dominates [16,17]. Hence  $T_x$  may be considered as the only radiative level for  $T_0$  in anthracene and also in phenazine, see fig. 1.

When taking SOC into account the wave function  $T_x$  can be written as

$$T_x = T_x^{(0)} + \sum_{S_n} \frac{\langle S_n | \mathcal{H}_{SO} | T_x^{(0)} \rangle}{E_{S_n} - E_{T_0}} S_n \quad (10)$$

Here  $T_x^{(0)}$  stands for the "pure" triplet state without SOC. Apparently  $T_x^{(0)}$  is coupled to  $B_{1u}$  singlet states, which owing to the antisymmetry for reflection in the plane  $z = 0$  of a  $B_{1u}$  state, must arise from  $1\sigma\pi^*$  - (and/or  $1\pi\sigma^*$ -) or  $1n\pi^*$  electron excitations. Further, it will prove significant that according to the discussion following (6) only the products of the  $x$  components,  $\ell_{xK}(i)S_x(i)$  in  $\mathcal{H}_{SO}$  (9) couple  $T_x$  with singlet states.

When substituting (9) into (10) and expanding the matrix element  $\langle S_n | \mathcal{H}_{SO} | T_x^{(0)} \rangle$  in integrals over atomic wave functions, then after the integration over the spin coordinates, we are left with sums of *one-electron* integrals of the type  $\langle a_K(i) | \ell_{xL}(i) | b_M(i) \rangle$ , where  $a_K$  and  $b_M$  are atomic orbitals and the labels  $K, L$  and  $M$  refer to individual nuclei in the molecule, not necessarily different. We remember that for aromatic hydrocarbons, and also for the aza-derivatives of the present interest,  $T_0$  corresponds to a  $\pi^* \leftarrow \pi$  promotion. Hence  $b_M$  is always a  $2p_z$  atomic wave function.

Because SOC happens only in regions very close to the nuclei, it is a reasonable approximation to keep only the *one-center* integrals in this sum, i.e.  $\langle a_K(i) | \ell_{xK}(i) | 2p_{zK}(i) \rangle$ . From the quantum theory of atoms we know that it follows from the commutation rules of the orbital angular momentum that  $\ell_x p_z = -i p_y$ . Thus the above one-electron-one-center integral - which in our situation always has a  $p_z$ -type A.O. in the ket - gives a non-vanishing contribution only when the atomic wave function  $a_K$  contains the atomic orbital  $2p_y$ .

Let us first consider phenazine. Here there is one term in the sum over singlet-states in (10), which dominates all the others: that involving the  $1n\pi^*$  state. This state lies very close in energy to  $T_0$  and therefore leads to an energy denominator which is only one-tenth of that of the other terms in (10). If we restrict ourselves to this dominant term we get the following picture. The lone-pair orbitals resemble pure  $sp^2$  hybrids on the  $n$  atoms [10]:  $(s+p_y\sqrt{2})/\sqrt{3}$  or  $(s-p_y\sqrt{2})/\sqrt{3}$ . In phenazine SOC thus may be considered to occur localized on the nitrogen nuclei.

In anthracene, however,  $S_n$  runs through all  $1\sigma\pi^*$  and  $1\pi\sigma^*$  states of the proper symmetry. Here the  $a_K(i)$  are trigonal  $(2s)(2p)^2$  hybrids  $t_{KK'}$  of carbon atom  $C_K$  pointing in the direction of a neighbouring H or C atom ( $K'$ ),

$$t_{KK'} = [s_{C_K} + (p_{y,C_K} \sin \alpha_{K,K'} + p_{x,C_K} \cos \alpha_{K,K'}) \sqrt{2}] / \sqrt{3},$$

$\alpha_{K,K'}$  is the angle between the vector pointing from  $C_K$  to atom  $K'$  and the

x-axis of the molecule. The  $s$ ,  $p_y$  and  $p_x$  stand for  $2s$ ,  $2p_y$  and  $2p_x$  atomic orbitals. In a large molecule like anthracene there are many  $\sigma$ -bonds making various angles with the  $x$  and  $y$  axes and, therefore, one expects that  $T_y$  must be coupled to  $^1\sigma\pi^*$  and  $^1\pi\sigma^*$  states via the terms  $\ell_{yK}(i)S_y(i)$  in (9) to about the same extent as  $T_x$  is coupled via  $\ell_{xK}(i)S_x(i)$ .

The overall symmetry of the electron distribution in the molecule governs the selection rules for dipolar radiation, hence  $T_y \rightarrow S_0$  is forbidden as a radiative transition. But as we shall see later in the chapters IV and V the observed near-quality of the absolute *non-radiative* decay rates for  $T_x$  and  $T_y$  in anthracene reflects the comparable coupling to singlet states of  $T_y$ . A satisfactory estimate of the probabilities for radiationless transitions can in fact be obtained by only considering the local symmetry.

#### 4. INTERSYSTEM CROSSING

During the last decade there has been a growing interest in the theoretical description of radiationless transitions in molecules, by which electronic energy of excitation is converted into vibrational energy. At the present time there have been a number of conferences on this subject: the next takes place in September 1974 in Munich.

The pioneering work on this subject has been done by Robinson and Frosch in 1962 [18,19]. Following these authors we discuss a molecular radiationless transition in terms derived from a comparison with a simple mechanical model [18]. When one of two weakly coupled oscillators, for instance two pendula connected by a spring, is excited, one observes the continuous build-up and decay of the oscillatory motion in the separate oscillators. However, if one of the two oscillators in addition is strongly coupled to a further oscillator system with many degrees of freedom (Robinson's famous "bedspring" [18]) the original motion will be dissipated into the many degrees of freedom. The time evolution of the amplitude of the pendulum that was initially excited here corresponds to the decay via the radiationless transition.

In the theoretical description of a molecular radiationless transition which converts electronic energy into vibrational energy the transition is identified with the development of an initially excited discrete quasi-stationary state into adjacent vibronic states, which belong to a lower lying electronic state [20], see fig. 2.

One has succeeded to prove experimentally that the non-radiative change

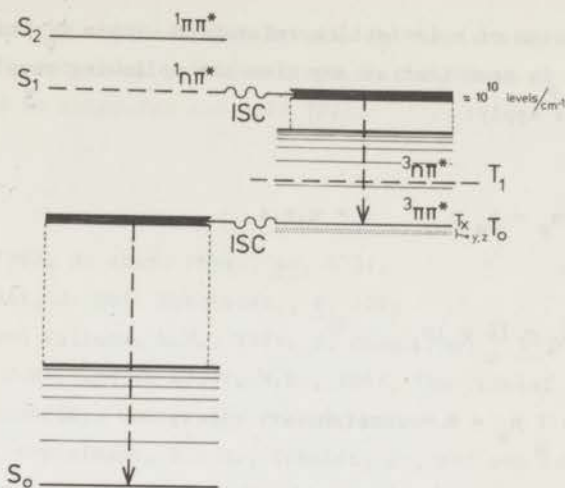


Fig. 2.

to a new electronic configuration occurs in an isolated molecule, provided it is sufficiently large, see for instance [21]. The subsequent vibrational relaxation, see fig. 2, is a consequence of the coupling between molecular vibronic (= vibrational x electronic) states and lattice phonons. Modern theories on radiationless transitions are based on intramolecular interactions; the medium acts as an additional perturbation and as a heat bath.

### 5. SPIN ALIGNMENT ON OPTICAL PUMPING

A simple kinetic scheme serves to illustrate how the spin selective processes of populating and decay of  $T_0$  may lead to spin alignment. We consider the five level diagram of fig. 3, in which we have drawn the relevant rates

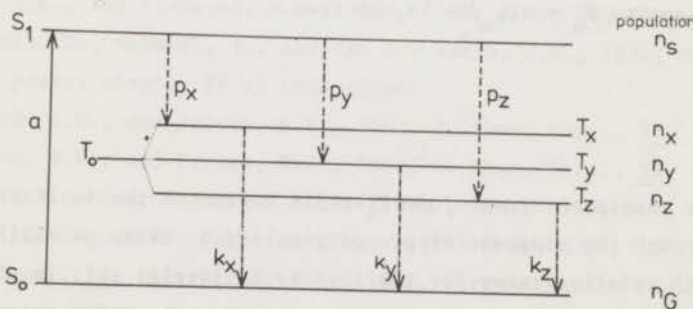


Fig. 3.

with the exception of spin-lattice relaxation within  $T_0$  which is not yet considered. It is seen that at any time the following coupled equations for the populations apply:

$$\frac{dn_u}{dt} = p_u n_s - k_u n_u \quad u = x, y, z \quad (13a)$$

$$\frac{dn_s}{dt} = a n_G - (\sum_u p_u) n_s \quad (13b)$$

$$n_G + n_s + \sum_u n_u = N = \text{constant} . \quad (13c)$$

The simplest case is the steady-state situation under continuous illumination (notation in capitals). Then the left hand sides of (13a, b) equal zero, and hence

$$N_u = \frac{p_u}{k_u} \frac{a}{\sum_u p_u} N_G .$$

As only a small fraction of the  $N$  molecules in the sample is excited, (13c) is usually approximated to

$$N_G = N , \quad (14)$$

hence 
$$N_u = \frac{p_u}{k_u} \frac{a}{\sum_u p_u} N .$$

In what follows we simplify things by introducing as the populating rate of  $T_0$  the quantity  $P_u = a(p_u/\sum_u p_u)N$ , so that

$$N_u = \frac{P_u}{k_u} . \quad (15)$$

Obviously the absolute values of the  $P_u$  still depend on the excitation condition through the constant of proportionality  $a$ . Since we shall only be concerned with relative rates for the three spin levels, this is not important and simply talk about these  $P_u$  as if they were the actual ISC-rates  $p_u$ . Spin selectivity in populating and decay of  $T_0$  in general will lead to a ratio

$P_u/k_u$  that varies for the separate spin levels. Such spin alignment, because of (15), caused the spectacular emissive lines in the ESR on  $T_0$  of naphthalene observed by Schwoerer and Wolf [22].

#### REFERENCES

- [1] Clementi, E., 1967, *J. chem. Phys.*, 46, 4731.
- [2] Goodman, L., 1961, *J. mol. spectrosc.*, 6, 109;  
Harris, R.A., and Falicov, L.M., 1971, *J. chem. Phys.*, 55, 2931.
- [3] van der Waals, J.H., and de Groot, M.S., 1967, *The Triplet State*, edited by A. Zahlan (Cambridge University Press), p. 101.
- [4] de Groot, M.S., Hesselmann, I.A.M., Schmidt, J., and van der Waals, J.H., 1968, *Molec. Phys.*, 15, 17.
- [5] Bethe, H.A., and Salpeter, F.E., *Handbuch der Physik*, vol. 35, p. 271, Ed. by S. Flügge, Springer, 1957, Berlin, Göttingen and Heidelberg.
- [6] Krishna, V.G., and Goodman, L., 1962, *J. chem. Phys.*, 36, 2217.
- [7] Mizushima, M., and Koide, S., 1952, *J. chem. Phys.*, 20, 765.
- [8] McClure, D.S., 1952, *J. chem. Phys.*, 20, 682.
- [9] Hameka, H.F., and Oosterhoff, L.J., 1958, *Molec. Phys.*, 1, 358.
- [10] Veeman, W.S., and van der Waals, J.H., 1970, *Molec. Phys.*, 18, 63.
- [11] Lim, E.C., 1962, *J. chem. Phys.*, 36, 3497.
- [12] Metz, F., Friedrich, S., and Hohlneicher, G., 1972, *Chem. Phys. Lett.*, 16, 353.
- [13] McWeeny, R., and Peacock, T.E., 1957, *Proc. Roy. Soc. London, A* 70, 41.
- [14] Slater, J.C., 1960, *Quantum Theory of Atomic Structure*, Vol. II (McGraw-Hill, London, New York and Toronto).
- [15] Grivet, J.Ph., 1970, thesis, Paris.
- [16] Lower, S.K., and El-Sayed, M.A., 1966, *Chem. Rev.*, 66, 199.
- [17] Antheunis, D., Schmidt, J., and van der Waals, J.H., 1974, *Molec. Phys.*, in the press; chapter IV of this thesis.
- [18] Robinson, G.W., and Frosch, R.P., 1962, *J. chem. Phys.*, 37, 1962.
- [19] Robinson, G.W., and Frosch, R.P., 1963, *J. chem. Phys.*, 38, 1187.
- [20] Jortner, J., Rice, S.A., and Hochstrasser, R.M., 1969, *Adv. Photochem.*, 7, 149; Schlag, E.W., Schneider, S., and Fischer, S.F., 1971, *Ann. Rev. Phys. Chem.*, 22, 465; Freed, K.F., 1972, *Current topics in Chem.*, 31, 105.
- [21] Jortner, J., 1969, *J. chim. Phys.*, 20e Réunion de la Société de chimie physique Paris, p. 9.

[22] Schwoerer, M., and Wolf, H.C., 1967, Proceedings XIVth Colloque Ampère, (Amsterdam, North-Holland Publishing Co.), p. 87.



## CHAPTER III

### EXPERIMENTAL

#### 1. THE MICROWAVE INDUCED PHOSPHORESCENCE EXPERIMENT

The optical detection of magnetic dipole transitions between pairs of zero-field levels of a phosphorescent triplet state  $T_0$  was first realized by Schmidt and van der Waals [1]. Conceived as a means for the direct observation of the zero-field resonances within  $T_0$ , the method became very promising when a brief transient microwave field at resonance with one of the zero-field transitions was applied. In particular spectacular transient changes in phosphorescence intensity can be produced by sweeping through a microwave transition at a given time *during the decay of the phosphorescence*, see fig. 1 (microwave induced delayed phosphorescence, MIDP).

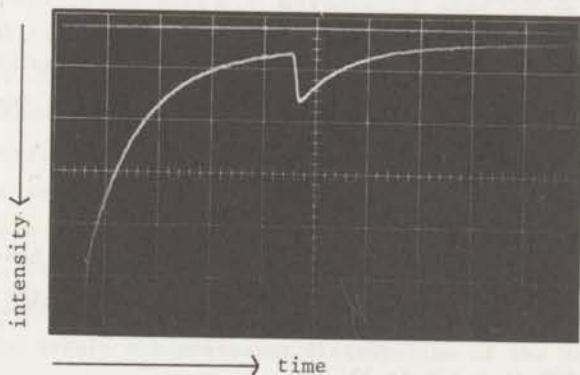


Fig. 1. MIDP signal for phenazine on sweeping through the  $T_x - T_z$  resonance.  $T = 1.2$  K. Horizontal 5 ms/div.

By virtue of the "dark" background the MIDP experiment is quite sensitive. The method soon was developed into a simple tool for a detailed investigation of the populating and decay processes of the separate spin

components of phosphorescent triplet states [2,3] and recently also for the study of spin-lattice relaxation transitions within  $T_0$  [4].

For a further description of the experiment we take phenazine in a biphenyl crystal as an example. The system is illuminated for a relatively long period, say 5 s, until a stationary distribution of the population over the spin levels of  $T_0$  is established. Then at the time  $t = 0$  the excitation is terminated and we observe the decay of  $T_0$  via the decreasing phosphorescence intensity with a photomultiplier connected to an oscilloscope. At the time  $t = t_1$  the frequency of a microwave field is swept through the  $T_x - T_z$  resonance at 2586 MHz and a sharp increase in light intensity occurs, see fig. 1.

To make the experiment useful for a quantitative analysis the full width  $\Delta\omega$  of the zero-field resonance must be covered within a time much shorter than the shortest of the lifetimes of the three levels. Hence if  $T_1$  is this shortest lifetime, the sweep rate  $\frac{d\omega}{dt}$  has to obey the condition

$$\frac{1}{\Delta\omega} \frac{d\omega}{dt} \gg T_1^{-1}. \quad (1)$$

This lifetime is either determined by the decay to the ground state if the isolation condition between the spin states is fulfilled, or by spin-lattice relaxation in the case of dominant relaxation. For the actual case of phenazine under conditions of isolation  $T_x - T_z$  is swept at a rate of about 20 MHz/ms.

When performing such fast sweeps, the total number of molecules in the two levels is the same just before and immediately after the sweep. Hence

$$\Delta N_x + \Delta N_z = 0. \quad (2)$$

The change of population  $\Delta N$  produced by the microwave sweep can be written as a fraction of the population difference of  $T_x$  and  $T_z$  before the sweep:

$$\Delta N_x = -\Delta N_z = f(N_z(t_1) - N_x(t_1)). \quad (3)$$

If  $k_x^r$  and  $k_z^r$  are the rates for radiative decay from  $T_x$  and  $T_z$ , the change in light intensity  $\Delta I$  at the time  $t_1$  resulting from the sweep, is given by [2]

$$\begin{aligned}\Delta I(t_1) &= (\Delta I(t_1))_x + (\Delta I(t_1))_z \\ &= c (\Delta N_x k_x^r + \Delta N_z k_z^r)\end{aligned}$$

and hence by substitution of (3)

$$\Delta I(t_1) = c f (N_z(t_1) - N_x(t_1)) (k_x^r - k_z^r) ; \quad (4)$$

where  $c$  is an instrumental constant. The fraction  $f$  is the "microwave transfer factor": it is the fraction of the population difference between  $T_x$  and  $T_z$  transferred by the microwaves at the time  $t_1$  and it has to be determined for the existing experimental conditions.

## 2. THE EQUIPMENT

### 2.1 Cryogenics

#### the dewars

Experiments at liquid He temperatures are done in the glass dewar of fig. 2. It has been made in this laboratory by Mr. L. van As. The volume of the He-chamber is 3.5 l. The system contains three suprasil I (Heraeus) quartz windows at the bottom. The upper one is fused to a quartz-glass transition,  $\phi_1 = 36$  mm. The middle window is connected to the nitrogen container in order to minimize I.R. irradiation into the He-bath. The system keeps liquid He for over 45 hours when operating at 4.2 K with a  $\text{NiSO}_4 + \text{CoSO}_4$  solution filter in the excitation light beam from a mercury arc.

For experiments above 4.2 K we used a stainless steel gas-flow cryostat (Leybold-Heraeus), see fig. 3. This dewar contains two He-chambers: the reservoir A for storage of the liquid with a volume of 3 l and a separate vessel B in which the experiments are done. Because the pressure in B is kept a little lower, say 10 to 20 cm Hg, than that in A the He is forced to flow via a needle valve V through a capillary C into the porous metal plug P. This plug P serves to attain a homogeneous distribution of the He entering the experimental space B. Before the He enters the chamber B it must be evaporated; the rate of evaporation is controlled by electric heating.

#### thermometry

In the bath cryostat the temperature is determined by the measurement of

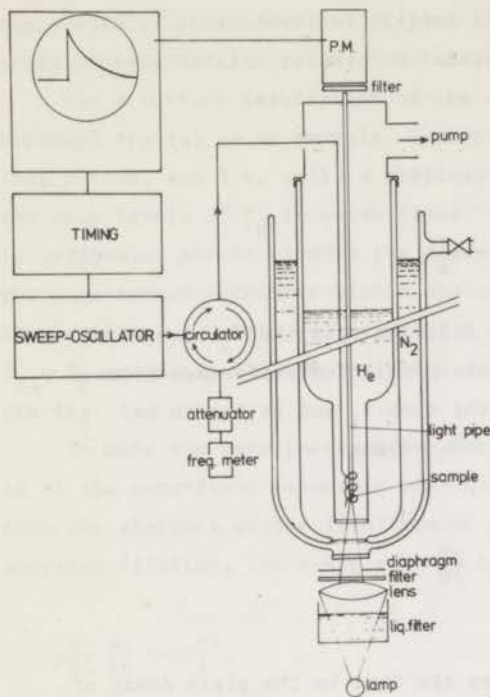


Fig. 2

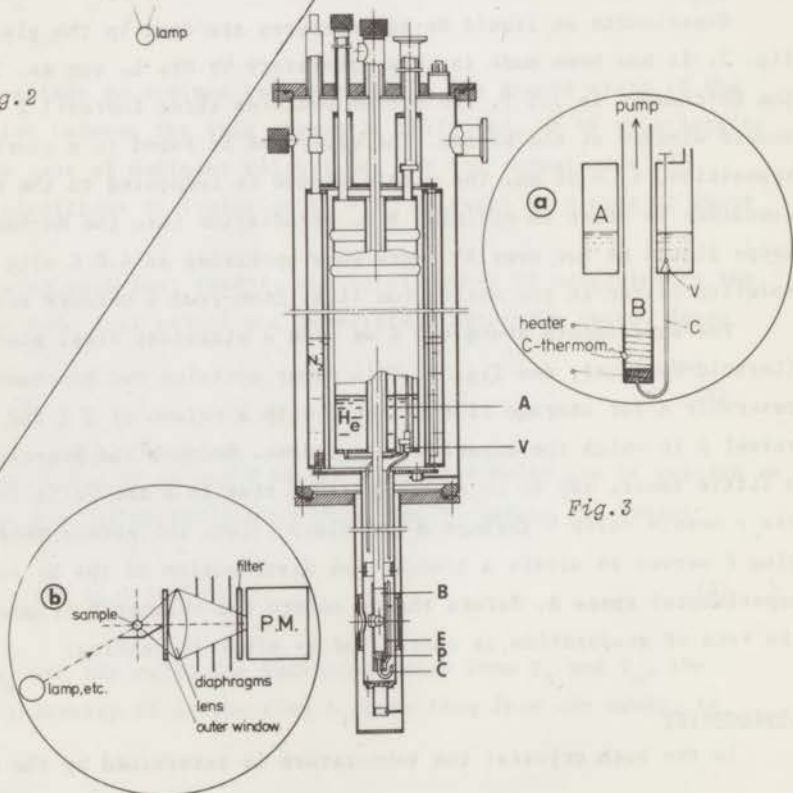


Fig. 3

the vapour pressure of the He.

In the gas flow dewar a Ge-resistor thermometer, placed very close to the sample, is used. Its resistance is measured in an A.C. wheatstone-bridge with phase sensitive detection. The thermometer is calibrated against the vapour pressures of  $^4\text{He}$ ,  $\text{H}_2$  and Ne in the respective temperature ranges  $3 \text{ K} \lesssim T \lesssim 5 \text{ K}$ ,  $14 \text{ K} \lesssim T \lesssim 22 \text{ K}$  and  $24.5 \text{ K} \lesssim T \lesssim 29.5 \text{ K}$ . In the intermediate temperature regions we compared its resistance with an accurately calibrated second Ge-thermometer from the thermometry-group of the Kamerlingh Onnes Laboratory. Interpolations are done by least-square polynomial fits. Care was taken that in all cases heating of the resistors was kept to a minimum.

### thermostats

In the bath cryostat the temperature was controlled with a manostat.

In the gas flow dewar we employed a simple electronic feed back system. Via valve V in fig. 3 a certain amount of He is supplied to the experimental space B in which the pressure is kept constant with a manostat. The temperature of the evaporator body E (the lower, heavy part of tube B) is determined with a carbon resistor thermometer in an A.C.-bridge with phase sensitive detection. The current through the heater on E is regulated by the D.C. output of the detector via a heater control unit. With this system we could keep the temperature constant to within 6 mK at 4.5 K and within 20 mK at 18 K for half an hour in both cases.

We have also verified that the temperature of the sample must be reasonably equal to that of its surroundings. We did this test with quinoxaline in durene under the excitation conditions used in the actual experiments and lowered the temperature of the gas gradually until finally the crystal became immersed in liquid He. During this cooling we repetitively monitored one of the zero-field transitions. No abrupt changes in the height of the signal or in its decay were observed when contact with the liquid was established. We believe that in the liquid under appropriate excitation conditions  $T_{\text{sample}} = T_{\text{bath}}$ , c.f. chapter IV, section 3.3. From the above experiment it seems safe to assume that also in gas  $T_{\text{sample}} = T_{\text{gas}}$ .

### *2.2 The microwaves*

The source is a Hewlett Packard HP 8690 B sweep oscillator containing a backward wave oscillator as a plug in. The transmission of the microwaves

occurs through coaxial lines, see fig. 2 for further details. A helix acts as a resonator. Double resonance experiments and multiple sweeps at different frequencies are carried out with two sweep oscillators. The power of both oscillators is fed into a single coaxial line via a coaxial hybrid or, if the frequencies differ much more than one octave, via suitable cut off filters and a simple coaxial T junction.

### 2.3 Optics

#### excitation

The light source is a Philips SP 1000 W mercury arc or an Osram 200 W mercury arc. A quartz lens focuses the light on the sample. In order to minimize heat input into the crystal the excitation beam passes through a solution filter (a  $\text{NiSO}_4 + \text{CoSO}_4$  or a  $\text{CuSO}_4$  solution), an optical glass filter (OX-7 Chance Pilkington or UG-5 Heraeus Schott) and a partly closed diaphragm.

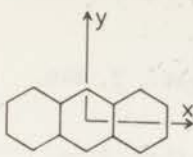
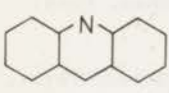
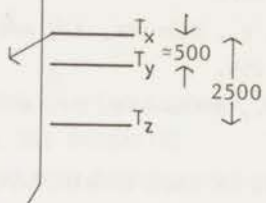
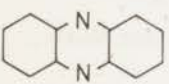
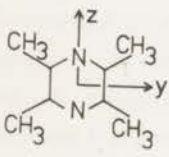
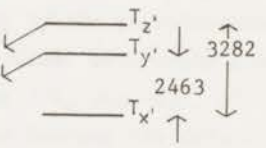
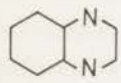
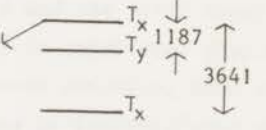
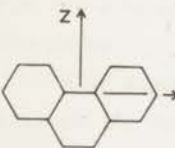
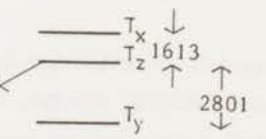



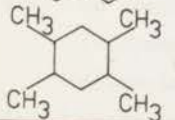
#### detection

In the glass dewar the sample is mounted against a light pipe through which the emitted light is passed. Via an appropriate filter we take care that only the phosphorescence emission reaches the cathode of a photomultiplier tube (EMI 9524 B or a Peltier cooled EMI 9558 A).

In the gas flow cryostat the crystal lies on a teflon bolt which screws into the helix and which contains a number of vertical holes to allow the He-gas to flow freely around the sample. The detection beam is at  $90^\circ$  with respect to the incident excitation beam. In order to minimize stray light, particularly in experiments done during continuous illumination of the crystal, we used a lens and some diaphragms in the emitted light beam, see fig. 3.

### 3. THE SYSTEMS STUDIED

The following may serve for quick reference to all systems studied in this thesis.

GUESTS		isomers	studied	zero-field splitting and radiative level(s)	host	chapter
	Anthracene	$-h_{10}, -d_{10}, -h_2 d_8$			B	IV
	Acridine	$-h_9, -d_9$			B	IV, VII
	Phenazine	$-h_8, -d_8$			B	IV
	Tetramethylpyrazine	$-h_{12}$			D	VI, VII [5]
	Quinoxaline	$-h_6$			D, N	VII [2]
	Phenanthrene	$-h_{10}$			B, F	VII [6]
HOSTS						
	Biphenyl	$-h_{10}$	(B)			
	Fluorene	$-h_9$	(F)			
	Naphthalene	$-d_8$	(N)			
	Durene	$-h_{14}$	(D)			

The zero-field splittings are expressed by the resonance frequencies in MHz.

## REFERENCES

- [1] Schmidt, J., and van der Waals, J.H., 1968, Chem. Phys. Lett., 2, 640.
- [2] Schmidt, J., thesis University of Leiden, 1971.
- [3] Schmidt, J., Veeman, W.S., and van der Waals, J.H., 1969, Chem. Phys. Lett., 4, 341.  
Antheunis, D., Schmidt, J., and van der Waals, J.H., 1970, Chem. Phys. Lett., 6, 255.  
Schmidt, J., Antheunis, D., and van der Waals, J.H., 1971, Molec. Phys., 22, 1.
- [4] Chapter VII of this thesis, with further references.
- [5] de Groot, M.S., Hesselmann, I.A.M., Reinders, F.J., and van der Waals, J.H., Molec. Phys., in the press.
- [6] Sixl, H., 1971, Thesis, University of Stuttgart.



## CHAPTER IV

### SPIN-FORBIDDEN RADIATIONLESS PROCESSES IN ISOELECTRONIC MOLECULES: ANTHRACENE, ACRIDINE AND PHENAZINE.

A STUDY BY MICROWAVE INDUCED DELAYED PHOSPHORESCENCE<sup>(\*)</sup>.

*Microwave induced delayed phosphorescence (MIDP) experiments have been performed to study the populating and decay of the phosphorescent triplet state  $T_0$  of seven aromatic three-ring molecules: anthracene ( $-h_{10}$ ,  $-h_2 d_8$  and  $-d_{10}$ ), acridine ( $-h_9$  and  $-d_9$ ) and phenazine ( $-h_8$  and  $-d_8$ ), all diluted in biphenyl crystals. We chose these molecules because the desactivation of  $T_0$  goes dominantly via radiationless processes and the total decay rates of the individual spin components of  $T_0$  determined in experiment thus equal the radiationless decay rates. The phosphorescence emission, used as a monitor for the triplet state population, here gives an insignificant contribution to the decay.*

*MIDP experiments only yield the true decay rates if thermal isolation between the levels is maintained throughout and the present investigations, in which the intensity of excitation has been varied over a wide range, uncover a possible source of systematic error that has been overlooked thus far.*

*The principal results of the experiments are (see fig. 1 for choice of axes)*

- (i) In the anthracene isomers the spin states  $T_x$  and  $T_y$  (corresponding to the in-plane axes of the molecule) are comparably active in both  $S_1 \rightarrow T_0$  as well as in  $T_0 \rightarrow S_0$  crossing.*
- (ii) We observe a deuterium effect on the radiationless decay rates which is independent of the particular spin state, but merely depends on the molecule.*
- (iii) Appreciable effects of aza-substitution on the decay rates of the "inactive" components  $T_y$  and  $T_z$  are noted:  $k_y/k_z$  and  $P_y/P_z$  decrease*

substantially on going from anthracene to the aza-derivatives;  $k_y$  and  $k_z$  increase by a factor of 2 in going from acridine to phenazine. The results on anthracene are compared with results from other workers and with quantitative estimates derived from recent theories on spin-forbidden radiationless transitions.

## 1. INTRODUCTION

In this chapter we present a systematic investigation of the dynamics of populating and decay of the lowest triplet state of anthracene and two of its aza-derivatives when excited by UV light in a biphenyl host crystal. The molecules studied are anthracene ( $A-h_{10}$ ), 9-azaanthracene (acridine,  $Ac-h_9$ ), 9,10-diazaanthracene (phenazine,  $P-h_8$ ), and also the deuterated species  $A-d_{10}$ ,  $A-h_{2,8}^d$  (hydrogen at the mesopositions),  $Ac-d_9$ ,  $P-d_8$ . The molecules have a lowest  $\pi\pi^*$  triplet state that in essence is the same for all seven, as demonstrated by nearly equal triplet state energies and zero-field splittings and a striking similarity in the triplet ESR spectra [1], see also table 1.

The idea behind the experiments was to gather a coherent set of data for testing certain aspects of recent theories on spin-forbidden radiationless processes in aromatic molecules [2]. The present molecules were chosen because their triplet state lies at such low energy that one may assume radiative decay to be (almost) negligible relative to the radiationless decay. Hence, as we shall show later in greater detail, the radiationless decay rates in which we are interested in good approximation may simply be assumed equal to the total decay rates observed in experiment.

The probability of radiationless singlet  $\leftrightarrow$  triplet transitions is known to be critically dependent on the spin-orbit coupling scheme and on vibronic coupling. In our experiments we determine the rate constants for the populating and decay of the individual spin levels of the phosphorescent state; from a comparison of these rates for the seven molecules we then get information on how changes in the two kinds of coupling affect the radiationless processes. By substituting one or two nitrogen atoms at the mesoposition(s) one alters the spin-orbit coupling in a specific manner, while the replacement of hydrogen by deuterium leads to changes in the vibrational modes that give rise to the well-known "deuterium effect" in the radiationless transition probabilities [2]. Furthermore, to illustrate the influence a change of host may have, we compare our results for anthracene in a single

crystal of biphenyl with data from the literature on anthracene in fluorene [3] and phenazine [4] and on anthracene X-traps [5].

The experiments have been carried out by the microwave induced delayed phosphorescence (MIDP) method [22] that has recently been described in detail [6,7] and which turns out to be particularly appropriate for the study of the present molecules for two reasons. First, because of the high rates of radiationless decay, the lifetimes of the individual spin levels of the triplet state for all seven molecules are short relative to spin-lattice relaxation at the temperature of the experiments, 1.2 K. Hence, the "isolation" condition of [6] proves to be rigorously fulfilled: when a steady-state population is first established over the three spin levels by irradiating the crystals for a period of a few seconds and the light is then shut off, the individual levels decay independently of one another.

The second reason is that a single spin level,  $T_x$  in fig. 1, will prove to carry nearly all ( $\approx 95\%$ ) of the radiative activity. This is a consequence of the orbital symmetry of the  $\pi\pi^*$  triplet state concerned ( $B_{2u}$  in  $D_{2h}$ ) and

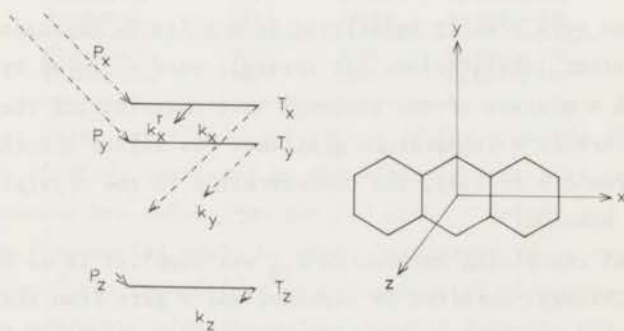


Fig. 1. Choice of axes in the three ring aromatics.

Anthracene serves as an illustration. The same coordinate frame and ordering of levels has been employed for the other molecules. The populating and decay rates  $P_u$  and  $k_u$  ( $u = x, y, z$ ) of the lowest triplet state are indicated. The length of the arrows measures the relative rate constants as observed for A-h<sub>10</sub> in biphenyl, see table 2. Radiative decay is of minor importance (section 4.1); only  $T_x$  carries some oscillator strength, symbolically represented by the full arrow originating from  $T_x$ .

the particular spin-orbit coupling route by which it interacts with  $\pi^*$  or  $\pi\sigma^*$  singlet states. Or, one may also look at it in another way: because of the high symmetry of our molecules ( $C_{2v}$  or  $D_{2h}$ ) the principal axes of the zero-field splitting must coincide with the molecular axes as in fig. 1 and from group theory it then follows that the out-of-plane polarized phosphorescence characteristic for  $\pi\pi^*$  triplet states can originate from a single spin component only [8]. The particular ordering and labelling of the states in fig. 1 has been taken from previous ESR studies by Grivet and Lhoste [1], it is different from the convention used in [9].

The molecules were chosen because of the predominance of radiationless decay, and as a result their phosphorescence is weak. The present experiments provide an example how with the aid of signal averaging the kinetics of populating and decay of a triplet state can be unravelled with the MIDP method, even for a very weakly phosphorescent molecule such as anthracene.

## 2. SAMPLES AND EQUIPMENT

### 2.1 The crystals

The present work greatly benefitted from gifts of crystals by several colleagues in other laboratories. All crystals were prepared by the Bridgman method in which a mixture of the biphenyl host material and the guest is very slowly passed through a temperature gradient. The solute concentration in the melts varied from 0.5 to 1.9%, the concentration in the crystals used in our experiments is unknown.

The crystal containing anthracene- $d_{10}$  was supplied to us by Dr. H.C. Brenner from Chicago. Acridine in biphenyl was a gift from the Koninklijke/Shell Laboratorium, Amsterdam. The biphenyl crystals doped with the phenazine isomers and the partially deuterated anthracene were gifts from Drs. J.M. Lhoste and J.Ph. Grivet in Paris.

The crystals anthracene in biphenyl and perdeutero-acridine in biphenyl were grown here by Mr. M. Noort: Both anthracene and acridine- $d_9$  were prepared by vacuum sublimation from commercial samples (Fluka scintill. grade, and Merck, Sharp and Dohme, respectively). Biphenyl (Fluka) was submitted to multiple zone refining. The crystals were grown from mixtures that contained 1.9% anthracene, or 0.8% acridine- $d_9$ .

## 2.2 The equipment

The experimental arrangement is similar to that given before, see fig. 3 of [6]. The crystal, which is mounted against a  $\phi = 5$  mm quartz light pipe and immersed in liquid helium, is surrounded by a helix that acts as the microwave resonator. Light from a Philips water-cooled SP 1000 W high-pressure mercury arc is focused on the sample via a  $\text{CuSO}_4$  solution filter and a UG-5 Heraeus-Schott glass filter. The phosphorescence, which passes through the light pipe and a suitable interference filter (see table 1) is detected with a Peltier-cooled photomultiplier, EMI type 9558 A. The MIDP signal is either directly recorded on a storage oscilloscope, or accumulated in a Hewlett Packard 5480 A signal analyzer.

	Zero-field splitting		Detection filter(s)
	$\nu_{x-y}$ MHz	$\nu_{x-z}$ MHz	
Anthracene- $h_{10}$	506	2396	RG 665
Anthracene- $h_2d_8$	506	2396	hp 650
Anthracene- $d_{10}$	506	2396	hp 650
Acridine- $h_9$	531.7	2491.2	hp 650/lp 650
Acridine- $d_9$	523.1	2468.8	hp 650/lp 750
Phenazine- $h_8$	666.9	2586	hp 600/lp 750
Phenazine- $d_8$	668.7	2580.7	hp 600/lp 750

Table 1. Triplet state zero-field splittings of the aromatic three-ring molecules studied, expressed as transition frequencies in MHz. The data for anthracene are taken from the ESR work of Grivet and Lhoste [1]. The other frequencies could be directly determined by optical detection of the zero-field transitions as a function of microwave frequency [?] and agree perfectly with the values derived from the ESR experiments [1]. In the last column we have indicated the filters used in the detection: RG 665 is an optical glass filter of Schott (Mains), all others are variable bandpass filters of Optics Technology, hp stands for high pass, lp stands for low pass.

## 3. THE EXPERIMENTS AND THEIR ANALYSIS

Let us briefly review the MIDP technique for the present, relatively simple situation where the one level  $T_x$  carries almost the entire radiative activity and the experimental conditions can be so chosen that spin-lattice relaxation is negligible.

The sample is first illuminated by UV light for some time at about 1.2 K until a stationary distribution of the excited molecules over the three spin levels of the lowest triplet state is established. At a time  $t = 0$  the illumination is terminated and the subsequent phosphorescence decay displayed on the oscilloscope, see fig. 2. The signal one initially observes is almost entirely due to the rapid decay of the radiative level with a rate  $k_x$ . At a time  $t_1$ , chosen long compared with the lifetime  $k_x^{-1}$  of  $T_x$ , one suddenly sweeps through the  $T_x - T_z$  transition, for instance. This causes a repopulation of the, by this time almost empty, radiative level  $T_x$  from the more slowly decaying "dark" level  $T_z$ , and an increase in phosphorescence intensity results.

By analyzing the height and decay of such "delayed signals" one can unravel the dynamics of populating and decay of the triplet state. That is, besides the *absolute* decay rates  $k_u$  one can determine the *relative* value of the radiative decay rates  $k_u^r$ , steady-state populations  $N_u(0)$  and populating rates  $P_u$  ( $u = x, y, z$ ). This analysis for the details of which we refer to [6],

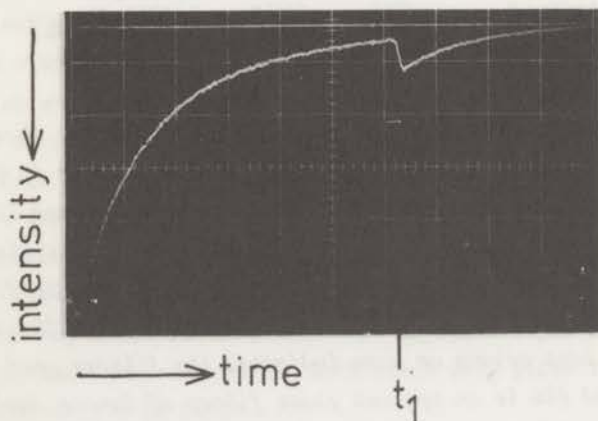


Fig. 2. Phosphorescence decay of  $Ac-h_0$  in biphenyl with a MDP signal appearing after a resonant microwave sweep through the  $T_x - T_z$  transition at the delay time  $t_1 = 61$  ms. One sees that the induced signal corresponds to an increase of the emission intensity, indicating that molecules are carried from the populated non-radiative level  $T_z$  to the radiative level  $T_x$  by the microwave field. The microwave frequency is swept at a rate of 10 MHz per ms. Temperature of He-bath 1.2 K, Horizontal 10 ms/div.

starts from a simple expression for the height  $h_{x-z}(t_1)$  of the delayed signal produced by sweeping the frequency of the microwave oscillator through the  $T_x - T_z$  transition, at the delay time  $t_1$  (formula (5) of [6])

$$h_{x-z}(t_1) = c f_{x-z} (N_z(t_1) - N_x(t_1)) (k_x^r - k_z^r) . \quad (1)$$

Here  $c$  is an instrumental constant and  $f_{x-z}$  the "microwave transfer factor", which is the fraction of the population difference between  $T_z$  and  $T_x$  transferred by the microwaves and which has to be determined for the existing experimental conditions, see section (3.2) of [6]. Without resonant microwaves  $f = 0$ , for saturation  $f = 0.5$ , but because of the possibility of population inversion [7,10] values between 0.5 and 1 may also occur.

### 3.1 The absolute decay rates and relative radiative rates

Since by definition

$$N_u(t_1) = N_u(0) \exp [-k_u t_1] \quad (2)$$

one has for sufficiently long delay times  $t_1 \gg k_x^{-1}$ , where the term  $N_x(t_1)$  in (1) becomes negligible,

$$h_{x-z}(t_1) = c f_{x-z} N_z(0) \exp [-k_z t_1] (k_x^r - k_z^r) . \quad (3)$$

Hence the slope  $k_z$  of a semi-logarithmic plot of  $h_{x-z}(t_1)$  versus  $t_1$  equals the rate  $k_z$ . This is shown in fig. 3a, where the curved part in the beginning corresponds to delay times that are not long compared with  $k_x^{-1}$  and where the active level  $T_x$  therefore is not yet empty when the sweep occurs (fig. 3b will be discussed with the temperature effect in section 3.3). The rate  $k_y$  of the other dark level is found from similar experiments in which the fast decaying level is now repopulated by hitting the  $T_x - T_y$  transition.

The decay rate  $k_x$  of the active level and the relative radiative rates were obtained from an analysis of the induced signal, as in section 3.1 and 3.3 of [6]. For instance, it is not difficult to see that apart from some small corrections the tail of the induced signal decays as  $\exp [-k_x(t-t_1)]$  and thus yields  $k_x$ .

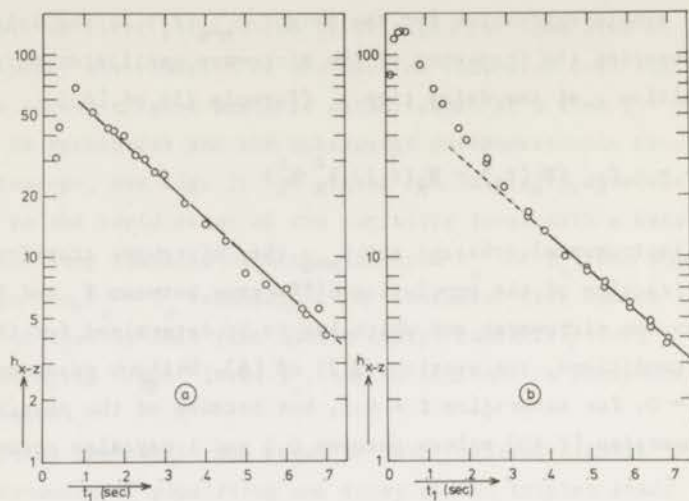


Fig. 3. A semilogarithmic plot of the height of the MIDP signal  $h_{x-z}(t_1)$  at different delay times  $t_1$  for  $Ac-h_9$  in biphenyl;  $T_{bath} = 1.2$  K.

a) Heights observed for low level excitation during a period  $\gg k_z^{-1}$ . The slope of the straight line for  $t_1 > 70$  ms yields  $\kappa_z = 4.0$  ( $\sigma = 0.3$ )  $s^{-1}$ , because of the isolation of the levels (cf. fig. 4),  $\kappa_z$  is equal to the true decay rate  $k_z$ . For delay times  $t_1 < 70$  ms the induced signals are smaller because  $T_x$  still carries a population. For  $t_1 = 0$  the signal becomes negative, demonstrating that in steady-state  $T_z$  is underpopulated relative to  $T_x$  (cf. table 2).

b) The results of MIDP experiments performed after intense irradiation. The intensity of the steady-state phosphorescence is approximately 150 times higher than in case a. Up to  $t_1 = 350$  ms the decay of  $T_z$  clearly does not follow a single exponential. In this region the decay is enhanced because of spin-lattice relaxation caused by the temperature effect of section 3.3. For delay times  $t_1 > 350$  ms the temperature of the sample apparently has dropped sufficiently for the observed decay rate again to be equal to  $k_z = 4.3$  ( $\sigma = 0.5$ )  $s^{-1}$ .

As in [6] we checked in every case whether the isolation condition was fulfilled by doing additional experiments at temperatures higher than 1.2 K. An example is shown in fig. 4 where for the system  $P-d_8$  in biphenyl the apparent decay rates  $\kappa_y$  and  $\kappa_z$ , as derived from a semi-logarithmic plot such as fig. 3a, are plotted against temperature. At temperature above 1.5 K  $\kappa_y$  and  $\kappa_z$  start to increase because the "dark" levels  $T_y$  and  $T_z$  now also begin



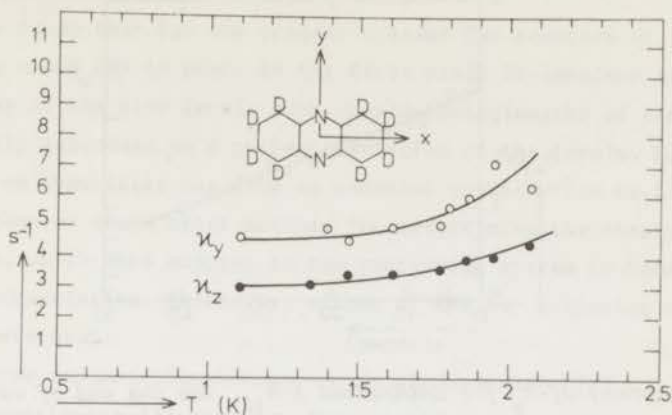


Fig. 4. The apparent decay rates  $\kappa_y$  and  $\kappa_z$  of  $P-d_8$  in biphenyl as a function of bath temperature. The MIDP experiments are performed in phosphorescence decay following low level excitation (fig. 3a). From the temperature independent behaviour of  $\kappa_u$  at lower temperatures one concludes that the isolation condition is fulfilled [6] and that the apparent rates  $\kappa_u$  are equal to the true decay rates  $k_u$ .

to decay through the active level  $T_x$  via spin-lattice relaxation (i.e. spinre-orientation no longer is slow with respect to  $k_y$  and  $k_z$  [6]). As before, the idea that at 1.2 K the values observed for  $\kappa_y$  and  $\kappa_z$  are equal to the true rate constants,  $k_y$  and  $k_z$ , tacitly involves the assumption that there is no appreciable temperature independent contribution to the spin relaxation.

A special situation arises for the three anthracene isomers, where the  $T_y$  level, although hardly radiative, has a decay rate comparable to that of the active level  $T_x$ . (This is quite analogous to what has been found for naphthalene [3], for instance, and we shall return to this point later). Whenever  $t_1 \gg k_x^{-1}$ , e.g. at  $t_1 = 150$  ms for  $A-h_{10}$ , not only  $T_x$  is practically empty, but also  $T_y$  and therefore no delayed signal is observed when sweeping through the transition  $T_x - T_y$ . However, since at  $t_1 = 150$  ms  $T_z$  still carries a substantial population one can first repopulate the  $T_y$  level by sweeping through the  $T_y - T_z$  transition at the time  $t_1$ . The population thus established in  $T_y$  will decay as  $\exp[-k_y \Delta t]$ , where  $\Delta t = t - t_1$ . This decay can be monitored by a second sweep, now through the  $T_x - T_y$  transition, which results in an induced signal. By analyzing the height of this delayed signal as a function of  $\Delta t$  for fixed  $t_1$  one obtains  $k_y$ , see fig. 5.

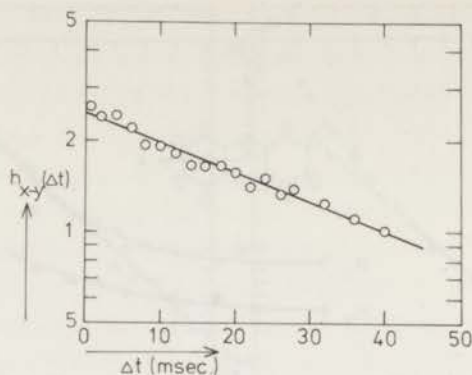


Fig. 5. Measurement of  $k_y$  for anthracene  $A-h_{10}$ . See the end of section 3.1 for an explanation.

### 3.2 Steady-state populations and populating rates

At sufficiently low temperature the spin levels behave independently and their populations are governed by the equations

$$\frac{dN_u}{dt} = P_u - k_u N_u \quad (u = x, y, z) . \quad (4)$$

For the present experiments the three equations for  $u = x, y, z$  are uncoupled. It may be mentioned in passing, however, that this is not always true. Under conditions of intense optical pumping an appreciable depletion of the ground state may occur [11] and then the terms  $P_u$  in (4) have to be replaced by  $P_u N_g$ . Here  $N_g$  is the relative population of the ground state and since  $N_g = 1 - \sum_u N_u$  this introduces coupling into the set (4).

Once the absolute decay rates  $k_u$  and the relative  $k_u^r$  have been obtained the relative values of the steady-state populations  $N_u(0)$  can be determined. Previously (section 3.4 of [6]) this was done by solving the ratio  $N_x(0) : N_y(0) : N_z(0)$  from the two equations (3) for  $h_{x-z}(t_1)$  and  $h_{x-y}(t_1)$  together with that for the total phosphorescence intensity,

$$I(0) = c \sum_u N_u(0) k_u^r . \quad (5)$$

In practice this procedure amounts to an extrapolation of the straight parts of the semi-logarithmic plots of  $h_{x-z}$  and  $h_{x-y}$  versus  $t_1$  back to  $t_1 = 0$  (see fig. 3a) and a subsequent comparison of the intercepts with the total

phosphorescence intensity.

It was found that for the present systems the accuracy of this method of determining the  $N_u(0)$  is poor. In the first place it involves extrapolations of the decay of the slow levels over considerable lengths of time and thus it is critically dependent on a perfect isolation of the levels. Further, emission from impurities may give an unwanted contribution to  $I(0)$ . To avoid these problems we chose other methods for determining the steady-state populations, which were adapted to the particular system in hand and avoided lengthy extrapolation. Basically, either of the two following types of procedure were used:

(i) *Microwave induced phosphorescence in steady-state* [12]

Under continuous illumination two experiments are done in which the microwaves are swept through the  $T_x - T_y$  and  $T_x - T_z$  resonances and the resulting changes in intensity are observed. These changes  $h_{x-y}(0)$  and  $h_{x-z}(0)$  must obey two equations identical to (1) for  $t_1 = 0$ ; together with a measurement of the total phosphorescence (5) one then has three equations from which the ratio  $N_x(0) : N_y(0) : N_z(0)$  can be solved.

(ii) *MIDP experiments with a very short delay time*

If  $t_1$  is chosen short relative to the lifetimes of the slowly decaying levels, i.e.  $t_1 \ll k_y^{-1}, k_z^{-1}$ , one may rewrite (1) as

$$h_{x-u}(t_1) = c f \{ N_u(0) - N_x(0) \exp(-k_x t_1) \} (k_x^r - k_u^r) \quad (6)$$

One can now solve the steady-state populations from the two equations (6) for  $u = y, z$  and that for the total phosphorescence intensity (5). An attractive alternative is to do two sets of experiments with two different delay times  $t_1$  and  $t_2$  which both are short relative to  $k_y^{-1}, k_z^{-1}$ . From the ratio  $h_{x-u}(t_2)/h_{x-u}(t_1)$  one then can directly obtain the relative population  $N_u(0)/N_x(0)$  with the aid of (6), without taking recourse to a measurement of the total phosphorescence intensity  $I(0)$ . The latter method is to be preferred whenever the phosphorescence is very weak and contaminated with impurity emission, as for anthracene. All the signals one uses for the determination of the populations now are induced by the resonant microwaves and one does not "see" the emission from non-resonant impurities.

The relative populating rates  $P_z : P_y : P_x$  are determined from the absolute rates  $k_u$  and the ratio  $N_z(0) : N_y(0) : N_x(0)$ , via the steady-state conditions  $dN_u/dt = 0$  in (4).

### 3.3 The temperature effect

Finally, a complication has to be considered. Although the specimen is in contact with superfluid helium, it was found that internal heating affects the measurements when these are carried out at a high level of excitation. This is not too surprising: of the energy absorbed to excite our molecules from  $S_0$  to  $S_1$ , a small fraction of at most a few percent is re-emitted as light and the bulk is dissipated as thermal energy in the specimen.

The experimental evidence for this is of several kinds. First, when using method (i) of section 3.2 for determining the steady-state populations, we found that the height of the microwave induced signals depends on the intensity of the incident light. As an example we show in fig. 6 some results of experiments for  $P-d_8$  where the incident light intensity was stepwise reduced by a diaphragm. In this figure the heights of the induced signals  $h_{x-z}(0)$  and  $h_{x-y}(0)$  relative to the total phosphorescence intensity  $I(0)$  are plotted as a function of  $I(0)$ . Since the intensity of excitation only enters into our equations via the constant  $c$ , it follows by dividing (6) by (5) that the quantity  $h_{x-u}(0)/I(0)$  must be independent of  $I(0)$ . Experimentally it is found that this is not true. At high levels of excitation the ratios  $|h_{x-z}(0)/I(0)|$  and  $|h_{x-y}(0)/I(0)|$  decrease, because relaxation processes set in that tend to decrease the population differences created by the optical pumping cycle.

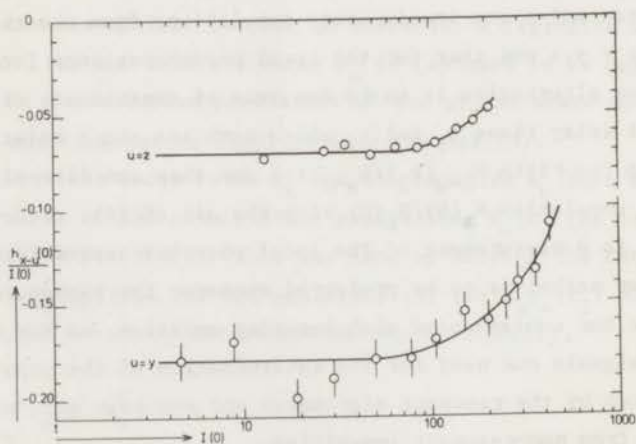


Fig. 6. The relative steady-state signal  $h_{x-u}(0)/I(0)$  as a function of the steady-state phosphorescence intensity  $I(0)$  for  $P-d_8$  in biphenyl.

A second manifestation of the temperature effect is illustrated in fig. 3a, b. In these figures we have plotted the height of the MDP signal  $h_{x-z}(t_1)$  versus the delay time  $t_1$  for  $\text{Ac-h}_9$  at two quite different levels of excitation. The curve of fig. 3b refers to excitation at maximum intensity, whereas that of fig. 3a is observed when the excitation is so far reduced that the phosphorescence intensity has dropped to 0.66% of its original value. The experiment of fig. 3a is the proper one, with a slope of the straight part that yields  $\tau_z = k_z^{-1} = 230$  ( $\sigma = 30$ ) ms. With the intense excitation of fig. 3b one finds a pronounced curvature of the plot up to a delay time of 350 ms; the final part is approximately straight with a slope that agrees with that of fig. 3a to within the experimental error ( $\tau_z = 260$  ( $\sigma = 20$ ) ms). Intense excitation apparently causes a departure from thermal equilibrium inside the crystal that is serious enough to cause relaxation to become non-negligible. After shutting off the light, the lattice cools down and relaxation comes to an effective stop.

Similar observations have been made by us in other photo-excited systems. For instance, we are currently investigating spin-lattice relaxation in the triplet state of phenanthrene in a biphenyl crystal. Here the heights of the signals induced by sweeping through a microwave transition under continuous illumination of the sample make a jump at the  $\lambda$  point of helium (2.2 K) if the level of excitation is high; clearly below 2.2 K the cooling by the bath is far more effective than at higher temperature.

The temperature effect is caused by the limited heat conductivity of the lattice of the host crystal, via which most of the incident energy has to be transported to the helium bath. If the incident energy is too high a rise in temperature inside the crystal results which is sufficient for spin-reorientation to set in and the isolation of the levels, on which the kinetic analysis rests, is destroyed. When doing experiments of the present kind it is very important to check that the lifetimes of the long-lived levels (and hence the steady-state populations) are not affected by relaxation effects caused through local heating. In the present work all experiments were performed at the minimum level of excitation permitted by the detection system and it was verified that the results did not change when varying the (low) intensity of excitation by a factor of 2 or 3.

Difficulties due to temperature rises caused by energy degradation within the sample, are known from other experiments, for instance from the spin-lattice relaxation studies by Rieckhoff and Griffiths on neodymium ethylsulfate [13].

	Anthracene in biphenyl			Acridine in biphenyl		Phenazine in biphenyl	
	A-h <sub>10</sub>	A-h <sub>8</sub> d <sub>8</sub>	A-d <sub>10</sub>	Ac-h <sub>8</sub>	Ac-d <sub>8</sub>	P-h <sub>8</sub>	P-d <sub>8</sub>
[msec] $\tau_x$	23.3	45	85	11.2	32.5	5.0	10.9
$\tau_y$	40.6	89	119	130	400	72	185
$\tau_z$	205	477	715	250	600	135	275
[s <sup>-1</sup> ] $k_x$	42.5 (2.2)	22.3 (1)	11.8 (1)	89 (2)	30.8 (0.5)	200 (4)	91.5 (3)
$k_y$	24 (2.2)	11.2 (1.2)	8.4 (0.6)	7.7 (0.6)	2.5 (0.3)	14 (1)	5.4 (0.2)
$k_z$	4.9 (0.9)	2.1 (0.11)	1.4 (0.1)	4 (0.2)	1.5 (0.3)	7.5 (0.3)	3.65 (0.15)
$k_x^r$	1	1	1	1	1	1	1
$k_y^r$	≤ 0.03	0.04	≤ 0.02	≥ 0.04	0.04 (0.02)	0.02 (0.002)	≤ 0.02
$k_z^r$	≤ 0.03	0.04	≤ 0.02	≥ 0.04	0.025 (0.005)	0.02 (0.002)	0.02 (0.003)
$P_x$	1	1	1	1	1	1	1
$P_y$	1.4 (0.7)	0.45 (0.1)	2 (0.4)	0.054 (0.005)	0.064 (0.008)	0.011 (0.007)	0.035 (0.004)
$P_z$	0.14 (0.03)	0.090 (0.007)	0.12 (0.02)	0.053 (0.003)	0.04 (0.008)	0.028 (0.004)	0.034 (0.002)
$N_x(0)$	1	1	1	1	1	1	1
$N_y(0)$	0.8 (0.4)	0.87 (0.1)	2.8 (0.4)	0.62 (0.02)	0.78 (0.03)	0.16 (0.1)	0.59 (0.05)
$N_z(0)$	1.2 (0.1)	0.95 (0.05)	1.05 (0.1)	0.78 (0.02)	0.80 (0.04)	0.67 (0.1)	0.86 (0.01)

## 4. RESULTS

In table 2 the results of our experiments are summarized. Previously [9] we applied the MIDP method to P-h<sub>8</sub> as a guest in a biphenyl crystal. The numbers for this system given in table 2 differ slightly from those of [9], since at the time we did not realize that our experiments were affected by the temperature effect described in section 3.3.

In this section we indicate a few striking aspects of the data presented in table 2. We further compare our results with some quantitative statements derived from theory and also with experimental results of other workers. Some general conclusions that may be drawn from our work are given in section 5.

### 4.1 The dominance of radiationless $T_0 \rightarrow S_0$ decay over the phosphorescence emission

For all molecules of this study one may assume  $k_u^d \gg k_u^r$ , so that to a good approximation  $k_u = k_u^d$ . This assumption is based on two arguments. First of all it is well known that for anthracene the quantum yield of phosphorescence is very low relative to the rate of intersystem crossing. For instance, from the data reported by Langelaar et al. [14] on phosphorescent anthracene in an ethanol glass at 77 K it follows that radiationless decay from  $T_0$  exceeds the radiative decay by a factor of about 4000. Or, when defining the mean decay rates  $k = 1/3 \sum k_u$  and  $k^r = 1/3 \sum k_u^r$ , one thus has for anthracene  $k^r/k^d = 2.5 \cdot 10^{-4}$ . We see from table 2 that the probability for radiative decay is highest for  $T_x$ , hence we have  $k_u^r/k_u^d \approx 5 \cdot 10^{-4}$  for  $u = x$

Table 2. Lifetimes  $\tau_u$  in ms, decay rates  $k_u = \tau_u^{-1}$  in  $s^{-1}$ , relative radiative decay rates  $k_u^r$ , relative populating rates  $P_u$  and relative steady-state populations  $N_u(0)$  of the three spin components  $T_u$ ,  $u = x, y, z$  as measured at about 1.2 K. All values are averages of at least three measurements, mostly performed on two or more different samples cut from the same crystal. The numbers in parentheses denote the standard deviation of the mean. Limiting numbers are derived from signal to noise ratios.

The values of the  $P_u$ , derived from the ratio  $N_u(0)/k_u$ , are the least reliable and the striking variation of  $P_y$  over the three anthracene isomers may not be significant. All that may be said with confidence is that  $P_x$  and  $P_y$  have nearly equal values, an order of magnitude larger than  $P_z$ .

and considerably lower values for  $u = y, z$ .

Secondly a detailed analysis of spin-orbit coupling has been made for naphthalene [15,16] and quinoxaline [15], and quantum yields have been determined for these molecules [14,17]. Although one may question the value of the spin-orbit coupling calculations as regards the a-priori estimate of radiative lifetimes, they seem to provide an acceptable basis for comparing anthracene with naphthalene, and phenazine with quinoxaline. With the aid of the expressions given in [15] we find  $k_y^r$  (anthracene)  $\approx 0.1 k_x^r$  (naphthalene),  $k_x^r$  (phenazine)  $\approx 0.1 k_x^r$  (quinoxaline). (Note the change of axes system in quinoxaline compared with [15]). When further taking  $k_x^r$  (naphthalene)  $= 0.03 \text{ s}^{-1}$  [3,14] and  $k_x^r$  (quinoxaline)  $= 7.4 \text{ s}^{-1}$  [6,17] one arrives at the values  $k_x^r/k_x$  (anthracene)  $\approx 7 \cdot 10^{-5}$  and  $k_x^r/k_x$  (phenazine)  $= 3.7 \cdot 10^{-3}$ . Since it follows from table 2 that the relative radiative decay rates vary more strongly for the different spin levels than the total decay rates, the values of  $k_y^r/k_y$  and  $k_z^r/k_z$  must be even lower. The deuterium effect on  $k_u$  in anthracene and phenazine decreases  $k$  with a factor of 3.33 and 2.2 respectively, hence assuming that  $k_u^{r,u}$  is not influenced on deuteration one expects  $k_x^r/k_x$  (A-d<sub>10</sub>)  $= 2.3 \cdot 10^{-4}$  and  $k_x^r/k_x$  (P-d<sub>8</sub>)  $= 8.1 \cdot 10^{-3}$ .

It is reasonable to assume that acridine is intermediate between anthracene and phenazine. In conclusion we may thus state that for all molecules in this study  $k_u = k_u^d$  to within 1%. Therefore the values we obtained for the total decay rates of the individual spin levels of  $T_0$  can be directly compared with theories on spin-forbidden radiationless transitions.

That  $k_u^r/k_u$  has such low values for the three ring aromatics is due to the small energy separation between the states  $S_0$  and  $T_0$ : this causes the probability for radiative decay (which contains a factor  $\nu^3$ ) to be low and that for radiationless decay to be high (the "energy gap law" [18,26]).

#### 4.2 Comparison with predictions from theory

Siebrand and coworkers [2a,19] have recently proposed a scheme for calculating non-radiative rates to and from individual spin levels of phosphorescent triplet states of aromatic hydrocarbons. Their results and those of Metz [20], who uses a similar scheme, provide the only quantitative theoretical estimates that may be tested on our results.

##### (i) Aza-molecules

The populating and decay of  $T_0$  go dominantly via its  $T_x$  spin component.



This once again demonstrates the efficient spin-orbit coupling between  $\pi\pi^*$  and  $n\pi^*$  states in intersystem crossing processes in nitrogen-hetero aromatics. The mechanism - as stated before [21] - is simple:  $P_x$  results from direct spin-orbit coupling of  $T_x$  ( $^3\pi\pi^*$ ) with  $S_1$  ( $^1n\pi^*$ ).

(ii) Anthracene

a. Decay rates

There exists a qualitative agreement between theory and experiment, in the sense that populating and decay are relatively improbable via the bottom component, which reflects the circumstance that  $T_x$  and  $T_y$  are more contaminated with singlet character (effective SOC with intermediate  $^1(\pi\sigma^*)$  and  $^1(\sigma\pi^*)$  states) than  $T_z$  (weak SOC with  $^1(\pi\pi^*)$  states).

When making a comparison with the quantitative predictions that have been published one finds for the relative decay rates

	$k_x$	$k_y$	$k_z$
Exper. A-h <sub>10</sub> (table 2)	1	: 0.56 (0.06)	: 0.11 (0.02)
Siebrand et al. [23]	1	: 0.063	: 0.15
Metz [20] <sup>†</sup> )	1	: 0.2 - 0.5	: 0.04 - 0.15

The calculations correctly predict that  $k_z$  is substantially smaller than the sum  $k_x + k_y$  which, as noted, simply originates from a difference in efficiency of the spin-orbit coupling pathways.

Decay from  $T_x$  and  $T_y$  is attributed to the same "mechanism" in Siebrand's terminology and thus one might have hoped [23] the ratio  $k_y/k_x$  to be amenable to theoretical prediction with his model. The result of Metz et al. [20]<sup>†</sup>) are limits predicted for polyacenes in general; their specific predictions which have only been published for naphthalene are in good accord with experiment. In both sets of calculations [2a, 19, 20] the same approach by perturbation theory is used and the final results prove critically dependent on which terms one chooses to neglect.

b. Deuterium effects

A surprising conclusion that emerges from the present work is that we encounter a spin component *independent* deuterium effect for

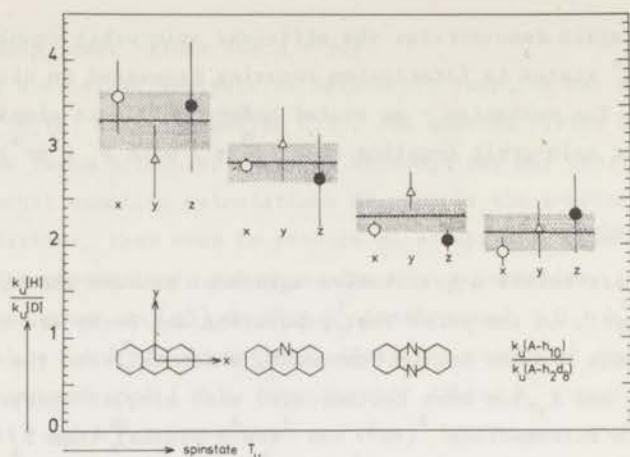


Fig. 7. The ratio of the decay rates of each of the spin levels  $T_u$  for pairs of isotopic isomers of the three-ring aromatics. H labels the protomolecule, D stands for the perdeutero compound. The vertical lines measure the standard deviations calculated with the aid of table 2. Each horizontal line is the average over the three spin components for a pair of isotopic isomers. The dotted area represents the error in this mean value.

the radiationless lifetimes. In fig. 7 we have plotted the ratio of the radiationless decay rate of spin level  $T_u$  ( $k_u[H]$ ) and its perdeutero isomer ( $k_u[D]$ ) for each molecule, and also a similar ratio for  $A-h_{10}$  and  $A-h_2d_8$ . From the picture one sees that the effect of deuteration on the radiationless decay rate of the individual spin states:

1. does not depend on the particular spin component to within experimental accuracy,
2. depends only on the molecule, i.e. on the average we observe  $k[H]/k[D]$  to be 3.3, 2.9 and 2.2 for anthracene, acridine and phenazine, respectively.

In a calculation of the  $k_u$  based on perturbation theory as first proposed by Siebrand [2a,19], and later used also by Metz [20], a deuterium effect arises in two manners. First there is an overall deuterium effect, which is the same for all three spin components and which is a consequence of the famous "energy gap law" [18,26]; it does not depend on detailed aspects of the radiationless transition

but merely on the energy difference between the triplet and ground electronic states (see section 5 below for further details and references). Secondly, one is led to expect an "additional deuterium effect" [2a,19,20] that varies for the three spin components and which is related to the properties of the particular promoting mode(s) thought to be involved in the decay from a given spin component. These predictions appear to be at variance with our present results, which indicate that for anthracene any spin specific deuterium effect can only be of a minor nature. When comparing the experimental data with the calculations one has

	$\frac{k_x[H]}{k_x[D]}$	$\frac{k_y[H]}{k_y[D]}$	$\frac{k_z[H]}{k_z[D]}$
Exp. (cf. fig. 7)	1	: 0.81 (0.12)	: 0.97 (0.21)
Siebrand et al. [23]	1	: 1	: 0.55
Metz et al. [20]	1	: 0.56	: 0.77

The results in the last line are for naphthalene but the authors [20] expect them to be typical for polyacenes in general<sup>†</sup>.

#### 4.3 Comparison with other experiments

So far the dynamics of  $T_0$  in aromatic hydrocarbons has been studied in greatest detail for anthracene. In table 3 we have summarized all known data. The numbers in the first column are from this research, the others are taken from the literature.  $k_x$  clearly shows a large host effect. It has the same value ( $43 \text{ s}^{-1}$ ) for anthracene diluted in biphenyl and fluorene crystals, while it increases via anthracene X-traps ( $64 \text{ s}^{-1}$ ) to a value twice as large ( $83 \text{ s}^{-1}$ ) for anthracene in a phenazine crystal.

The shortening of the lifetime of the top level in situations where the phosphorescent anthracene molecules have phenazine molecules as neighbours, is attributed to inter-molecular spin-orbit coupling. Because of the presence of the two meso-nitrogens the phenazine  $T_x$  component mixes to singlet states, and this results in a marked effect on populating [5] and decay of the corresponding anthracene spin state.

	Anthracene-h <sub>10</sub>			in phenazine
	in biphenyl	in fluorene	X-traps	
$k_x$ [s <sup>-1</sup> ]	42.5 (2.2)	44 (6)	64 (6)	83 (6)
$k_y$	24 (2.2)	23 (4)	24 (3)	28 (4)
$k_z$	4.9 (0.9)	2 (2)	5 (3)	8 (0.6)

	Anthracene-d <sub>10</sub>		
$k_x$ [s <sup>-1</sup> ]	11.8 (1)	11 (1.5)	24
$k_y$	8.4 (0.6)	11 (1)	11
$k_z$	1.4 (0.1)	0.6 (0.6)	3.8

Table 3. Decay rates  $k_u$  of the three spin states of  $T_0$  for A-h<sub>10</sub> and A-d<sub>10</sub> in different hosts. The data in the first column are taken from table 2 and those in the other columns from the literature: Sixl studied anthracene in fluorene [3,5] and as "X-traps", which occurs when an anthracene crystal is doped with phenazine [5], Clarke studied the anthracene isomers in a phenazine host-crystal [4]<sup>(+)</sup>.

One gets the impression that  $k_z$  also depends on the host, but one has to remember that the decay rate of the long-lived level  $T_z$  is most susceptible to experimental error and it is not known whether isolation of the levels was attained in the experiments in a phenazine host [4]. The numbers in the last column of table 4 have been used to conclude to a deuterium effect in anthracene that varies significantly over the three spin components [19]. This conclusion is not supported by our experiments of the three ring aromatics in biphenyl and Clarke's findings may have been influenced by the phenazine host and (or) imperfect isolation<sup>(+)</sup>.

	Anthracene		
	in biphenyl	in fluorene	in phenazine
$k_x$ [H]/ $k_x$ [D]	3.6 (0.4)	4 (1)	3.48
$k_y$ [H]/ $k_y$ [D]	2.9 (0.4)	2.1 (0.6)	2.71
$k_z$ [H]/ $k_z$ [D]	3.5 (0.7)	3.3 (3.3)	2.09
Average	3.3	3.1	2.76

Table 4. The effect of deuterium substitution on the decay rates of the separate spin components of the phosphorescent triplet state of anthracene as a guest in different hosts. The data are derived from those of table 3 (cf. fig. 7).

#### 4.4 The effect of aza substitution on $k_y$ and $k_z$

We have seen that aza substitution in the 9 (and 10) position leads to a marked and understandable increase in  $k_x$ . But in addition it has a striking effect on the behaviour of the ratio  $k_y/k_z$ . In anthracene  $k_y/k_z = 5$ , while in acridine and phenazine this ratio has decreased to about 2. A similar effect is even more pronounced for the populating rates:  $P_y/P_z$  drops by an order of magnitude when anthracene is compared with acridine, where it becomes unity, see fig. 8. In the two-ring aromatics  $k_y/k_z$  also decreases in going from the hydrocarbon to the aza-derivatives, see fig. 9.

Another outstanding fact deserves attention, namely both  $k_y$  and  $k_z$  increase by a factor of about 2 in going from the mono-aza compound (acridine or quinoline) to the di-aza compound (phenazine or quinoxaline), see table 5.

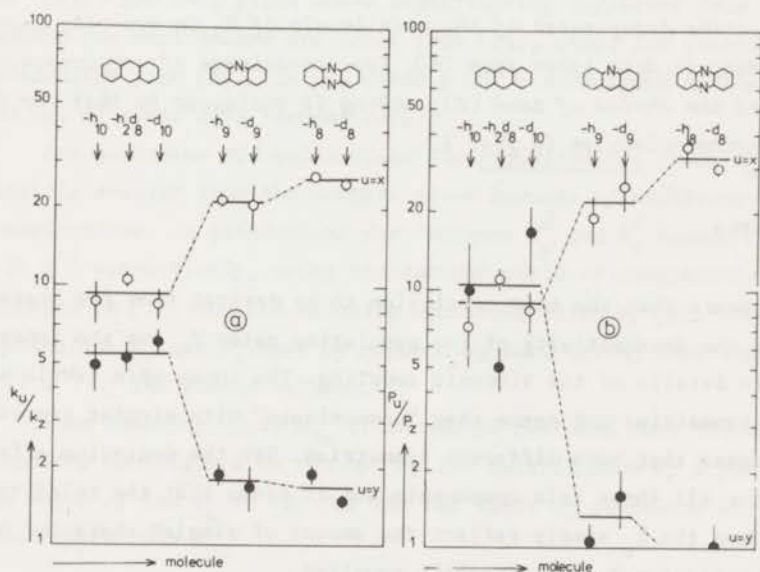


Fig. 8. Relative radiationless intersystem crossing rates for the lowest triplet state of the different three-ring aromatics.

a) relative decay rates  $k_x/k_z$  (open circles) and  $k_y/k_z$  (black dots),  
 b) relative populating rates  $P_x/P_z$  (open circles) and  $P_y/P_z$  (black dots).

Note that we here normalize to  $k_z$  and  $P_z$ , as opposed to table 2 where we chose  $P_x = 1$ .

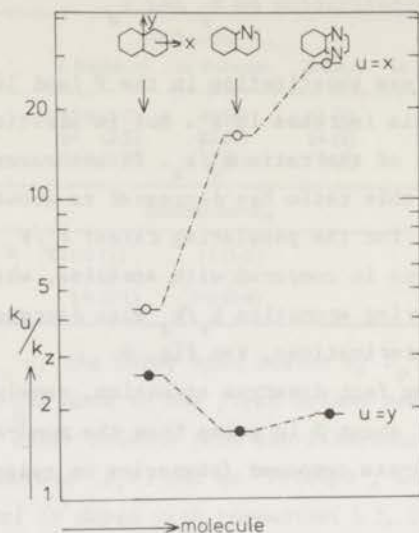


Fig. 9. Relative decay rates of the spin levels of  $T_0$  in two-ring aromatics according to data taken from [6]. For convenience of comparison we changed the choice of axes [6], making it analogous to that for the three-ring molecules in fig. 1.

## 5. CONCLUSION

It appears that the main conclusion to be derived from the present results is the insensitivity of the populating rates  $P_u$  and the decay rates  $k_u$  relative to details of the vibronic coupling. The three spin levels have different symmetries and hence they "communicate" with singlet states via inducing modes that have different symmetries. Yet the deuterium effect is the same for all three spin components and it seems that the relative values of the  $P_u$  and the  $k_u$  simply reflect the amount of singlet character mixed into the particular  $T_u$  by spin-orbit coupling.

The bottom level  $T_z$  is inactive in populating and decay because in a first approximation it can only couple very weakly to  $\pi\pi^*$  singlet states [2a,19,20]<sup>(o)</sup>. In anthracene the ratio  $k_x/k_y$  roughly reflects the relative amounts of singlet contamination of  $T_x$  and  $T_y$  acquired by spin-orbit coupling with  $1\sigma\pi^*$  and  $1\pi\sigma^*$  states [15]. Unfortunately, the data on the  $P_u$  for anthracene are of very poor accuracy because of its very weak phosphorescence; an accurate knowledge of the populating rates should be quite valuable. On

<i>u</i>	$k_u(\text{A-h}_{10})\text{s}^{-1}$	$M_{1,u}$	$k_u(\text{Ac-h}_9)\text{s}^{-1}$	$M_{2,u}$	$k_u(\text{P-h}_8)\text{s}^{-1}$
<i>y</i>	24	0.31 (0.04)	7.7	1.8 (0.1)	14
<i>z</i>	4.9		4	1.9 (0.1)	7.5
	$k_u(\text{naphthalene})\text{s}^{-1}$		$k_u(\text{quinoline})\text{s}^{-1}$		$k_u(\text{quinoxaline})\text{s}^{-1}$
<i>y</i>	0.40		0.32	2.5 (0.2)	0.80
<i>z</i>	0.10		0.19	2.2 (0.1)	0.42

Table 5. Behaviour of  $k_y$  and  $k_z$  in aromatic two- and three-ring molecules on *aza*-substitution.

The intermediate columns in italics are ratios with their standard deviations:

$M_{1,u} = k_u(\text{mono-aza derivative})/k_u(\text{hydrocarbon})$ ,

$M_{2,u} = k_u(\text{di-azamolecule})/k_u(\text{mono-azamolecule})$ .

The ratios are only given where significantly different from unity. The numbers for naphthalene are taken from [24], those for quinoline and quinoxaline from [6]. (In all cases *y* and *z* correspond to the short - and out of plane axis respectively).

For quinoline and quinoxaline the radiationless rates  $k_u^d$  should be slightly smaller than the numbers given because of radiative contributions. In quinoxaline for instance  $k_y^d$  and  $k_z^d$  become 0.70 and 0.36  $\text{s}^{-1}$  respectively, using the quantum yield of phosphorescence reported in [17] and the relative radiative rates of [6]. (For naphthalene  $k_y$  and  $k_z$  must be reduced by subtracting less than 0.01  $\text{s}^{-1}$  of the stated values).

When thinking about  $M_{2u}$  it should be realized that the number of accepting oscillators is reduced by the substitution of N for C-H. Thus the ratio of the  $C_u$  in (9) for the two kinds of compounds should be even larger than  $M_{2u}$ .

- (o) It is valuable to point to an interesting result of Metz et al. [20]. In addition to the weak  $\pi\pi^*$  singlet character mixed into  $T_1$  via small three center spin-orbit coupling terms, they recognize the occurrence of one-center spin-orbit coupling contributions. These arise due to interaction between  $\sigma\pi$  or  $\pi\sigma^*$  states via higher order Herzberg-Teller expansion terms which were omitted by Siebrand. Such terms might also contribute to the explanation of some of the effects of section 4.4 and table 5. Then spin-orbit coupling between  $n\pi^*$  and  $\sigma\pi$  states might also contribute some singlet character to  $T_2$ , see chapter V.

aza-substitution in the meso-position(s) a new path for strong spin-orbit coupling is opened: the  $T_x$  level then couples to the first excited  $n\pi^*$  singlet state and this level becomes the preferred "door" of the triplet manifold for populating and decay [21]. The data on naphthalene [3], quinoline and quinoxaline [6], show a similar picture, and although less is known about benzene it does not seem to be an exception [25].

In terms of the recent theories on radiationless transitions (see e.g. [26] and [2] for references to the extensive literature) the above conclusion can be illustrated as follows. If one considers the radiationless decay from the component  $T_u$  of the lowest triplet state to the ground state  $S_o$  in the present polyatomic molecules at liquid helium temperature, then the rate of decay is given by

$$k_u = \frac{2\pi}{\hbar} C_u^2 \sum_v |S(T_{u,o}; S_{o,v})|^2 \delta(E_{T_{u,o}} - E_{S_{o,v}}) \quad (7)$$

Here we have chosen Englman and Jortner's formalism from the great many papers on this subject; see (1.10) of [26] with an obvious change in notation. In (7)  $C_u$  is a coupling matrix element and  $S(T_{u,o}; S_{o,v})$  the familiar Franck-Condon overlap integral between the vibrationless triplet component  $T_u$  and a vibrationally excited level of the ground state  $S_o$  with energy  $E_{S_{o,v}}$ ; the summation extends over a quasi-continuum of vibronic states coupled to  $T_u$ .

The precise form the coupling matrix element takes depends on the basis from which one starts and we shall not consider this problem in any detail. In the model of Englman and Jortner, (1.7 b) of [26],

$$C_u = \sum_{k \neq T_u, S_o} \sum_{\gamma} (K_{T_u \gamma}^k J_{\gamma S_o}^k + J_{T_u \gamma}^k K_{\gamma S_o}^k) \frac{(X_{T_o k}(Q_k, 0) \left| \frac{\delta}{\delta Q_k} \right| X_{S_o k}(Q_k, v_{S_o k}))}{(X_{T_o k}(Q_k, 0) X_{S_o k}(Q_k, v_{S_o k}))} \quad (8)$$

In this expression two types of electronic matrix elements appear which combine the electronic states  $T$  and  $S_o$  with intermediate states labelled with the index  $\gamma$ : the  $J$ 's for  $\frac{\delta u}{\delta Q}$  (from the kinetic energy operator) of the  $k^{\text{th}}$  normal mode and the  $K$ 's for the spin-orbit coupling. The function  $X_{S_o k}(Q_k, v_{S_o k})$  is a harmonic oscillator function for the  $k^{\text{th}}$  mode in the state  $S_o$  with  $v_{S_o k}$  quanta, for further details see [26]. (The extra overlap factor in the denominator has been introduced by us in order to bring the formalism of Englman and Jortner more closely in line with the expressions used by Siebrand et al. in their calculations).



Now Englman and Jortner have shown that the summation in (7) can be carried out to give the "energy gap law" [18,26] in the form

$$k_u = \frac{C_u^2 \sqrt{2\pi}}{h\sqrt{h\omega_m \Delta E}} \exp(-\gamma \Delta E/h\omega_m) \quad (9)$$

Here  $\Delta E$  is the energy separation between the electronic states  $T_u$  and  $S_0$ ,  $\omega_m$  the C-H (or C-D) stretching frequency, and  $\gamma$  a parameter that accounts for the displacement of the potential surfaces for the electronic states  $S_0$  and  $T_u$  and which is estimated to lie in the range 1.31 - 0.50 [26]. All that matters here is that the only term that varies for the different spin states is the coupling element  $C_u$ ; we have checked that this remains true when working in the basis used by Siebrand et al. [2a,19] who obtain  $C_u$  as a sum of many different terms by expanding their coupling element in a Herzberg-Teller series about  $Q_k = 0$ .

The overall deuterium effect arises because of the factor  $\omega_m^{-1/2} \times \exp(-\gamma \Delta E/h\omega_m)$  in (9). Further Siebrand et al. pointed out that one would expect an "additional deuterium effect" depending on  $u$  and originating from the integrals involving the promoting modes which cause the fraction on the right of (8) to become isotope dependent [2a,19,20]. This effect does not show up in the present experiments, so if it exists, it must be smaller than originally estimated by Siebrand [2a,19,23].

The pioneering calculations by Siebrand, Henry and others [2a,19,23] have shed a lot of light on the quantitative aspects of radiationless transitions involving the triplet state. In Siebrand's expressions, which are based on perturbation theory and a Herzberg-Teller expansion of the matrix elements, the factor  $C_u$  in (7) corresponds to the sum of a number of terms which are identified with "mechanisms" for radiationless transitions. Since the number of terms is large, and the distinction between the different kinds tricky [2a,19,20], it may be questionable whether they correspond to mechanisms in a physical sense. The data on the three- and two-ring (aza) aromatic molecules bear out a simplicity which one would like to see reflected in the theoretical description. Perhaps the realization by Metz et al. [20] that for all three levels it is the spin-orbit coupling to highly excited  $\sigma\pi^*$  and  $\pi\sigma^*$  states that is responsible for their decay is an important step forward.

(†) *Notes*

1. After the present manuscript was finished a further article by Metz (Chem. Phys. Lett. 1973, 22, 186) appeared on  $T_0 + S_0$  ISC rates in aromatic hydrocarbons. He there reports the results of specific calculations for anthracene, whereas the results [20] quoted in section 4.2 related to estimates for polyacenes in general. He finds for  $A-h_{10}$ :

$$k_x : k_y : k_z = 1 : 0.48 : 0.118$$

and for the deuterium effect:

$$\frac{k_x[H]}{k_x[D]} : \frac{k_y[H]}{k_y[D]} = 1 : 0.63 .$$

These numbers agree surprisingly well with our experimental results (see section 4.2 a and b):

$$k_x : k_y : k_z = 1 : 0.56 (0.06) : 0.11 (0.02)$$

and

$$\frac{k_x[H]}{k_x[D]} : \frac{k_y[H]}{k_y[D]} = 1 : 0.81(0.12) .$$

2. Dr. Clarke has kindly informed us that he has revised his previous values of the  $k_u$  of anthracene in a phenazine host (last column of table 4). His new values do not differ significantly from those here reported for anthracene in biphenyl.

*Acknowledgement*

We thank Drs. J.M. Lhoste and J.Ph. Grivet, Dr. H.C. Brenner and the Koninklijke/Shell Laboratorium, Amsterdam for their generosity in providing us with some of the crystals used in the present investigation. We are also grateful to Mr. M. Noort of our laboratories who prepared the mixed crystals of anthracene in biphenyl and perdeuteroacridine in biphenyl for us.

## REFERENCES

- [1] Grivet, J.Ph., and Lhoste, J.M., 1969, Chem. Phys. Lett., 3, 445.  
Grivet, J.Ph., 1969, Chem. Phys. Lett., 4, 104; *ibid.* 1971, 11, 267.  
Grivet, J.Ph., 1970, thesis, Paris.
- [2] Henry, B.R., and Siebrand, W., 1971, J. chem. Phys., 54, 1072. Schlag, E.W., Schneider, S., and Fischer, S.F., 1971, Ann. Rev. phys. Chem., 22, 465, with further references.
- [3] Sixl, H., 1971, thesis, University of Stuttgart.
- [4] Clarke, R.H., 1971, Chem. Phys. Lett., 12, 157.
- [5] Gromer, J., Sixl, H., and Wolf, H.C., 1972, Chem. Phys. Lett., 12, 574.
- [6] Schmidt, J., Antheunis, D.A., and van der Waals, J.H., 1971, Molec. Phys., 22, 1.
- [7] Schmidt, J., 1971, thesis, University of Leiden.
- [8] Van der Waals, J.H., and de Groot, M.S., 1967, The Triplet State, edited by A. Zahlan (Cambridge University Press), p. 101.
- [9] Antheunis, D.A., Schmidt, J., and van der Waals, J.H., 1970, Chem. Phys. Lett., 6, 255.
- [10] Harris, C.B., 1971, J. chem. Phys., 54, 972. Ref. [7], p. 83.
- [11] Schwoerer, M., and Sixl, H., 1969, Z. Naturforsch., A 24, 952.  
Van Dorp, W.G., Schaafsma, T.J., Soma, M., and van der Waals, J.H., 1973, Chem. Phys. Lett., 21, 221. Schweitzer, D., Zuclich, J., and Maki, A., 1973, Molec. Phys., 25, 193.
- [12] Winscom, C.J., and Maki, A.H., 1971, Chem. Phys. Lett., 12, 264.
- [13] Rieckhoff, K.E., and Griffiths, D.J., 1963, Can. J. Phys., 41, 33.
- [14] Langelaar, J., Rettschnick, R.P.H., and Hoytink, G.J., 1971, J. chem. Phys., 54, 1.
- [15] Veeman, W.S., and van der Waals, J.H., 1970, Molec. Phys., 18, 63.
- [16] Henry, B.R., and Siebrand, W., 1969, J. chem. Phys., 51, 2396.
- [17] Li, R., and Lim, E.C., 1972, J. chem. Phys., 57, 605.
- [18] Robinson, G.W., and Frosch, R.P., 1962, J. chem. Phys., 37, 1962; *ibid.*, 1963, 38, 1187.
- [19] Lawetz, V., Orlandi, G., and Siebrand, W., 1972, J. chem. Phys., 56, 4058.
- [20] Metz, F., Friedrich, S., and Hohlneicher, G., 1972, Chem. Phys. Lett., 16, 353.
- [21] De Groot, M.S., Hesselmann, I.A.M., Schmidt, J., and van der Waals, J.H.,

1968, Molec. Phys., 15, 17.

[22] Schmidt, J., Veeman, W.S., and van der Waals, J.H., 1969, Chem. Phys. Lett., 4, 341.

[23] Henry, B.R., and Siebrand, W., 1970, Chem. Phys. Lett., 7, 533.

[24] McClure, D.S., 1952, J. chem. Phys., 20, 682.

[25] Van Egmond, J., and van der Waals, J.H., 1973, Molec. Phys., 26, 1147.

[26] Englman, R., and Jortner, J., 1970, Molec. Phys., 18, 145.

(\*) This chapter has been submitted for publication in Molecular Physics by D. Antheunis, J. Schmidt and J.H. van der Waals.

## CHAPTER V

### THE DEPENDENCE ON SPIN STATE OF THE RATES FOR NON-RADIATIVE TRANSITIONS.

The preceding chapter is a published paper [1]. At the time we finished the manuscript we did not yet realize how Metz's conclusions on spin-orbit coupling (SOC) in relation to the radiationless decay rates of the three spin states of anthracene [2,3] might be extended in two directions: to include the populating rates and to take account of the effect of aza-substitution. In the present chapter we therefore give a further interpretation of the experimental results on the intersystem crossing (ISC) processes in the series of three-ring aromatic molecules of chapter IV.

We begin by drawing attention to the remarkable quantitative agreement between our experimental results and Metz's calculation on  $T_0^u \rightarrow S_0$  crossing in anthracene, as shown in the note added to the previous chapter. This not only holds for the absolute decay rates of the three levels, but also for the deuterium effect.

In this chapter we intend to show that by generalizing the ideas of Metz, it is possible to give a *qualitative* interpretation of the effect of aza-substitution on the relative radiationless rates of the three spin states. To facilitate the discussion we have rearranged some of the data of table 2 of chapter IV in table 1. The two most striking trends revealed by this table are:

- (i) Both  $k_x/k_y$  and  $k_z/k_y$  and also the corresponding ratios of the populating rates,  $P_x/P_y$  and  $P_z/P_y$ , increase on aza-substitution.
- (ii) The populating ratios show a sharper rise than the decay ratios, for instance

$$\frac{[P_x/P_y]_{\text{Acridine}}}{[P_x/P_y]_{\text{Anthracene}}} = 25 > 6 = \frac{[k_x/k_y]_{\text{Acridine}}}{[k_x/k_y]_{\text{Anthracene}}}$$

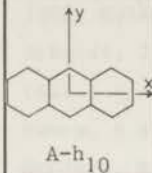
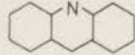
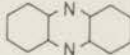
	 A-h <sub>10</sub>	 Ac-h <sub>9</sub>	 P-h <sub>8</sub>	deutero isomers		
				A-d <sub>10</sub>	Ac-d <sub>9</sub>	P-d <sub>8</sub>
$\frac{P_x}{P_y}$	0.7 (0.4)	18	90 (10)	0.5 (0.2)	16	29
$\frac{P_z}{P_y}$	0.10 (0.05)	1 (0.12)	2.5 (0.3)	0.06 (0.02)	0.6 (0.2)	1.0 (0.1)
$\frac{k_x}{k_y}$	1.8 (0.2)	11 (1)	14 (1)	1.4 (0.2)	12 (1)	17 (1)
$\frac{k_z}{k_y}$	0.20 (0.04)	0.52 (0.06)	0.54 (0.06)	0.17 (0.02)	0.6 (0.2)	0.68 (0.05)

Table 1. Relative non-radiative rates for the spin-components of  $T_0$  in three-ring aromatic molecules.

The present table contains the same information as fig. 8 of chapter IV. However for reasons to be explained we have here normalized the rates relative to the spin state  $T_y$ .

## 1. THE MODEL

The next two statements, taken from previous work on the evaluation of non-radiative rates, provide the point of departure for the present discussion:

I. Let in a large molecule  $K_u$  denote a non-radiative transition rate that involves the spin level  $T_u$  and which may either be the populating rate  $P_u$  or the decay rate  $k_u$ . Then it is possible to show that  $K_u$  is separable into a product of two factors, where one factor contains everything that depends on the spin state  $T_u$  and the other factor the dependence on the Franck-Condon overlap integrals between the two states connected by the radiationless process, cf. (9) of chapter IV.

II. In the expression for  $K_u$  one has to consider only those matrix elements of the spin-orbit coupling (SOC) operator which on expansion in integrals over atomic wave functions yield one-center one-electron integrals. All

contributions which would contain multicenter SOC integrals only may be neglected.

The first point emerges from various theories on radiationless transitions [4,5,6]. It is very useful in the interpretation of experiments on the spin selectivity of the ISC processes, i.e. on the way in which  $P_u$  and  $k_u$  vary with the spin state  $T_u$  for a given molecule. Only one factor of the expression for  $K_u$  then has to be evaluated. We shall present a brief outline how the separation can be achieved when starting from a general expression for  $K_u$ .

The second point recently has been expressed by Metz et al. [2]. In the present context the contribution of these authors to the understanding of SOC in aromatic hydrocarbons is that the above rule applies to the non-radiative rates of all spin components of  $T_o$ , including the long-lived level  $T_z$ . Following McClure [7], it previously had always been assumed that SOC coupling of  $T_z$  is predominantly to  $^1\pi\pi^*$  states [8,5] via the small three-center contributions first calculated by Hammett and Oosterhoff for benzene [8]. But as we shall see, and as shown by Metz [2], in higher order SOC between highly excited states involving the  $\sigma$ -core appears to contribute appreciably, because of the one-center integrals that then arise. The experiments on aza-molecules when compared with the experiments on the parent hydrocarbons support the suggestion of Metz et al.

In what follows we shall take the  $T_o^u \rightarrow S_o$  crossing as an example and assume that the system initially is in the lowest vibronic level of the triplet state, with a total wave function denoted by  $T_o^u$ . For a large molecule in the "statistical limit" [9] at low temperature in a solid, the rate for  $T_o^u \rightarrow S_o$  ISC,  $K_u(T_o^u \rightarrow S_o) = k_u^d$ , is given by (see for instance [4,10]):

$$K_u(T_o^u \rightarrow S_o) = \frac{2\pi}{h} \sum_v | \langle T_o^u | \Omega | S_{o,v} \rangle |^2 \delta(E(T_o^u) - E(S_{o,v})) \quad (1)$$

Here  $S_{o,v}$  stands for a "hot" state of the ground state approximately degenerate with  $T_o$  and the  $\delta$ -function implies conservation of energy. The operator  $\Omega$  is the level shift operator [10,11]; we are interested in its off-diagonal matrix elements which can be represented as a perturbation series. One has

$$\langle T_o^u | \rho | S_{o,v} \rangle = \langle T_o^u | V | S_{o,v} \rangle + \sum_{\{m\}} \frac{\langle T_o^u | V | m \rangle \langle m | V | S_{o,v} \rangle}{E(T_o^u) - E_m} + \text{h.o.t.} \quad (2)$$

Bold brackets  $\langle \rangle$  mean integration over *vibronic* space, i.e. over *vibrational* and *electronic* coordinates.  $V$  is the interaction hamiltonian; its explicit form depends on the choice of basis set.

If, with Siebrand et al. [5] and with Heller et al. [6] we choose pure spin adiabatic Born Oppenheimer (BO) wave functions as a basis, then

$$\begin{aligned} V &= \mathcal{H} - \mathcal{H}^{(o)} \\ &= T_N + \mathcal{H}_{SO} \end{aligned} \quad (3)$$

The BO functions

$$\begin{aligned} T_o^u &= {}^3\psi_{o,o}^u(q,s,Q) = T_o^u(q,s;Q)\Lambda_{o,o}^3(Q) \\ S_{o,v} &= {}^1\psi_{o,v}^u(q,s,Q) = S_o(q,s;Q)\Lambda_{o,v}^1(Q) \\ \text{and } m &= {}^\mu\psi_{m,v}^u(q,s,Q) = {}^\mu\phi_m^u(q;s;Q)\Lambda_{m,v}^u(Q) \end{aligned} \quad (4)$$

are the eigenfunctions of the zeroth order hamiltonian  $\mathcal{H}^{(o)}$ .  $T_N$ , the operator for nuclear kinetic energy, and  $\mathcal{H}_{SO}$ , the hamiltonian for SOC, are non-diagonal in the basis set of the pure spin BO functions (4).  $Q$  and  $q$  represent the full sets of nuclear and electronic coordinates  $\{Q\}$  and  $\{q\}$ ;  $s$  labels the spin variable.  $\phi$  and  $\Lambda$  are the electronic and nuclear wave functions;  $m$  labels the electronic state,  $v$  stands for a set of quantum numbers representing the number of quanta with which all separable vibrational modes are excited in  $\Lambda$ . Finally  $\mu$  and  $u$  are spin labels:  $\mu$  is the multiplicity, and  $u$  denotes the spin component for triplet states.

The specific calculations of non-radiative decay rates of aromatic hydrocarbons that recently have been made in principle are based on the substitution of (3) and (4) into (2) and then making a sensible guess as to what terms should be retained in working out the result. Now there is a fundamental distinction between the first order and second order terms in the perturbation expansion (2), in which the higher order terms are always neglected. This distinction arises because in the coupling operator  $V$  the term



$T_N$  in (3) which takes account of the breakdown of the BO approximation, can only connect states of the same multiplicity, whereas  $\mathcal{K}_{S_0}$  may couple singlets with triplets. Hence the first order term in (2) may arise from SOC alone, whereas a significant contribution from the second order sum only arises if an appreciable breakdown of the Born Oppenheimer approximation occurs. It is here that the recent treatment of Metz et al. [2] differs from the earlier work of Siebrand, Henry, Lawetz and Orlandi [5,12]: Siebrand attributed most of the decay of the second order term, whereas Metz has shown that the breakdown of the BO approximation can altogether be neglected and everything follows from the first term in (2) with simply  $V = \mathcal{K}_{S_0}$ . Since this controversy at first sight may seem strange, we note that  $\langle T_o^u | V | S_{o,v} \rangle$  is a complicated matrix element between vibronic states, which can only be evaluated by introducing further simplification. This will become clear from what is to follow and, in greater detail, from the appendix to this chapter.

We further follow Metz et al. and restrict ourselves to the first term of (2). This matrix element of  $V$  between a triplet and a singlet state for the present choice of basis reads

$$\langle T_o^u | V | S_{o,v} \rangle = \langle T_o^u(q,s;Q) \Lambda_{o,o}^3(Q) | \mathcal{K}_{S_0}(q,s,Q) | S_o(q,s;Q) \Lambda_{o,v}^1(Q) \rangle \quad (5)$$

On substituting (5) via (2) into  $\langle T_o^u | \dot{n} | S_{o,v} \rangle$  of (1) we obtain a formal expression for the rate one would like to estimate. The integral in this expression is over the electronic coordinates (including spin) and subsequently over the nuclear coordinates. In order to reduce this integral to a more manageable form for a quantitative calculation, Siebrand expanded the electronic integrals in a Herzberg-Teller series about a suitable nuclear equilibrium configuration  $\{Q\} = 0$ . The details of such an expansion are given in the appendix. All what matters here is that one then obtains  $K_u(T_o^u \rightarrow S_o)$  as a sum of individual contributions, each arising from a term in the Herzberg-Teller series:

$$K_u(T_o^u \rightarrow S_o) = k_u^{(0)} + k_u^{(1)} + k_u^{(2)} \quad (6)$$

The upper indices label the order of the term in the Herzberg-Teller expansion of the electronic integral in (5) from which the contribution arises. Now the nice thing is that all  $k_u^{(i)}$  in (6) contain the same vibrational factor independent of the labels  $u$  and  $i$ , see appendix (A 14), and hence statement I

is fulfilled.

For the present purpose we are merely interested in the *relative* behaviour of the  $K_u(T_o^u \rightarrow S_o)$ , the  $k_u^d$  of previous chapters, with respect to the separate spin states of  $T_o$ , and similarly for the  $K_u(S_1 \rightarrow T_o^u)$  (the "P<sub>u</sub>'s"). Then there is no need for us to consider the evaluation of the vibrational factor. An evaluation of this factor has been carried out, for instance, by Englman and Jortner [4] and by Freed and Jortner [13] and in a different formalism also by the German school [14].

At this stage we return to the second statement (II). In § 3.1 of chapter II we gave a sketch of SOC in aromatic molecules. We argued that the one-center one-electron integrals arising from matrix elements of  $\mathcal{H}_{SO}$  between a  $\sigma\pi^*$  and a  $\pi\pi^*$  state must exceed by over 100 times the multi-center integrals which appeared in a pure  $\pi$  electron description; the squares of these integrals enter in the expressions for the transition probabilities between singlet and triplet states. Therefore, with Metz, we look for only those matrix elements of the SOC of each individual spin state which lead to one-electron one-center SOC integrals in the lowest order Herzberg-Teller expansion of (5).

Let us consider the  $T_o^u \rightarrow S_o$  transition in an aromatic hydrocarbon, for instance anthracene.

(o) Here  $k_u^{(o)}$  vanishes because  $\langle T_o^u | \mathcal{H}_{SO} | S_o \rangle$  is zero by symmetry for all  $u = x, y, z$ , cf. fig. II.1.  $\langle \rangle$  is an electronic integral, cf. appendix.

(1) When coming to the next terms,  $k_x^{(1)}$  and  $k_y^{(1)}$  both contain one-center SOC integrals via SOC of  $T_o^{x,y}$  with highly excited  $\sigma\pi^*$  and  $\pi\sigma^*$  singlet states, see the discussion in the last paragraph of § 3.1 of chapter II. We have summarized this in table 2. For the long-lived level  $T_z$ , however,  $k_z^{(1)}$  relates to SOC between  $\pi\pi^*$  states only, which results in three- and more-center integrals over atomic orbitals, which Metz et al. [2] decided to neglect.

(2) For  $u = z$ ,  $k_z^{(2)}$  is the lowest order term which yields one-center integrals. In this case the effective SOC occurs between singlet and triplet electron configurations which both involve the  $\sigma$ -core ( $\sigma\pi^*$  and  $\pi\sigma^*$  states); because of vibronic coupling such configurations contribute to the total wave functions  $S_{o,v}$  and  $T_o^z$ .

In table 2 we have schematically represented the occurrence of the one-center SOC integrals in the lowest order Herzberg-Teller term for each spin component. The scheme not only applies to the decay of  $T_o$  but also the populating rates of  $T_o$  for aromatic hydrocarbons.

	(0)	(1)	(2)
$k_x, P_x$	-	$T_0(3\pi\pi^*) \leftarrow \text{SOC} \rightarrow 1\sigma\pi^*, 1\pi\sigma^*$	...
$k_y, P_y$	-	$T_0(3\pi\pi^*) \leftarrow \text{SOC} \rightarrow 1\sigma\pi^*, 1\pi\sigma^*$	...
$k_z, P_z$	-	-	$1\sigma\pi^*, 1\pi\sigma^* \leftarrow \text{SOC} \rightarrow 3\sigma\pi^*, 3\pi\sigma^*$

Table 2. The populating and decay rates of  $T_0$  in aromatic hydrocarbons. The numbers between brackets in the head of the table indicate the order of the terms in the Herzberg-Teller series. For each spin component the lowest order term in which one-center SOC integrals occur are listed.

We started by mentioning the surprising agreement between Metz's calculations, based on a scheme like that of table 2, and the experimental results for anthracene  $C_{14}H_{10}$ . We notice two further aspects that support this scheme, namely the near equality observed for the non-radiative rates ( $k$ 's and  $P$ 's) involving the spin levels that correspond to the in-plane spin axes  $x$  and  $y$ :

all anthracene isomers of chapter IV have  $k_x \approx k_y$  and  $P_x \approx P_y$ , phenanthrene has  $k_x \approx k_y$  [15] and for a number of compounds in hosts of different alkanes  $P_x \approx P_y$  [16].

## 2. THE POPULATING AND DECAY FOR AZA-AROMATIC MOLECULES

Extension of the model to aza-molecules leads to a further support for the idea that only one-center SOC integrals contribute significantly. Aza-substituents provide a new and interesting aspect. We shall show that in this case the scheme analogous to table 2 differs for the populating and decay rates of  $T_0$ .

As discussed in chapter II the main difference of the present nitrogen heterocycles with aromatic hydrocarbons is that  $n\pi^*$  states at low energy are inserted into the original energy level diagram of the parent hydrocarbon.

Let us first consider the populating processes  $S_1 \rightarrow T_0^u$  in aza-molecules. We limit ourselves to compounds which have their lone-pair orbital(s) parallel to the molecular  $y$ -axis and for which  $T_0$  is  $3\pi\pi^*$  as, for instance, phenazine, see fig. 1 of chapter II. The populating rates  $P_u$  must be calculated from expressions analogous to (1) with matrix elements  $\langle S_1 | \Omega | T_{0,v}^u \rangle$ , where  $T_{0,v}$

represents a "hot" state of the lowest triplet state. The expansion of  $\langle S_1 | \mathcal{H}_{SO} | T_0^u \rangle$  in a Herzberg-Teller series about  $\{Q\} = 0$  finally leads to an expression similar to (6):

$$P_u(S_1 \rightarrow T_0^u) = P_u^{(0)} + P_u^{(1)} + P_u^{(2)} . \quad (7)$$

$P_u^{(0)}$  contains  $\langle S_1 | \mathcal{H}_{SO} | T_0^u \rangle_0$ . Here the important difference with the parent hydrocarbon shows up. In the present case  $S_1$  itself is  $1_{n\pi}^*$  ( $\Gamma(S_1) = B_{1u}$  for phenazine, see fig. 1 of chapter II) and thus it directly couples to the spin component of  $T_0$  having the same total (= orbital  $\otimes$  spin) symmetry, i.e. to  $T_x$ . Hence  $P_x$  now is determined by "direct" SOC between  $S_1$  and  $T_0$ , i.e. by the zeroth order term in (7). For  $T_y$  and  $T_z$  this term vanishes, as before. Consequently  $P_x \gg P_y, P_z$ , a fact first observed and explained by de Groot et al. [17] for quinoxaline in durene. In phenazine, acridine, and similar molecules like quinoxaline and quinoline, the selective populating mechanism into  $T_x$  reflects the large one-center integrals on the nitrogen atom(s) of the type

$$\langle p_y(N) | l_x(N) | p_z(N) \rangle . \quad (8)$$

For the discussion of the first order term  $P_u^{(1)}$  we must consider the two levels  $T_y$  and  $T_z$  separately.

For  $T_y$  nothing has been changed relative to the parent hydrocarbon. The spin-orbit coupling route still is determined by coupling of  $T_0$  to highly excited singlet states involving the  $\sigma$ -core.

For  $T_z$  however the fact that  $S_1$  is an  $1_{n\pi}^*$  state with the n-orbital parallel to the y-axis brings about SOC of this state with highly excited triplet states involving the  $\sigma$ -core via one-center integrals of the type

$$\langle p_y(N) | l_z(N) | p_x(N) \rangle . \quad (9)$$

The recognition of the importance of this higher-order SOC route from  $S_1$   $1_{n\pi}^*$  into the  $T_z$  component of  $T_0$  led us to give the analysis of the present chapter. This route is specific for aza-molecules. In an aromatic hydrocarbon the first order term only allows of the ineffective SOC between  $1_{\pi\pi}^*$  and  $3_{\pi\pi}^*$  states for  $T_z$ , which we decided to neglect in the construction of table 2.

In table 3 we show where the one-center SOC integrals first occur in the

Herzberg-Teller expansion for the populating rate of each spin level.

	(0)	(1)	(2)	change relative to parent hydrocarbon
$P_x$	$S_1(1n\pi^*) + \text{SOC} \rightarrow T_0(3\pi\pi^*)$	...		SOC involving $1n\pi^*$ ; one order higher
$P_y$	-	$T_0(3\pi\pi^*) + \text{SOC} \rightarrow 1\sigma\pi^*, 1\pi\sigma^*$	...	$\approx$ unaltered
$P_z$	-	$S_1(1n\pi^*) + \text{SOC} \rightarrow 3\sigma\pi^*$	...	SOC involving $1n\pi^*$ ; one order higher

Table 3. The populating rates of  $T_0$  in aza-aromatic molecules with  $n/y$ -axis. The numbers between brackets in the head of the table indicate the order of the terms in the Herzberg-Teller series. For each spin component the lowest order term in which one-center SOC integrals occur are listed.

From table 2 and 3 we observe that, in the expressions for the populating rates  $P_x$  and  $P_z$  of the aza-substituted molecules, as compared with the hydrocarbons, the one-center integrals occur *one order lower* in the Herzberg-Teller series. On the other hand  $P_y$  is not affected. As a result both the populating ratios  $P_x/P_y$  and  $P_z/P_y$  are expected to increase on aza-substitution just as observed in table 1.

Finally we consider the decay processes  $T_0^u \rightarrow S_0$ . Here no  $n\pi^*$  states are directly involved in transition. Hence the zeroth order contributions to  $k_u$  vanish for each spin level. For what concerns the first order term,  $k_y^{(1)}$  can not be different as compared with that of the hydrocarbon, while for  $T_x$  SOC is to  $S_1(1n\pi^*)$ . This  $(3\pi\pi^*)^x \leftrightarrow 1n\pi^*$  coupling is highly effective relative to the  $(3\pi\pi^*)^x \leftrightarrow 1\sigma\pi^*$  ( $1\pi\sigma^*$ ) SOC, which existed already in the hydrocarbon, because of a strongly reduced energy gap ( $E(S_1) - E(T_0) \approx 0.1\{E(1\sigma\pi^*) - E(T_0)\}$ ), as explained in § 3 of chapter II. The same reduction of energy separation causes the second order term involving SOC to  $S_1(1n\pi^*)$  to be the dominant contribution in the decay of  $T_z$ , as before via integrals of the type (9).

In table 4 we present the scheme for SOC in the decay rates in aza-molecules.

Thus for the decay again  $n\pi^*$  states are involved in the SOC routes for  $T_x$  and  $T_z$ . SOC involving  $T_y$  is not altered relative to the parent hydrocarbon. As a result the decay ratios  $k_x/k_y$  and  $k_z/k_y$  also are expected to increase on

	(0)	(1)	(2)	change relative to parent hydrocarbon
$k_x$	-	$+ T_0(^3\pi\pi^*) + SOC + S_1(^1n\pi^*)$	...	additional but more effective SOC involving $n\pi^*$
$k_y$	-	$T_0(^3\pi\pi^*) + SOC + ^1\sigma\pi^*, \pi\sigma^*$	...	= unaltered
$k_z$	-	...	$+ S_1(^1n\pi^*) + SOC + ^1\sigma\pi^*$	additional but more effective SOC involving $n\pi^*$

Table 4. The decay rates of  $T_0$  in aza-aromatic molecules with  $n \parallel y$ -axis. The numbers between brackets in the head of the table indicate the order of the terms in the Herzberg-Teller series. For each spin component the lowest order term in which one-center SOC integrals occur are listed.

aza-substitution. In table 1 we see this reflected in the experimental results.

Another striking manifestation that results from the above analysis is the following. Since the effective  $^3\pi\pi^* \leftrightarrow ^1n\pi^*$  SOC for the populating processes to  $T_x$  and  $T_z$  occurs in terms that are one order lower than for the decay rates, the populating ratios  $P_x/P_y$  and  $P_z/P_y$  are expected to increase more strongly on aza-substitution than the corresponding decay ratios  $k_x/k_y$  and  $k_z/k_y$ . This also agrees with the experimental results of table 1.

It is interesting to note that the available data on non-radiative transitions in a number of naphthalene derivatives also lend support to the present qualitative analysis based on the schemes of tables 2 - 4. We have represented these data in table 5. The same appears to be true even for recent measurements of van Dorp et al. [19] of the decay rates of  $T_0$  of free-base porphyrin.

In the extensive, rather formal discussions of spin-forbidden radiationless processes of the past five years it has often been unclear how to think of these in a physical sense. Is the rate determining "mechanism" to be sought in a breakdown of the Born Oppenheimer approximation, via the operator for the kinetic energy of the nuclei, or in the flipping of the electron spin, represented by the spin orbit coupling terms in the Hamiltonian? The early conclusion of de Groot et al. [17] that the selectivity of intersystem crossing with respect to the three spin states arises from SOC alone is

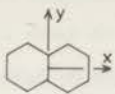
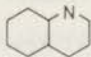
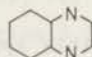
	 naphthalene	 quinoline	 quinoxaline
$k_x/k_y$	1.5	15	10
$k_z/k_y$	0.37	0.5	0.6
$P_x/P_y$	0.4	50	50
$P_z/P_y$	0.17	0.5	1.5

Table 5. Relative rates for the spin components of  $T_0$  in two-ring aromatic molecules. The data for naphthalene are from work of Sixl [15] and El-Sayed et al. [18]. The numbers for the nitrogen heterocyclics are taken from Schmidt et al. [18]. The values for the decay rates must still be corrected for radiative contributions, but this turns out to be of minor importance.

clearly maintained. The only limitation is that these authors considered the matrix element of  $\mathcal{H}_{SO}$  between BO states in a fixed frame; in Metz's work this is extended by taking into account some of the higher order terms in the Herzberg-Teller expansion of the matrix elements.

The striking agreement of Metz's calculations with our results on anthracene and the success with which a generalization of his idea can account for the effects of aza-substitution lend strong support to the idea that spin selectivity in ISC is a manifestation of the spatial anisotropy of SOC in large planar molecules.

APPENDIX

In this appendix we first rewrite the vibronic matrix element (5). Subsequently we show that this leads to an expression for  $K_u(T_o^u \rightarrow S_o)$  given by (6).

We abbreviate the states in matrix element (5):

$$\langle T_o^u(q,s;Q)\Lambda_{o,o}^3(Q) | \mathcal{H}_{SO}(q,s;Q) | S_o(q,s;Q)\Lambda_{o,v}^1(Q) \rangle \quad (A1)$$

by  $T_o^u = T_o^u(q,s;Q)$ ,  $S_o = S_o(q,s;Q)$ ,  $\Lambda_{o,o}^3 = \Lambda_{o,o}^3(Q)$ ,  $\Lambda_{o,v}^1 = \Lambda_{o,v}^1(Q)$  and we write for  $\mathcal{H}_{SO}(q,s;Q)$  simply  $\mathcal{H}_{SO}$ . For evaluating (A1) we follow the recipe first given by Henry and Siebrand [5]. The vibronic integration  $\langle \rangle$  is performed by first taking the integral over electronic coordinates including the spin and subsequently integrating over the space of the nuclear coordinates. Hence we write for (A1)

$$\langle T_o^u \Lambda_{o,o}^3 | \mathcal{H}_{SO} | S_o \Lambda_{o,v}^1 \rangle = (\Lambda_{o,o}^3 \langle T_o^u | \mathcal{H}_{SO} | S_o \rangle \Lambda_{o,v}^1) \quad (A2)$$

The electronic matrix element  $\langle T_o^u | \mathcal{H}_{SO} | S_o \rangle$  depends on the nuclear coordinates, because  $T_o^u$ ,  $S_o$  and  $\mathcal{H}_{SO}$  depend on  $Q$ . Hence it cannot yet be taken out of the nuclear integral, denoted by ( ).

The dependence of the electronic matrix element on the nuclear conformation is obtained by expanding it in a Herzberg-Teller series about an equilibrium conformation  $\{Q\} = 0$ :

$$\begin{aligned} \langle T_o^u | \mathcal{H}_{SO} | S_o \rangle &= [\langle T_o^u | \mathcal{H}_{SO} | S_o \rangle]_o + \sum_p \left[ \frac{\delta \langle T_o^u | \mathcal{H}_{SO} | S_o \rangle}{\delta Q_p} \right]_{Q_p} + \sum_{pr} \left[ \frac{\delta^2 \langle T_o^u | \mathcal{H}_{SO} | S_o \rangle}{\delta Q_p \delta Q_r} \right]_{Q_p Q_r} + \dots \\ &= u_{h_{SO}}^{(0)} + u_{h_{SO}}^{(1)} \{Q_p\} + u_{h_{SO}}^{(2)} \{Q_p\}^2 + \dots \quad (A3) \end{aligned}$$

$u$  as before labels the spin component of  $T_o$ . The upper indices denote the order of the Herzberg-Teller expansion. The terms in square brackets  $[ ]_o$  are independent of  $\{Q\}$ , since they have to be evaluated at  $\{Q\} = 0$ . This is indicated by the subscript  $o$ .  $\{Q_p\}^2$  symbolically denotes the second order dependence  $Q_p Q_r$ .

For aromatic hydrocarbons  $u_{h_{SO}}^{(0)}$  vanishes by symmetry for  $T_o^u \rightarrow S_o$ .



crossing for every spin component, see for instance fig.1 of chapter II. However, in other cases where it does not vanish by symmetry it dominates, for instance in  $S_1 \rightarrow T_0$  crossing in aza-aromatics, see chapter II and section 5.2, and also [17]. Therefore we shall keep  $u_{h_{SO}}^{(0)}$  in what follows.

Before we proceed with the evaluation of (A2) a remark may be in order on how the expressions between square brackets in the first and second order terms  $u_{h_{SO}}^{(1)}\{Q_p\}$  and  $u_{h_{SO}}^{(2)}\{Q_p\}^2$  of (A3) are related to the familiar integrals of vibronic coupling and SOC. Using standard Herzberg-Teller theory [5,20,21] we may write:

$$\begin{aligned} \left[ \frac{\delta \langle T_0^u | \mathcal{H}_{SO} | S_0 \rangle}{\delta Q_p} \right]_0 &= \left[ \langle \frac{\delta T_0^u}{\delta Q_p} | \mathcal{H}_{SO} | S_0 \rangle + \langle T_0^u | \mathcal{H}_{SO} | \frac{\delta S_0}{\delta Q_p} \rangle + \langle T_0^u | \frac{\delta \mathcal{H}_{SO}}{\delta Q_p} | S_0 \rangle \right]_0 \\ &= \left[ \sum_m \frac{\langle T_0^u | \frac{\delta \mathcal{H}^{(0)}}{\delta Q_p} | T_m^u \rangle \langle T_m^u | \mathcal{H}_{SO} | S_0 \rangle}{E(T_0) - E(T_m)} + \right. \\ &\quad \left. + \langle T_0^u | \mathcal{H}_{SO} | S_m \rangle \frac{\langle S_m | \frac{\delta \mathcal{H}^{(0)}}{\delta Q_p} | S_0 \rangle}{E(S_0) - E(S_m)} + \langle T_0^u | \frac{\delta \mathcal{H}_{SO}}{\delta Q_p} | S_0 \rangle \right]_0. \end{aligned} \quad (A4)$$

For the present qualitative discussion, the only important fact is that (A4) contains products of SOC matrix elements and matrix elements of vibronic coupling.

Similarly, the second derivative of the electronic matrix element in  $u_{h_{SO}}^{(2)}\{Q_p\}^2$  contains triple products such as

$$\left[ \frac{\langle T_0^u | \frac{\delta \mathcal{H}^{(0)}}{\delta Q_p} | T_m^u \rangle \langle T_m^u | \mathcal{H}_{SO} | S_n \rangle \langle S_n | \frac{\delta \mathcal{H}^{(0)}}{\delta Q_p} | S_0 \rangle}{E(T_0) - E(T_m)} \frac{1}{E(S_0) - E(S_n)} \right]_0 \quad (A5)$$

arising from  $\left[ \langle \frac{\delta T_0^u}{\delta Q_p} | \mathcal{H}_{SO} | \frac{\delta S_0}{\delta Q_p} \rangle \right]_0$ . We bear this in mind, but for the sake of brevity keep everything as expressed in (A3).

Subsequently we substitute (A3) into (A2). This gives

$$\langle T_0^u \Lambda_{o,o}^3 | \mathcal{H}_{SO} | S_0 \Lambda_{o,v}^1 \rangle = \langle \Lambda_{o,o}^3 | u_{h_{SO}}^{(0)} + u_{h_{SO}}^{(1)}\{Q_p\} + u_{h_{SO}}^{(2)}\{Q_p\}^2 | \Lambda_{o,v}^1 \rangle$$

$$\begin{aligned}
&= (\Lambda_{o,o}^3 |u_{hSO}^{(0)} | \Lambda_{o,v}^1) + (\Lambda_{o,o}^3 |u_{hSO}^{(1)} \{Q_p\} | \Lambda_{o,v}^1) + \\
&\quad + (\Lambda_{o,o}^3 |u_{hSO}^{(2)} \{Q_p\}^2 | \Lambda_{o,v}^1) \\
&= u_{\mathcal{H}_{SO}}^{(0)} + u_{\mathcal{H}_{SO}}^{(1)} + u_{\mathcal{H}_{SO}}^{(2)} \quad (A6)
\end{aligned}$$

with

$$\begin{aligned}
u_{\mathcal{H}_{SO}}^{(0)} &= (\Lambda_{o,o}^3 \langle T_o^u | \mathcal{H}_{SO} | S_o \rangle | \Lambda_{o,v}^1) \\
&= \langle T_o^u | \mathcal{H}_{SO} | S_o \rangle | \Lambda_{o,o}^3 | \Lambda_{o,v}^1) \\
&= C_u^{(0)} N(v) . \quad (A7)
\end{aligned}$$

Since  $[\langle T_o^u | \mathcal{H}_{SO} | S_o \rangle]_o$  is independent of  $Q$  we take it out of the nuclear integral. We abbreviate it by  $C_u^{(0)}$ . The symbol  $N(v)$  stands for the Franck-Condon overlap integral  $(\Lambda_{o,o}^3 | \Lambda_{o,v}^1)$ .

$$\begin{aligned}
u_{\mathcal{H}_{SO}}^{(1)} &= (\Lambda_{o,o}^3 | \sum_p \left[ \frac{\delta \langle T_o^u | \mathcal{H}_{SO} | S_o \rangle}{\delta Q_p} \right]_o Q_p | \Lambda_{o,v}^1) \\
&= \sum_p \left[ \frac{\delta \langle T_o^u | \mathcal{H}_{SO} | S_o \rangle}{\delta Q_p} \right]_o (\Lambda_{o,o}^3 | Q_p | \Lambda_{o,v}^1) , \quad (A8)
\end{aligned}$$

and

$$u_{\mathcal{H}_{SO}}^{(2)} = (\Lambda_{o,o}^3 | \sum_{p,r} \left[ \frac{\delta^2 \langle T_o^u | \mathcal{H}_{SO} | S_o \rangle}{\delta Q_p \delta Q_r} \right]_o Q_p Q_r | \Lambda_{o,v}^1) . \quad (A9)$$

With the aid of (A7) - (A9) we can now cast the transition rate  $K_u(T_o^u \rightarrow S_o)$  in the form (6). Namely with (2) and (5) the expression for  $K_u(T_o^u \rightarrow S_o)$  can be written as

$$K_u(T_o^u \rightarrow S_o) = \frac{2\pi}{h} \sum_v \left| \langle T_o^u \Lambda_{o,o}^3 | \mathcal{H}_{SO} | S_o \Lambda_{o,v}^1 \rangle \right|^2 \delta(E(T_o) - E(S_{o,v})) \quad (A10)$$

with (A6) - (A9) we write for this rate:

$$K_u(T_o^u \rightarrow S_o) = \frac{2\pi}{\hbar} \sum_v |C_u^{(o)}| N(v) + |u_{SO}^{(1)} + u_{SO}^{(2)}|^2 \delta(E(T_o) - E(S_{o,v})) \quad (A11)$$

In the present qualitative approach we only take into account the first term in the Herzberg-Teller expansion (A3) where a matrix element of  $\mathcal{H}_{SO}$  appears that on expansion in integrals over atomic orbitals yields one-center integrals. Then (A11) may be approximated to:

$$\begin{aligned} K_u(T_o^u \rightarrow S_o) &= \frac{2\pi}{\hbar} |C_u^{(o)}|^2 \sum_v N^2(v) \delta(E(T_o) - E(S_{o,v})) + \\ &+ \frac{2\pi}{\hbar} \sum |u_{SO}^{(1)}|^2 \delta(E(T_o) - E(S_{o,v})) + \\ &+ \frac{2\pi}{\hbar} \sum |u_{SO}^{(2)}|^2 \delta(E(T_o) - E(S_{o,v})) . \end{aligned} \quad (A12)$$

It follows further, see for instance [5,13] and formula (2) - (4) of [3], that

$$\frac{2\pi}{\hbar} \sum |u_{SO}^{(1)}|^2 \delta(E(T_o) - E(S_{o,v})) \quad \text{may be}$$

written as  $\frac{2\pi}{\hbar} |C_u^{(1)}|^2 \sum_v N^2(v) \delta(E(T_o) - E(S_{o,v}))$ ,

$$\text{where } C_u^{(1)} = \sum_p f(\omega_p) \left[ \frac{\delta \langle T_o^u | \mathcal{H}_{SO} | S_o \rangle}{\delta Q_p} \right]_o . \quad (A13)$$

The term with  $u_{SO}^{(2)}$  can be reduced in a similar way. In total we get

$$\begin{aligned} K_u(T_o^u \rightarrow S_o) &= \frac{2\pi}{\hbar} |C_u^{(o)}|^2 F + \frac{2\pi}{\hbar} |C_u^{(1)}|^2 F + \frac{2\pi}{\hbar} |C_u^{(2)}|^2 F \\ &= k_u^{(o)} + k_u^{(1)} + k_u^{(2)} . \end{aligned} \quad (A14)$$

Here F stands for the Franck-Condon factor

$$\sum_v N^2(v) \delta(E(T_o) - E(S_{o,v})) .$$

## REFERENCES

- [1] Antheunis, D., Schmidt, J., and van der Waals, J.H., 1974, *Molec. Phys.*, in the press.
- [2] Metz, F., Friedrich, S., and Hohlneicher, G., 1972, *Chem. Phys. Lett.*, 16, 353.
- [3] Metz, F., 1973, *Chem. Phys. Lett.*, 22, 186.
- [4] Englman, R., and Jortner, J., 1970, *Molec. Phys.*, 18, 145.
- [5] Henry, B.R., and Siebrand, W., 1971, *J. chem. Phys.*, 54, 1072.
- [6] Heller, D.F., Freed, K.F., and Gelbart, W.M., 1972, *J. chem. Phys.*, 56, 2309.
- [7] McClure, D.S., 1952, *J. chem. Phys.*, 20, 682.
- [8] Hameka, H.F., and Oosterhoff, L.J., 1958, *Molec. Phys.*, 1, 358.
- [9] Bixon, M., and Jortner, J., 1968, *J. chem. Phys.*, 48, 715.
- [10] Freed, K.F., and Gelbart, W.M., 1971, *Chem. Phys. Lett.*, 10, 187.
- [11] Goldberger, M., and Watson, K., *Collision theory*, (Wiley, New York, 1964).
- [12] Lawetz, V., Orlandi, G., and Siebrand, W., 1972, *J. chem. Phys.*, 56, 4058.
- [13] Freed, K.F., and Jortner, J., 1970, *J. chem. Phys.*, 52, 6272.
- [14] Stanford, A.L., and Fischer, S.F., 1973, *Chem. Phys.*, 1, 99.
- [15] Sixl, H., Thesis, 1971, University of Stuttgart.
- [16] El-Sayed, M.A., Moomaw, W.R., and Chodak, J.B., 1973, *Chem. Phys. Lett.*, 20, 11.
- [17] de Groot, M.S., Hesselmann, I.A.M., Schmidt, J., and van der Waals, J.H., 1968, *Molec. Phys.*, 15, 17.
- [18] Schmidt, J., Antheunis, D., and van der Waals, J.H., 1971, *Molec. Phys.*, 22, 1; Schmidt, J., Thesis, 1971, University of Leiden.
- [19] van Dorp, W.G., private communication.
- [20] Murrell, J.N., and Pople, J.A., 1955, *Proc. Roy. Soc.*, 69 A, 245.
- [21] Albrecht, A.C., 1960, *J. chem. Phys.*, 33, 156.

## CHAPTER VI

### KINETICS OF POPULATING AND DECAY OF THE PHOSPHORESCENT STATE OF TETRAMETHYLPYRAZINE IN DURENE. A SYSTEM WITH SKEW SPIN AXES<sup>(\*)</sup>.

*Using microwave induced phosphorescence techniques we determined the rate constants for populating and decay of the lowest triplet state of tetramethylpyrazine (TMP) in a durene crystal. The dynamic behaviour of the spin states  $T_y$ , and  $T_z$ , corresponding to the in-plane spin axes (principal axes of the dipolar coupling tensor)  $y'$  and  $z'$  proves to be identical:  $k_y^r = k_z^r$ , (radiative decay),  $k_y = k_z$ , (absolute decay rates) and  $P_y = P_z$ , (populating rates). This result supports the suggestion of de Groot et al., based on ESR experiments, that for the phosphorescent state of TMP in the durene host the in-plane spin axes  $y'$  and  $z'$  have undergone an appreciable ( $\approx 45^\circ$ ) rotation with respect to the in-plane molecular axes  $y$  and  $z$ .*

#### 1. INTRODUCTION

Recently de Groot et al. [1] reported ESR experiments on the lowest triplet state of tetramethylpyrazine (TMP) in a durene single crystal (see fig. 1) and in three different glasses. The authors explained their data by assuming that in the durene host the in-plane principal axes of the zero-field splitting tensor are considerably rotated with respect to the symmetry axes of the molecule. The present work has been undertaken to investigate whether support for this explanation is provided by the way in which the three spin components participate in intersystem crossing into and decay from the lowest triplet state.

In fig. 1 we define the system of axes for TMP and indicate the frequencies of the zero-field transitions in its phosphorescent state. In the notation used by de Groot [1] the principal axes of the zero-field splitting

tensor ("spin axes") are distinguished from the symmetry axes of the molecule ( $D_{2h}$ ) by a bar; we use primes. According to the ESR experiments [1] the  $x'$  axis coincides with the out-of-plane molecular axis, while the pair  $y', z'$  roughly bisects the angle between  $y$  and  $z$ , see fig. 2 where the ESR data still leave an option between two possibilities.

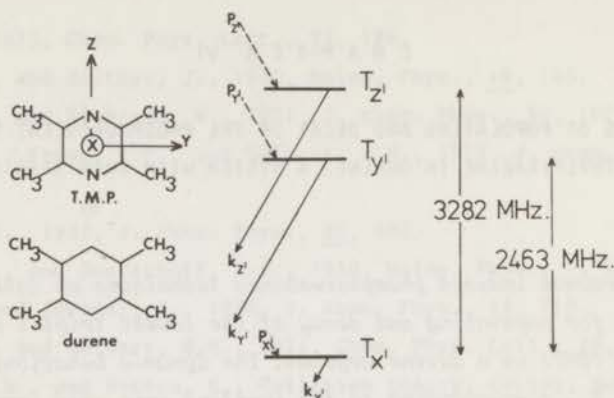


Fig. 1. Definition of the system of axes for TMP. Spin axes are primed. The zero-field splitting is expressed in the resonance frequencies of the  $T_{x'}' - T_{z'}'$  and  $T_{x'}' - T_{y'}'$  transitions. The populating and decay rates  $P_u$  and  $k_u$  ( $u = x', y', z'$ ) of the lowest triplet state of TMP in a durene host are indicated. The length of the arrows measures the relative rate constants (see table 2).

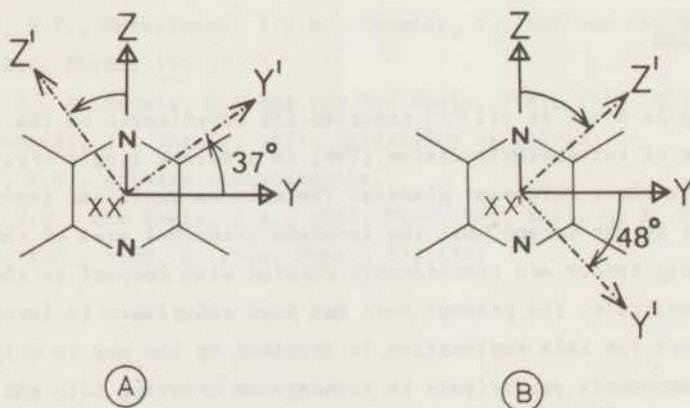


Fig. 2. The two possible sets of spin axes (primed) for the phosphorescent triplet state of TMP in durene, which follow from the ESR experiments by de Groot et al. [1].

From the theory of spin-orbit coupling it follows that for a  $\pi\pi^*$  triplet state of an aza-aromatic molecule the relative radiative activities of the two zero-field spin components related to the in-plane principal axes are determined by the orientation of these two relative to the direction of the lone-pair orbital(s) on the nitrogen atom(s) [2]. Hence, if the above explanation is correct one expects that for TMP in durene the unusual property of non-coincident spin and symmetry axes must be reflected in the decay properties of its phosphorescent state. The results to be presented in this chapter are in perfect accord with the assumed skewness of the spin axes of the lowest ( $\pi\pi^*$ ) triplet state of TMP in a durene host.

## 2. EXPERIMENTAL AND RESULTS

### 2.1 Equipment and principle of the experiments

We have used the equipment for microwave induced phosphorescence experiments described elsewhere [3]. The crystal, immersed in liquid He, was irradiated with light from a Philips SP 1000 Watt super high pressure mercury arc via a  $\text{NiSO}_4 + \text{CoSO}_4$  solution filter and an OX-7 Chance Pilkington optical glass filter. The phosphorescence was detected by an EMI 9524 B photo-multiplier tube. No filters were used in the detection.

In our experiments we observe the change in the intensity of phosphorescence brought about by the sudden application of microwaves that are resonant with one of the transitions between the spin levels. The majority are so-called microwave induced delayed phosphorescence (MIDP) experiments in which one applies the microwaves during phosphorescence decay [4]. Additional experiments are done under continuous illumination [5] and these will be referred to as steady-state experiments.

In the MIDP experiments the sample is illuminated for a short period, here 10 seconds, and then the exciting light is cut out by a shutter. The phosphorescence decay is followed on an oscilloscope and at a time  $t_1$  after closing the shutter one sweeps rapidly through one of the resonant microwave transitions between the spin levels. This causes a redistribution of the populations of the levels that participate in the transition and, as a rule, a change in light emission results. When considering the  $T_{x_1} - T_{z_1}$  transition the height  $h_{x_1-z_1}(t_1)$  of the induced signal is given by [3]

$$h_{x_1-z_1}(t_1) = c f_{x_1-z_1} \{N_{z_1}(t_1) - N_{x_1}(t_1)\} (k_{x_1}^r - k_{z_1}^r) . \quad (1)$$

Here  $N_u$  is the fractional population of the level  $T_u$  and  $k_u^r$  its rate of radiative decay,  $c$  is a constant and  $f_{x,-z}$ , the microwave transfer factor. The transfer factor either has to be determined in separate experiments [3], or the experimental conditions can be so chosen (e.g. by frequency modulation of the microwaves [5]) that saturation between the two levels is attained ( $f = 0.50$ ). For experiments in steady-state the same formula holds with  $t_1 = 0$ .

## 2.2 Decay rates

As previously explained [3,4], the absolute decay rates  $k_u$  of the individual spin levels may be determined from an analysis of  $h(t_1)$  as a function of  $t_1$  for the different transitions, provided spin-lattice relaxation between the levels is slow compared to the  $k_u$  (isolation condition, section 3.1 of [3]). In addition the relative radiative rates  $k_u^r$  can be found by comparing the height of the MIDP signals with the change in phosphorescence decay observed when the microwave transition is saturated continuously (section 3.3 of [3]).

For TMP in the durene host we observe two MIDP signals; one at 2463 MHz corresponding to the  $T_x, -T_y$  transition and one at 3282 MHz corresponding to  $T_x, -T_z$ . Except for the difference in frequency the two signals show exactly the same time dependent behaviour; the two decay rates found by plotting the heights of the signals as a function of delay time  $t_1$  are equal ( $\tau_{\max}^{-1}$  in table 1) and also the two decay rates obtained from the individual MIDP signals ( $\tau_{\min}^{-1}$  in table 1). This is an unusual situation and the interpretation of the results then still presents a problem which can only be solved by additional experiments to be described below. All one can say at this stage is that the decay of the triplet manifold is governed by two characteristic lifetimes and that the ratio of the radiative rates observed in the  $T_x, -T_y$  transition equals that for  $T_x, -T_z$ , to within the experimental accuracy of the order of 1 percent. From these observations one concludes that for the lowest triplet state of TMP in durene either of the two following situations must arise

- (i) the levels  $T_y$  and  $T_z$  have equal total decay rates and equal radiative rates; so far the experiments do not allow us to make a unique assignment and the two patterns represented in fig. 3 are still feasible;
- (ii) the populations of the levels  $T_y$  and  $T_z$  are tightly coupled by very



fast spin-lattice relaxation within this pair.

In the next section we investigate possibility (i) and show that, under the assumption of negligible spin-lattice relaxation between  $T_y$ , and  $T_z$ , situation a of fig. 3 is the correct one. Then in section 2.4 we report the results of a number of experiments that were designed to exclude the possibility of fast spin-lattice relaxation between  $T_y$ , and  $T_z$ , (ii).

	$T_x, -T_y$ , trans.	$T_x, -T_z$ , trans.
$\tau_{\max}$ in s	1.24 (0.02)	1.24 (0.02)
$\tau_{\min}$ in s	0.155 (0.002)	0.154 (0.003)
$k_{\max}^r/k_{\min}^r$	7.80 (0.08)	7.75 (0.10)

Table 1. Analysis of microwave induced delayed phosphorescence experiments on the  $T_x, -T_y$ , and  $T_x, -T_z$ , transitions.

The upper numbers represent the two distinct lifetimes  $\tau_{\max}$  and  $\tau_{\min}$  in seconds as determined from the MIDP measurements on each resonance. The lower numbers are the ratios of the radiative rates of the levels involved in each of the two transitions. Standard deviations of the mean are written in parentheses (cf. table 2).

	$k_U (s^{-1})$	$k_U^r$ (rel.)		$k_U (s^{-1})$	$k_U^r$ (rel.)
$ T_z\rangle$	6.5 [0.1]	7.75 [0.10]	—————	0.808 [0.007]	0.129 [0.002]
$ T_y\rangle$	6.45 [0.09]	7.80 [0.08]		0.81 [0.01]	0.128 [0.002]
$ T_x\rangle$	0.806 [0.005]	1	—————	6.48 [0.07]	1

Fig. 3. The two possible assignments of the decay rates of the lowest triplet state of TMP. The numbers in parentheses represent the standard deviations of the mean (cf. table 2).

### 2.3 Assignment of the decay rates

To choose between a and b of fig. 3 we did the following experiments. After illuminating the crystal during 10 s we shut off the exciting light and start to sweep  $T_x, -T_y$ , repeatedly at a rate of 100 Hz. When with a delay  $t_1 = 1.9$  s we then suddenly saturate  $T_x, -T_z$ , no induced signal appears.

At the time  $t_1 = 1.9$  s  $T_x$ , and  $T_y$ , are empty for both schemes a and b, because one of them is decaying at a rate of  $6.5 \text{ s}^{-1}$  and the other must be depleted via the continuous contact provided by the microwaves. Now remember that according to (1) the height of a microwave induced signal is proportional to the product of a population difference and the difference in radiative rates of the spin levels involved in the transition, and note that  $k_x^r$ , and  $k_z^r$ , differ by a factor of 8 in either scheme. It then follows that the failure to observe a signal after sweeping through the  $T_x, -T_z$ , transition at  $t_1 = 1.9$  s in the above experiment must mean  $N_z(t_1) = 0$ , which is only compatible with scheme a. In scheme b there would always be an appreciable population in  $T_z$ , at  $t = 1.9$  s with or without the constant contact field between  $T_x$ , and  $T_y$ ,. Hence one expects the MIDP signal to be unaffected by this contact field; a conclusion which is in contradiction with the experimental observation.

Because of the similarity in behaviour of the levels  $T_x$ , and  $T_y$ , one can just as well do the previous experiment in an inverse manner. When from  $t = 0$  onward  $T_x, -T_z$ , is swept continuously and at  $t_1 = 1.9$  s the transition  $T_x, -T_y$ , suddenly saturated, again no MIDP signal is observed. This provides additional support for the correctness of scheme a<sup>†</sup>.

In fig. 3a we see that from the MIDP experiments on the  $T_x, -T_y$ , and  $T_x, -T_z$ , transitions it follows that  $k_y^r = k_z^r$ , to within a relative accuracy of about one percent. However, in some additional experiments in which two transitions are swept in succession, it could be established that  $k_z^r$ , is in

<sup>†</sup> As an alternative to the situations of figures 3a and b one might suggest schemes in which decay is predominantly via radiationless processes in such a way, for instance, that  $T_y$ , and  $T_z$ , are short-lived owing to a substantial radiationless decay whereas the long-lived level  $T_x$ , is responsible for the emission,  $k_y^r = k_z^r = 1/8 k_x^r$ . Not only is a hypothesis of this nature unlikely on theoretical grounds, but it also is untenable from an experimental point of view. Even after very long delay times  $t_1$ , the MIDP signals observed are always *positive* which would be impossible for a system where the radiation comes from a relatively long-living level.

fact slightly larger than  $k_y^r$ . If at  $t_1 = 1$  s we sweep through  $T_x' - T_y'$ , (which yields the normal MIDP signal) and subsequently at  $t_1 + 0.002$  s through  $T_y' - T_z'$ , a further small *increase* in light intensity is observed. Here population was transferred to  $T_y'$ , via the first sweep. Then contacting  $T_y' - T_z'$ , populates the empty level  $T_z'$ . A light increase then means that  $k_z^r > k_y^r$ . Inversely when we first sweep through  $T_x' - T_z'$ , and then through  $T_y' - T_z'$ , we observe a small *decrease* in intensity for the second transition. This also leads to the above conclusion.

#### 2.4 Isolation between the spin states

That isolation between  $T_x'$  and  $T_y'$ , and between  $T_x'$  and  $T_z'$ , prevails at 1.2 K has been tested in the familiar way [3]. The apparent decay rate  $\kappa_x$ , derived from two sets of MIDP experiments on the two microwave transitions  $T_x' - T_y'$  and  $T_x' - T_z'$ , was measured as a function of temperature, see fig. 4. Below about 1.5 K the effective decay rate  $\kappa_x$ , of the long-lived level appears to be constant within the experimental accuracy: above this temperature it starts to increase because spin-lattice relaxation sets in. If, as before [3], we assume spin-lattice relaxation to decrease with temperature over the whole region of fig. 4, then the value of  $\kappa_x$ , measured at 1.2 K may be taken to represent the true decay rate  $k_x$ .

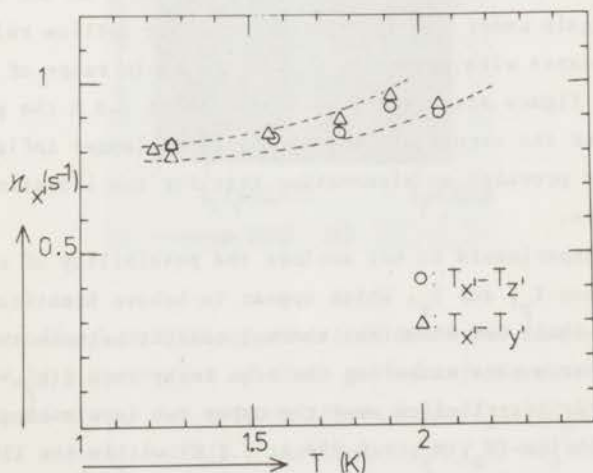


Fig. 4. Apparent decay rate  $\kappa_x$ , as a function of bath temperature.

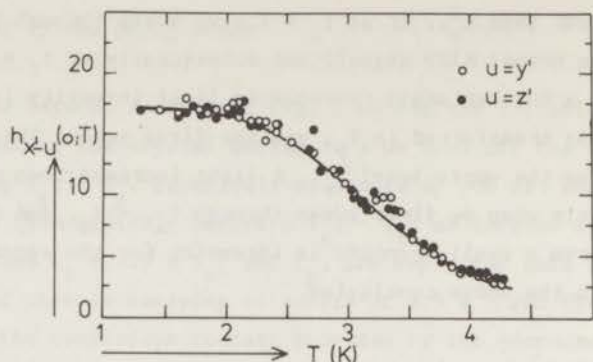


Fig. 5. Steady-state microwave induced phosphorescence signals  $h_{x'-u}(0)$  ( $u = y', z'$ ) as a function of temperature.

Each point in fig. 4 represents the results of a series of MIDP experiments with different delay times  $t_1$ . A quicker test for isolation between the levels is provided by the results of steady-state experiments, where we measured the heights  $h_{x'-y'}(0)$  and  $h_{x'-z'}(0)$  of the signals induced by microwaves under continuous UV illumination. The results are shown in fig. 5. From (1) we see that

$$h_{x'-u}(0;T) \sim \{N_{x'}(0;T) - N_u(0;T)\}; \quad u = y', z' . \quad (2)$$

From fig. 5 it follows that  $h_{x'-y'}(0;T)$  and  $h_{x'-z'}(0;T)$  and thus  $N_{x'}(0;T) - N_{y'}(0;T)$  and  $N_{x'}(0;T) - N_{z'}(0;T)$  are independent of  $T$  in the region of lower temperatures. Again under the assumption that spin-lattice relaxation between the levels decreases with temperature over the whole range of fig. 5, the results of this figure also prove that below about 1.8 K the population distribution over the zero-field components is no longer influenced by such relaxation. This provides an alternative test for the isolation between triplet substates.

The above experiments do not exclude the possibility of effective relaxation between  $T_{y'}$  and  $T_{z'}$ , which appear to behave identically in our experiments. We shall now show that thermal contact between these levels is not established at a rate exceeding the mean decay rate  $\frac{1}{2}(k_{y'} + k_{z'}) = 6.5 \text{ s}^{-1}$ . Thus the molecular distribution over the upper two levels cannot reach Boltzmann equilibrium ( $N_{z'}:N_{y'} = 0.958$  at 1.2 K) within the lifetimes  $\tau_{y'}$  and  $\tau_{z'}$ , and hence the "fast" decay rate exhibited in the MIDP experiments, which is the reciprocal of  $\tau_{\min}$  of table I, is not a Boltzmann average of two unequal rates  $k_{y'}$ ,  $k_{z'}$ .

First we have already noted at the end of the previous section that when the  $T_y, -T_z$ , transition is swept immediately after saturating either  $T_x, -T_y$ , or  $T_x, -T_z$ , a small change in emission intensity results. This change was *positive* in the first case and *negative* in the latter. If there had been relaxation on a time scale short with respect to the interval of the order of 1 ms between the successive sweeps, the sign of the second signals would have been the same for both cases (positive, because of the slightly larger value of  $k^T$  for the upper level).

That no relaxation between  $T_y$ , and  $T_z$ , occurs has further been tested in another experiment especially designed for this purpose. At  $t_1 = 1$  s we first sweep through  $T_x, -T_y$ , and observe an MIDP signal with a height  $h_1$ . Then at  $t_1 + 0.001$  s we saturate  $T_x, -T_z$ , continuously during 0.01 s with a microwave field centered at 3282 MHz and having a 6 kHz frequency modulation to ensure equipartition between  $T_x$ , and  $T_z$ , ( $f = 0.5$  [5]); this results in a signal with the height  $h_2$ , see fig. 6. Finally at  $t_1 + 0.013$  s we again sweep through  $T_x, -T_y$ , which yields  $h_3$ . From fig. 6 we see that  $h_1 : h_2 : h_3 \approx 1 : 0.5 : -0.25$ . This result is exactly what one expects if no dominant

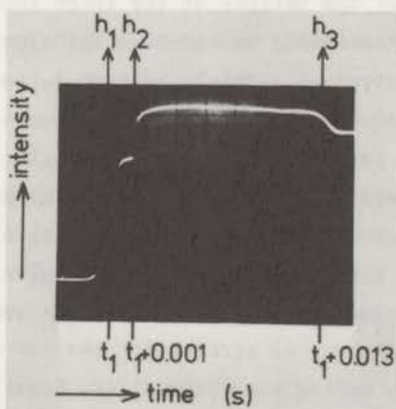


Fig. 6. The result of an MIDP experiment in which the sample has been perturbed by a succession of three periods of microwave irradiation. At the delay time  $t_1 = 1$  s we swept through the  $T_x, -T_y$ , transition. From  $t_1 + 0.001$  s to  $t_1 + 0.011$  s the transition  $T_x, -T_z$ , was continuously saturated via a 6 kHz frequency modulated microwave field. At  $t_1 + 0.013$  s we again swept through the  $T_x, -T_y$ , resonance. Horizontal 2 ms/div.,  $T_{bath} = 1.2$  K.

relaxation between  $T_y$ , and  $T_z$ , occurs. Namely, the effect of the microwaves on the relative populations is as follows:

$$\text{at } t_1 = 1 \text{ s} \quad N_x = n \quad N_y = 0 \quad N_z = 0 \quad (\text{a})$$

$$\text{end of 1st period} \quad N_x = (1-f)n \quad N_y = fn \quad N_z = 0 \quad (\text{b})$$

$$\text{end of 2nd period} \quad N_x = \frac{1}{2}(1-f)n \quad N_y = fn \quad N_z = \frac{1}{2}(1-f)n \quad (\text{c})$$

$$\begin{aligned} \text{Thus } h_1 : h_2 : h_3 &\approx f\{N_x(a) - N_y(a)\} : \frac{1}{2}\{N_x(b) - N_z(b)\} : f\{N_x(c) - N_y(c)\} \\ &= f : \frac{1}{2}(1-f) : f(\frac{1}{2} - (3/2)f) \end{aligned}$$

$$\text{for } f = \frac{1}{2} \quad = 1 : 0.5 : -0.25 .$$

If fast relaxation had occurred this would have tended to equalize the population of  $T_y$ , and  $T_z$ , and  $|h_2|$  and  $|h_3|$  would have been smaller relative to  $h_1$ . In an experiment in which  $T_x - T_y$ , and  $T_x - T_z$ , are interchanged the same ratio is measured for the heights of the three successive signals.

From the previous experiments we may reject the possibility of appreciable relaxation between  $T_y$ , and  $T_z$ , within a time of the order of 1 ms. However we must also check whether relaxation acts on a time scale in the order of 10-100 ms. This possibility was eliminated in our determination of the microwave transfer factor  $f$  [3] in which  $f$  is measured by sweeping the same transition twice in succession. We varied the time duration  $\Delta t$  between the two sweeps; up to  $\Delta t \approx 20$  ms the factor  $f$ , e.g. for  $T_x - T_z$ , does not change. Experiments with longer delay times have not been carried out; in such experiments one would have to correct for the non-negligible decay from the short-lived level  $T_z$ , during the interval  $\Delta t$ . Finally it is noted that we observed a single exponential decay of the individual MIDP signals with corrected base line used in the determination of  $k_z$ , and  $k_y$ , (see section 3.7 and fig. 7 of [3]). If  $k_y$ , and  $k_z$ , would have been different with relaxation between the two levels acting on a time scale comparable to  $\frac{1}{2}(k_y + k_z)^{-1}$  a biexponential decay would have been observed.

Concluding we may state that with the proceeding experiments we have rejected possibility (ii) of 2.2 that  $T_y$ , and  $T_z$ , are tightly coupled by fast spin-lattice relaxation within this pair.

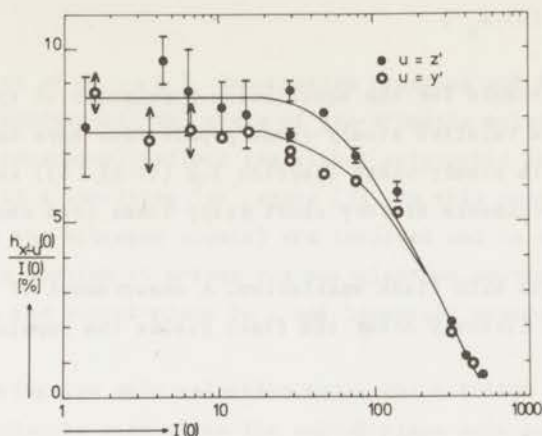


Fig. 7. The temperature effect in TMP. The relative steady-state signal  $h_{x'-u}(0)/I(0)$  is plotted versus the steady-state phosphorescence intensity  $I(0)$ . At high levels of excitation, corresponding to large values of  $I(0)$ , the relative steady-state signal becomes a function of  $I(0)$ ,  $T_{\text{bath}} = 1.2$  K.

Finally we note that the experiments have been performed under conditions of low level excitation. At high excitation levels we again observe the so-called "temperature-effect" (see section 3.3 of [6]: the ratios  $|h_{x'-z}(0)/I(0)|$  and  $|h_{x'-y}(0)/I(0)|$ , where  $I(0)$  is the steady-state phosphorescence intensity were found to decrease with increasing  $I(0)$ , because effective relaxation sets in, see fig. 7. In all investigations of the present kind it is important to verify that the results have not been influenced by such effects, since these may introduce large systematic errors.

### 2.5 Populating rates

So far we have shown that the dynamic behaviour of  $T_y$  and  $T_z$ , with respect to the decay is exactly the same:  $k_y = k_z$ , and from further experiments, the results of which are summarized in table 2, it follows that  $T_y$  and  $T_z$  are also equally populated:  $P_y = P_z$ .

As before [3], the populating rates were determined independently in two ways:

- (i) By calculation from the steady-state equation

$$P_u = N_u(0) k_u, \quad (3)$$

where  $N_u(0)$  stands for the equilibrium population of spin state  $T_u$ . The values of the relative steady-state populations have been determined via experiments in steady-state (section 3.2 (i) of [6]) and independently via MDP experiments at very short delay times (see section 3.2 (ii) of [6]).

- (ii) In experiments with flash excitation. A measurement of the population distribution directly after the flash yields the populating rates, because [3]

$$P_u \sim N_u^f.$$

$N_u^f$  stands for the population of  $T_u$  following a flash. This technique may be used whenever the duration of the flash is much shorter than the reciprocal of the highest rate constant, which may either be a decay rate to the ground state, or a relaxation rate when spin-lattice relaxation is faster than  $T_0 \rightarrow S_0$  decay.

	$\tau_u$	$k_u$	$k_u^r$	$N_u(0)$	$N_u(0)k_u$	$P_u$ flash
	(s)	( $s^{-1}$ ) (rel.)	(rel.)	(rel.)	(rel.)	(rel.)
$T_z$	0.154 (0.002)	6.5 8.1 (0.1)	7.75 (0.10)	0.74 (0.01)	6.0 (0.1)	5.8
$T_y$	0.155 (0.002)	6.45 8.0 (0.1)	7.80 (0.08)	0.74 (0.01)	5.9 (0.1)	5.8
$T_x$	1.242 (0.008)	0.81 1	1	1	1	1

Table 2. Summary of the results.

Lifetimes  $\tau_u$  in s, decay rates  $k_u$  ( $= \tau_u^{-1}$ ) in  $s^{-1}$ , relative radiative rates  $k_u^r$ , relative steady-state populations  $N_u(0)$  and relative populating rates  $P_u$  of the spin components of the phosphorescent triplet state of tetramethylpyrazine in a durene host as measured at about 1.2 K.

The values are averages of  $n$  measurements:  $n = 15$  for  $\tau_x$ ,  $n = 4$  for  $\tau_y$  and  $\tau_z$ ,  $n = 10$  for  $k_y^r/k_x^r$  and  $k_z^r/k_x^r$ , and  $n \geq 3$  for all values of the relative  $N_u(0)$  and  $P_u$ . The experiments are done on different samples, cut from one large single crystal. The numbers in parentheses represent the standard deviation of the mean.



### 3. DISCUSSION

The high rates of  $S_1 \rightarrow T_0$  intersystem crossing and fast (radiative) decay of the phosphorescent  $^3\pi\pi^*$  state of aza-aromatic molecules, as compared to the parent hydrocarbons, reflect the strong spin-orbit coupling (SOC) of the  $^3\pi\pi^*$  state with a low-lying  $^1n\pi^*$  state [7]. In this coupling the lone pair electrons on the nitrogen atom(s) are involved and in an LCAO-MO description of the problem it arises via one-electron one-centre SOC integrals between the out-of-plane  $2p_x$ , and lone-pair orbitals on the nitrogen.

When considering the spin selection rules which follow from the above mechanism for a molecule with  $x'$  as its out-of-plane axis and  $y'$ ,  $z'$  as the in-plane spin axes, one predicts a preferential contamination with singlet character of one or both of the triplet components  $T_{y'}$ ,  $T_{z'}$ , related to the in-plane axes [2]. This component (or these components) then are expected to be dominant in the  $S_1 \rightarrow T_0$  intersystem crossing and  $T_0 \rightarrow S_0$  decay. From theory it further follows that the distribution of singlet contamination over the two states  $T_{y'}$ ,  $T_{z'}$ , due to SOC on a given nitrogen nucleus reduces to a simple geometrical problem. If the direction of the lone pair orbital makes an angle  $\alpha$  with the  $y'$  axis then one expects in a first approximation [2,4]

$$k_{y'}^r/k_{z'}^r = \sin^2\alpha / \cos^2\alpha \quad (5)$$

with, in general, a similar formula for the ratio of the populating rates  $P_{y'}/P_{z'}$ , (compare [2] and [8]).

That this simple picture is not a figment of the imagination is illustrated by a comparison of the data on the  $S_1 \rightarrow T_0$  intersystem crossing and decay of  $T_0$  for quinoline (1-azanaphthalene) and isoquinoline (2-azanaphthalene). In quinoline, where  $\alpha = 0$ , one has  $k_{y'}^r/k_{z'}^r$ , and  $P_{y'}/P_{z'}$ ,  $< 0.04$ , but in isoquinoline where  $\alpha \approx 60^\circ$  (here  $\alpha$  is not known with precision) one finds  $k_{y'}^r/k_{z'}^r = 2.8$  [4] and that  $P_{y'}$ , and  $P_{z'}$ , have the same order of magnitude [9,10].

The remarkable finding that for TMP in durene the ratios  $k_{y'}^r/k_{z'}^r$ ,  $P_{y'}/P_{z'}$ , are all equal to unity, to within an experimental accuracy of better than 2 percent, may therefore be taken as a proof of the suggestion by de Groot et al. [1] that the ESR results for the triplet state of TMP in a durene host must be interpreted on the basis of in-plane spin axes that are rotated away from the symmetry axes of the free TMP molecule. The alternative

explanation that the TMP guests have undergone a molecular rotation relative to the durene molecules they replace, is not only unlikely on steric grounds, but also most improbable in the light of the paths of populating and decay of the phosphorescent state of TMP in durene established in the present study. The ESR studies left a choice between two values of  $\alpha$  [1]; when interpreting the present results on the basis of (5) one would favour  $\alpha = 48^\circ$  rather than  $\alpha = 37^\circ$  (fig. 2).

The present results suggest trying an intriguing experiment. The rate of intersystem crossing (ISC) from the singlet to the triplet manifold is determined by matrix elements of the spin-orbit coupling [6,8]. In an aromatic molecule the dominant contribution to this SOC comes from the one-electron one-center integrals on the N nuclei [2]. As a result, in the optical pumping cycle of TMP in durene one would expect the triplet spin to be generated in the state  $T_y$ , i.e. with its spin angular momentum lying in the plane  $y = 0$  of fig. 2, just as for quinoxaline or phenazine. However, after the fast relaxation into the vibrationless phosphorescent state,  $T_y$  is not an eigenstate but a superposition of the zero-field spin states  $T_y$  and  $T_z$ .

Now suppose one excites the crystal with a pico-second laser flash; if the ISC occurs within  $10^{-10}$  s one would then expect the ensemble to be prepared in a coherent superposition of the spin states  $T_y$  and  $T_z$ . Such coherence, which previously has been created in other (aza)-aromatic molecules by a  $\pi/2$  pulse at the  $T_y - T_z$  resonance frequency [11,12], will manifest itself by the appearance of a macroscopic magnetization in the x-direction oscillating at a frequency of 819 MHz (the  $T_y - T_z$  resonance frequency). The experimental proof that one can prepare a coherent superposition of spin states through optical excitation would not merely be a neat trick of applied quantum mechanics, but it would also further our understanding of the radiationless ISC processes.

#### *Acknowledgement*

We thank Dr. M.S. de Groot of the Koninklijke/Shell Laboratorium, Amsterdam for his stimulating interest in this investigation and the gift of a mixed crystal.

(\*) This chapter has been submitted for publication in *Molecular Physics* by D. Antheunis, B.J. Botter, J. Schmidt and J.H. van der Waals.

## REFERENCES

- [1] De Groot, M.S., Hesselmann, I.A.M., Reinders, F.J., and van der Waals, J.H., to be published in *Molec. Phys.*
- [2] Veeman, W.S., and van der Waals, J.H., 1970, *Molec. Phys.*, 18, 63.
- [3] Schmidt, J., Antheunis, D.A., and van der Waals, J.H., 1971, *Molec. Phys.*, 22, 1.
- [4] Schmidt, J., Veeman, W.S., and van der Waals, J.H., 1969, *Chem. Phys. Lett.*, 4, 341.
- [5] Winscom, C.J., and Maki, A.H., 1971, *Chem. Phys. Lett.*, 12, 264.
- [6] Antheunis, D.A., Schmidt, J., and van der Waals, J.H., 1974, *Molec. Phys.*, in the press; chapter IV of this thesis.
- [7] El-Sayed, M.A., 1963, *J. chem. Phys.*, 38, 2834.
- [8] De Groot, M.S., Hesselmann, I.A.M., Schmidt, J., and van der Waals, J.H., 1968, *Molec. Phys.*, 15, 17.
- [9] Schmidt, J., unpublished results.
- [10] Clarke, R.H., and Hayes, J.M., 1973, *J. chem. Phys.*, 59, 3113.
- [11] Schmidt, J., 1972, *Chem. Phys. Lett.*, 14, 411;  
Van 't Hof, C.A., Schmidt, J., Verbeek, P.J.F., van van der Waals, J.H., 1973, *ibid.*, 21, 437.
- [12] Breiland, W.G., Harris, C.B., and Pines, A., 1973, *Phys. Rev. Lett.*, 30, 158;  
Harris, C.B., Schlupp, R.L., and Schuch, H., 1973, *ibid.*, 30, 319.

## C H A P T E R V I I

### SPIN-LATTICE RELAXATION IN PHOSPHORESCENT TRIPLET STATES

#### 1. INTRODUCTION

Although spin-lattice relaxation in the paramagnetic ground state of a great variety of compounds in ionic solids at low temperatures has been studied during the past forty years [1] a very limited amount of data is available for excited states. Particularly Geschwind and his school succeeded in studying spin-lattice relaxation in optically excited doublet states of ruby and ruby like systems using optical techniques [2,3]. In 1970 Schwoerer [4] and in 1971 Wolfe [5] were the first to present investigations on spin-lattice relaxation in localized excited triplet states in molecular crystals. All these experiments were performed in external magnetic fields and the spin-lattice relaxation rate turned out to be highly anisotropic with respect to the direction of the field [5,6].

In this final chapter we summarize our results on spin-lattice relaxation in the phosphorescent state  $T_0$  in zero magnetic field. The idea behind the present study was to try out in how far one could extend the microwave induced phosphorescence experiments that were so successful in the study of populating and decay of  $T_0$  and apply these to situations where the spin components of  $T_0$  become effectively coupled by spin-lattice relaxation. The motivation for our interest is simple: it is an unanswered question how, in our case, the electronic spin is coupled to the phonon field of the lattice. But even if this fundamental question cannot yet be answered, any data on relaxation in zero-field that become available will be very helpful for the "molecular engineering" required by future experiments.

## 2. SAMPLES AND EQUIPMENT

For the crystals used in the present investigation we refer to the table in § 3 of chapter III. In that chapter we also discussed the principle of the microwave induced phosphorescence experiments together with details of the equipment.

## 3. THE KINETICS OF THE TRIPLET STATE

Here we present a brief outline of the kinetics of the phosphorescent state  $T_0$  in situations where spin-lattice relaxation within  $T_0$  is no longer negligible relative to the decay to the ground state. In the next section we discuss the experiments from which the relaxation rates can be obtained.

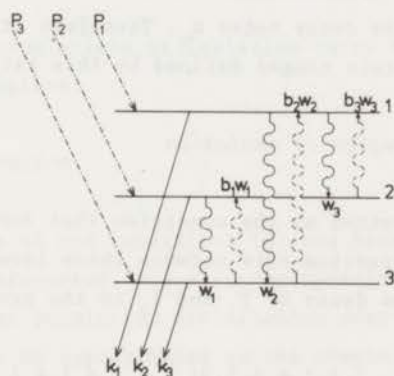


Fig. 1. The kinetic parameters of the phosphorescent triplet state.

In fig. 1 we have indicated all kinetic parameters of the triplet state. The spin components are labelled with 1,2,3 in the order of decreasing energy. As usual  $P_u$  stands for the populating rate of level  $T_u$  and  $k_u = k_u^r + k_u^d$  represents its absolute decay rate;  $u = 1,2,3$ . Relaxation rates are denoted by  $w$ 's; we indicate  $w(1 \rightarrow 2)$  by  $w_3$  for instance (cyclic notation) and the backward rate towards higher energy  $w(2 \rightarrow 1)$  by  $b_3 w_3$ , where  $b_3$  is the Boltzmann factor  $b_3 = \exp(-\Delta E_{1-2}/kT)$  [7,8].

The master equations that describe the time evolution of the population distribution over the three magnetic states are given by

$$\frac{d}{dt} \begin{pmatrix} n_1 \\ n_2 \\ n_3 \end{pmatrix} = \begin{pmatrix} P_1 \\ P_2 \\ P_3 \end{pmatrix} + \begin{pmatrix} -(k_1 + w_2 + w_3) & b_3 w_3 & b_2 w_2 \\ w_3 & -(k_2 + b_3 w_3 + w_1) & b_1 w_1 \\ w_2 & w_1 & -(k_3 + b_1 w_1 + b_2 w_2) \end{pmatrix} \begin{pmatrix} n_1 \\ n_2 \\ n_3 \end{pmatrix} \quad (1)$$

Here  $n_u = n_u(t)$  stands for the instantaneous population of level  $T_u$  at the time  $t$ . We shall reserve capitals for steady-state populations. When working under the condition of low intensity excitation one may assume that there is no saturation so that the relative values of the populating rates  $P_u$  are not affected by depletion of the ground state [9].

As a rule spin-lattice relaxation rates increase with increasing temperature. On the contrary the rate constants determined by the optical pumping process, the  $P_u$ ,  $k_u^r$  and  $k_u^d$ , are essentially temperature independent in the low temperature region of present interest, cf. chapter I. On changing temperature one expects a considerable variation of the ratio between the relaxation rates  $w_v$  and the decay rates  $k_u$ . Therefore it is practical to distinguish three temperature ranges defined by this ratio [7].

### 3.1 The low temperature region of isolation

This region is determined by the condition that for each pair of spin components  $T_j, T_l$  the relaxation rate between these levels,  $w_{jl}$ , must be negligible relative to the decay of  $T_j$  and  $T_l$  to the ground state; hence

$$w_{ij} \ll \min(k_j, k_l); \quad i, j, l = 1, 2, 3; \quad i \neq j \neq l. \quad (2)$$

Then (1) simplifies to

$$\frac{d}{dt} \begin{pmatrix} n_1 \\ n_2 \\ n_3 \end{pmatrix} = \begin{pmatrix} P_1 \\ P_2 \\ P_3 \end{pmatrix} + \begin{pmatrix} -k_1 & & \\ & -k_2 & \\ & & -k_3 \end{pmatrix} \begin{pmatrix} n_1 \\ n_2 \\ n_3 \end{pmatrix} \quad (3)$$

These equations are uncoupled and the spin levels behave independently.

When the isolation condition (2) is satisfied information about the spin-lattice relaxation can not be obtained, but instead, one can study the process of filling into and decay from the individual spin components of  $T_0$ . By lowering of the temperature through pumping of the helium bath molecules with a short-lived phosphorescence, say less than 0.5 s, usually can be made to

fulfil the isolation condition. For instance, for the series of three-ring aromatic molecules studied in chapter IV this condition was satisfied at 1.2 K for all members of the series. Hence the relaxation times for  $T_0$  of anthracene in a biphenyl crystal must be at least one second, see chapter IV. Also in isotopically mixed crystals of aromatic hydrocarbons relaxation occurs at the time scale of seconds at temperatures of pumped helium [4,10]. However, as we shall see, phenanthrene in biphenyl or fluorene provides intriguing exception. Even at 1.2 K the relaxation times are about 1 ms, approximately 1000 times faster than the decay of  $T_0$  to the ground state.

After illuminating the sample during a relatively long period of time  $\gg \max\{k_i^{-1}\}$ , all  $dn_i/dt = 0$  and a steady-state population distribution is established. When isolation prevails one has

$$P_i = k_i N_i^1. \quad (4)$$

For what follows the populations at isolation carry the upper label 1, denoting lowest temperature.

### 3.2 The intermediate region

When at least one of the conditions (2) has broken down then not only the populating and decay processes, but also the spin-lattice relaxation takes part in determining the population distribution over the zero-field levels. Then (1) can no longer be approximated to the simple diagonal form (3) and one must consider the full set of equations. Without further simplifications these equations present a considerable problem, since they contain *all nine* kinetic parameters  $P_u$ ,  $k_u$  and  $w_v$  and have solutions for the time evolution of the populations of the spin states which are the sums of three exponentials.

It is evident that reliable results for the  $w$ 's can be obtained only when the other constants, i.e. the  $P_u$  and  $k_u$ , are known from experiments at a lower temperature where the isolation condition (2) is fulfilled. Then one may try to obtain the three  $w$ 's from a tri-exponential fit to an experimental decay curve, for instance the decay of the phosphorescence intensity after termination of the illumination of the sample. Such a procedure is quite tricky and one should try to avoid it. Nevertheless there is a singlet report in the literature where the relaxation rates are determined by adjusting a sum of three exponentials to the decay of the phosphorescence intensity [11].

Very recently, Zuchlich et al. [12] simplified the set (1) by generating a quasi-two-level system via continuous saturation of one of the zero-field transitions with a resonant microwave field. Then one considers a new set of only *two* coupled differential equations and the solutions for the time evolution of the spin state populations now are sums of two exponentials, which certainly results in a more manageable problem.

Apart from the inherent inaccuracy arising in the analysis of experimental curves by sums of more than a single exponential, there is another motive against such methods, in particular when the total phosphorescence intensity is monitored. Since the intensity emitted in a relatively wide wavelength interval is far from specific for the molecules one tries to study, contributions from impurity emissions may introduce large systematic errors.

We have developed a method in which the analysis of the time evolution of signals is avoided, and where instead one observes the change in the steady-state situation brought about by saturating one of the zero-field microwave transitions specific for the molecule of interest. An example of this will be given in § 4.1, while the basic idea is as follows. After a transient period the time dependence disappears when the sample is continuously illuminated because a steady-state situation then is established. The steady-state equations that result when setting all  $dn_i/dt = 0$  in (1), can be rewritten into a form in which the relaxation rates are the unknowns:

$$\begin{pmatrix} k_1 N_1 - P_1 \\ k_2 N_2 - P_2 \\ k_3 N_3 - P_3 \end{pmatrix} = \begin{pmatrix} 0 & -(N_1 - b_3 N_3) & -(N_1 - b_3 N_2) \\ -(N_1 - b_1 N_3) & 0 & N_1 - b_3 N_2 \\ N_1 - b_1 N_3 & N_1 - b_3 N_3 & 0 \end{pmatrix} \begin{pmatrix} w_1 \\ w_2 \\ w_3 \end{pmatrix} \quad (5)$$

Only two of the equations are linearly independent and so the determinant of the coefficients matrix on the right vanishes. This follows by taking the sum of the three equations (5) which reads:

$$P_1 + P_2 + P_3 = k_1 N_1 + k_2 N_2 + k_3 N_3 \quad (6)$$

This merely expresses the condition for steady-state: the total rate of entering into the triplet state must be equal to the total that disappears from it, irrespective of what happens within the manifold of zero-field states.



Now the idea is that the steady-state population distribution in the intermediate region is determined by *all* kinetic parameters. Thus in the case that the  $P_u$  and  $k_u$  are already known the  $w$ 's must follow from the measurement of the steady-state population distribution. Although we need three equations only two are provided by (5). In § 4 we show how, by continuous saturation of a zero-field transition, one can generate a new steady-state and thus add an independent equation to (5). The  $w$ 's will then be expressed in terms of simple experimental observables, viz. the heights of microwave induced phosphorescence signals.

### 3.3 The high temperature region of dominant relaxation

Here all relaxation rates exceed the decay to the ground state, i.e.

$$w_i \gg \max(k_j, k_l); \quad i, j, l = 1, 2, 3; \quad i \neq j \neq l. \quad (7)$$

Hence after a perturbation the triplet system relaxes towards Boltzmann equilibrium according to:

$$\frac{d}{dt} \begin{pmatrix} n_1 \\ n_2 \\ n_3 \end{pmatrix} = \begin{pmatrix} -(w_2+w_3) & b_3 w_3 & b_2 w_2 \\ w_3 & -(b_3 w_3 + w_1) & b_1 w_1 \\ w_2 & w_1 & -(b_1 w_1 + b_2 w_2) \end{pmatrix} \begin{pmatrix} n_1 \\ n_2 \\ n_3 \end{pmatrix}. \quad (8)$$

Again, when writing these equations into a form with the relaxation rates as the unknowns, only two of them are linearly independent. This can be visualized by adding the three equations (8), which gives

$$\frac{d}{dt} (n_1 + n_2 + n_3) = 0. \quad (9)$$

Equations (8) and (9) only hold during a period of time short relative to the shortest of the life times  $k_u^{-1}$ .

Because of (9), the general solution of (8) is a sum of two exponentials:

$$n_i(t) = c_{i,1} e^{-\lambda_1 t} + c_{i,2} e^{-\lambda_2 t} + c_{i,3}. \quad (10)$$

The constants depend on the particular level  $T_i$  and on the initial conditions.

Approximating the Boltzmann factors  $b_i$  by unity the exponents can be

shown to read:

$$\lambda_{1,(2)} = \frac{(w_1+w_2+w_3)}{(-)} + \frac{\sqrt{w_1(w_1-w_2)+w_2(w_2-w_3)+w_3(w_3-w_1)}}{(-)} \quad (11)$$

$$= w_{+(-)} w_{-} .$$

Hence  $w_{+} = (\lambda_1 + \lambda_2)/2$  is a measure for the mean relaxation rate  $\bar{w}$ ,

$$w_{+} = 3 \bar{w} . \quad (12)$$

Further  $w_{-}$  is determined by the difference  $(\lambda_1 - \lambda_2)/2$  and proportional to the r.m.s. deviation of the mean, viz.

$$w_{-} = 3 \sqrt{\frac{(w_1 - \bar{w})^2 + (w_2 - \bar{w})^2 + (w_3 - \bar{w})^2}{3.2}} . \quad (13)$$

#### 4. THE MEASUREMENT OF SPIN-LATTICE RELAXATION RATES

We have done a large number of experiments to try and find out what methods work best for determining spin-lattice relaxation rates in the different regions of the previous section. We here give some of the results obtained thusfar. These are meant to illustrate what can be done and how; they should be regarded as a starting point for future work rather than as a report of a completed investigation.

##### 4.1 Acridine in biphenyl

Acridine in biphenyl between about 1.5 K and 4 K provides an illustrative example for a system in the intermediate temperature region, where spin-lattice relaxation and decay to the ground state roughly occur on the same time scale, see § 3.2.

As noted in § 3.2 we can only solve the separate relaxation rates if we can generate at least one further equation in addition to the set (5) by doing experiments in which the steady-state distribution has been altered in a known way. In practice it was found that a convenient way to do this is the following. One does a set of three experiments in each of which two of the steady-state populations are forced to be equal by continuous irradiation of

the corresponding microwave transition; at a certain moment one then breaks this contact, sweeps immediately through one of the other transitions and observes the change in phosphorescence intensity.

Suppose, for instance, that  $T_x - T_y$  at 531.7 MHz in fig. 2 is saturated and let  $(x=y)$  express this situation with continuous microwave contact between  $T_x$  and  $T_y$ . Then are the *new* steady-state populations

$$N_x(x=y) = N_y(x=y) \text{ and } N_z(x=y)$$

to which the set (5) still applies. After identifying the labels 1 with x, 2 with y and 3 with z, and approximating the Boltzmann exponents  $b_i$  by unity, we form from (5) a linear combination by taking the sum of  $k_z$  x the first line and  $-k_x$  x the third line. This gives

$$k_z(N_x(x=y) - N_z(x=y)) - (P_x/k_x - P_z/k_z) = -(N_x(x=y) - N_z(x=y))w_{y-z} - (1+k_z/k_x)(N_x(x=y) - N_z(x=y))w_{x-z} \quad (14)$$

Here we have already used  $N_x(x=y) = N_y(x=y)$ , by which the term containing  $N_y - N_x$  in (14) is eliminated. Because  $P_u = k_u N_u^1$ , see (4), we may replace  $P_x/k_x$  and  $P_z/k_z$  by  $N_x^1$  and  $N_z^1$  respectively. Then (14) is rewritten as:

$$w_{y-z} + (1+k_z/k_x)w_{x-z} = \left( \frac{N_z^1 - N_x^1}{N_z(x=y) - N_x(x=y)} - 1 \right) k_z = \left( \frac{h_{x-z}(0; \text{ISOL.})}{h_{x-z}(0; T; x=y)} - 1 \right) k_z \quad (15)$$

$h_{x-z}(0)$  stands for the height of the microwave induced phosphorescence signal in steady-state on sweeping through the  $T_x - T_z$  resonance and ISOL. refers to isolation.

For the evaluation of all three relaxation rates it is simplest to perform two additional experiments. For instance during which  $T_y - T_z$  is continuously saturated and the other where  $T_x - T_z$  is in constant contact. In both cases we monitor the signal that results after a sweep through the  $T_x - T_y$  resonance,  $h_{x-y}$ . The equations for the relaxation rates that belong to these experiments read:

$$(k_y/k_x + 1)w_{x-y} + (k_y/k_x)w_{x-z} = \left( \frac{h_{x-y}(0; \text{ISOL.})}{h_{x-y}(0; T; y=z)} - 1 \right) k_y \quad (16)$$

$$(k_y/k_x + 1)w_{x-y} + w_{y-z} = \left( \frac{h_{x-y}(0; \text{ISOL.})}{h_{x-y}(0; T; x=z)} - 1 \right) k_y \quad (17)$$

The result that we have obtained via the system of equations (15), (16) and (17) is represented in fig. 2.

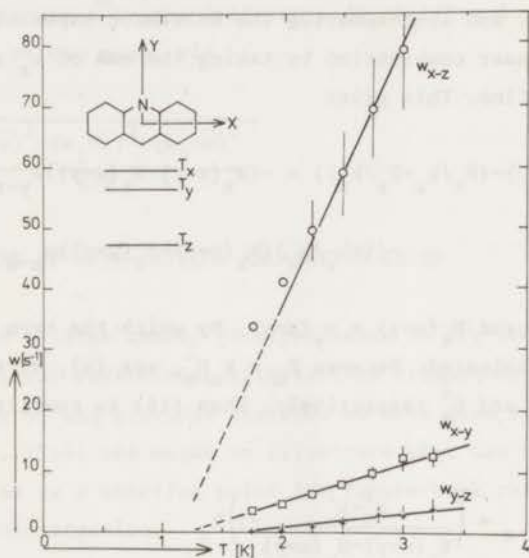


Fig. 2. Spin-lattice relaxation rates between the separate pairs of zero-field levels of  $T_0$  as a function of temperature for acridine in biphenyl in the intermediate temperature region.

The straight lines are only meant as a connection through the experimental points, because the temperature range is too limited to give an explicit temperature dependence. The dotted lines indicate that at 1.2 K the relaxation rate must be smaller than the decay rate  $k_z = 4 \text{ s}^{-1}$  of  $T_z$ , in order to fulfil the isolation condition (2), which applies for the present system, see chapter IV.

We see that the rates differ considerably,  $w_{x-z}$  exceeds  $w_{x-y}$  by a factor of about 8 and  $w_{y-z}$  by a factor in the order of 30. The temperature range is too limited for allowing us to give the explicit temperature dependence of the separate rates. But the example nicely demonstrates how the individual relaxation rates can be measured via experiments under various steady-state conditions and second it shows that such rates may be quite different for different pairs of zero-field levels. We are presently studying acridine at temperatures above 4.2 K.

We conclude this part on acridine with a final remark on how the experiment is done, for instance for the measurement of  $h_{x-z}(0;T;x=y)$ .  $T_x - T_y$  is saturated by setting the microwave oscillator at the resonance frequency of 531.7 MHz and in addition applying a frequency modulation at a rate that is much higher than the largest kinetic constant of the spin levels involved in the transition. This constant may be a decay rate to the ground state or a spin-lattice relaxation rate. For acridine we have used a modulation frequency of about 5 kHz. Although, as usual, the signal  $h_{x-z}$  is generated by a microwave sweep through the  $T_x - T_z$  transition, we must take special precautions that the saturating microwave field at the  $T_x - T_y$  transition does not disturb the measurement in an uncontrolled way. Therefore we change the central frequency at 531.7 MHz to 570 MHz, which is far from resonance, just before the sweep through  $T_x - T_z$  occurs.

#### 4.2 Quinoxaline in durene and perdeuteronaphthalene

Quinoxaline is such a widely studied system that it might almost be called the "ruby" in the field of aromatic phosphors. Therefore we initially chose this compound for our experiments on spin-lattice relaxation in triplet states. We here present the results in the region of dominant relaxation.

Above about 2.5 K quinoxaline- $h_6$ , when dissolved in a single crystal of durene- $h_{14}$  or of naphthalene- $d_8$ , provides an illustration of a system with dominant relaxation, see § 3.3, for which we cannot use the simple steady-state methods described above. In the steady-state the populations of the spin components are in Boltzmann equilibrium. This distribution depends only on the zero-field splitting and on the temperature; it is insensitive to the precise values of the relaxation rates. Hence one is forced to study relaxation by some perturbation creating a non-Boltzmann distribution, followed by a subsequent monitoring of the transient towards equilibrium. Similar methods

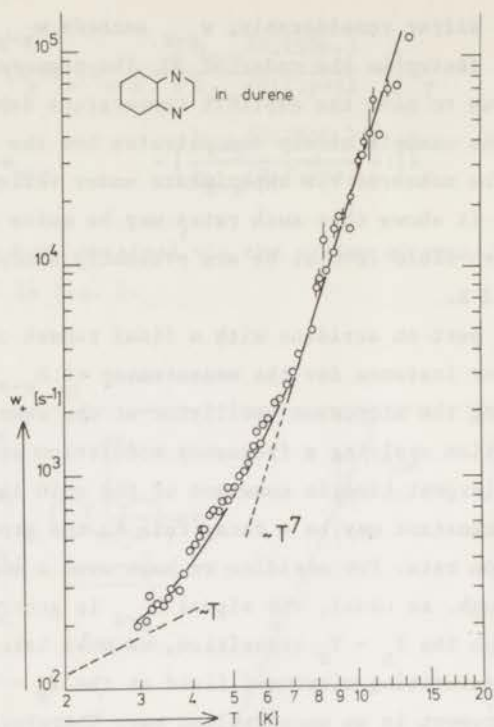


Fig. 3. A double logarithmic plot of the relaxation rate  $w_+ = 3 \bar{w}$  for quinoxaline- $h_6$  in durene- $h_{14}$  against the temperature.

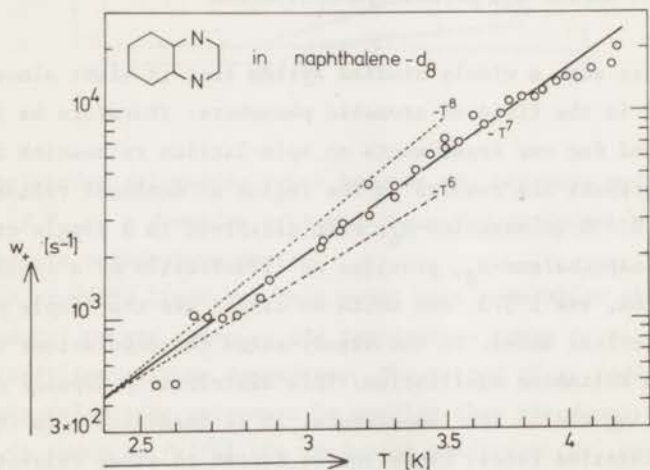


Fig. 4. A double logarithmic plot of the relaxation rate  $w_+ = 3 \bar{w}$  for quinoxaline- $h_6$  in naphthalene- $d_8$  against the temperature.

are well-known from the studies of spin-lattice relaxation rates in substances like ruby with excited doublets [2,3]. We have used two different methods for creating a non-Boltzmann situation:

- (i) *The microwave induced phosphorescence (MIP) experiment in steady-state.*

When the system is continuously illuminated a steady-state population according to a Boltzmann distribution is established. When at the time  $t = 0$  one suddenly sweeps through the  $T_x - T_z$  resonance at 3641 MHz and momentarily equalizes the populations of the two levels an abrupt increase of the phosphorescence intensity is observed and the signal decays biexponentially. One can show that if one takes the steady-state intensity as a base line the constant term arising from  $c_{i,3}$  in (10) vanishes.

Later, in fig. 9, we shall see an example for tetramethylpyrazine in durene which clearly shows that the decay of the transient after an MIP experiment in steady-state contains two time constants corresponding to the constants  $\lambda_1^{-1}$  and  $\lambda_2^{-1}$  in (10).

We have represented the temperature dependence of the quantity  $w_+$ , equal to three times the mean relaxation rate in  $T_0$ , of quinoxaline in durene and in naphthalene- $d_8$  in figs. 3 and 4. The naphthalene mixed crystal has only been studied below 4.2 K. Remark that in this host the relaxation is much faster at the lower temperatures and moreover depends on  $T^7$  with a higher constant of proportionality. Quinoxaline in durene in a magnetic field was studied by Wolfe [5] and Schwoerer et al. [4], who studied also the perdeuteronaphthalene mixed crystal. Particularly in the latter case we found appreciably faster relaxation in zero-field.

- (ii) *Sudden excitation of the system by a light flash.*

When the duration of the flash is short relative to the time scale of the relaxation, the population distribution over the levels just after the flash is proportional to the populating rates  $P_u$ , cf. section 2.5 (ii) of VI. Then the total phosphorescence intensity,  $I(t) = \sum n_u(t) k_u^r$ , decays biexponentially, of course only during a limited  $u$  period of time because it is subject to the same limitations as (8). On a longer time scale the triplet state decays while its spin levels maintain Boltzmann equilibrium. Then the phosphorescence decays via a single exponent at the mean rate  $\bar{k} = 1/3 \sum k_u^r$ .

In order to avoid contributions from impurity emissions the  $u$  biexponential decay can best be monitored via microwave induced delayed phosphorescence experiments.

We have checked that the continuous illumination experiment and the experiments after flash excitation yield the same result.

#### 4.3 Phenanthrene in biphenyl and fluorene

Clearly phenanthrene would be an interesting system for studying the populating and decay of  $T_0$ . This proved impossible with our zero-field methods (MIDP), because to our surprise for phenanthrene in a biphenyl or fluorene crystal we observe a spin-lattice relaxation that is of the order of 1000 times faster than the decay to the ground state ( $\tau(T_0) \approx 2.8$  s) [7]. Nevertheless Sixl has succeeded to determine the lifetimes of the separate spin levels via ESR in a magnetic field [7].

Let us first see how in practice one can check whether there is dominant relaxation or not. For a system with dominant relaxation a Boltzmann distribution over the three zero-field levels is established under steady-state conditions. Thus, when  $N_z$  is the steady-state population of the spin component  $T_z$  at the temperature  $T$ , then

$$N_y = N_z \exp(-\Delta E_{y-z}/kT) \approx N_z (1 - \Delta E_{y-z}/kT),$$

so that  $N_z - N_y = N_z (\Delta E_{y-z}/kT)$ .

Since the total number of molecules in the excited state  $T_0$ , see (6), hardly changes with temperature in the region of dominant relaxation, the height of the MIP signal  $h_{z-y}(0)$ , which is proportional to  $N_z - N_y$ , varies as the inverse temperature:

$$h_{z-y}(0;T) \sim \frac{1}{T}. \quad (18)$$

A behaviour according to (18) is shown in fig. 5 where we have plotted  $1/h_{z-y}$  versus  $T$  for phenanthrene in biphenyl and moderately intense irradiation of the sample. At the  $\lambda$ -point of helium,  $\approx 2.2$  K, a discontinuity appears: the heights of the signal makes a sudden jump by a factor of about 1.5. This change must be attributed to the temperature effect of section 3.3 of chapter IV. Below 2.2 K, where the helium contains a super fluid part, the cooling by the bath is far more effective than at higher temperature. At maximum irradiation with a 1kW mercury arc the jump in signal height even increases to a factor 3.5; but on reducing the intensity to about one percent



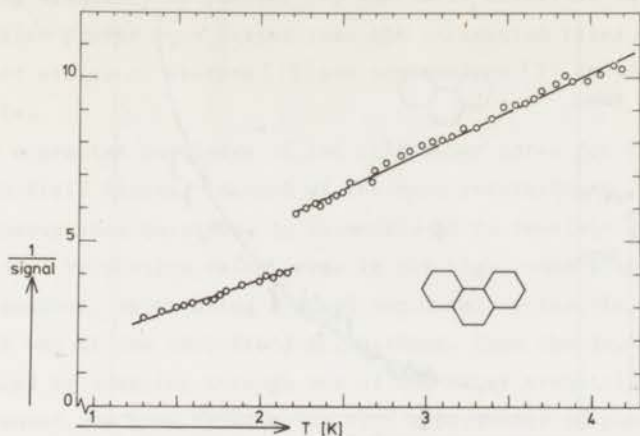


Fig. 5. The inverse of the height of the microwave induced phosphorescence signal on sweeping through the  $T_z - T_y$  resonance,  $1/h_{z-y}(0)$  versus temperature for phenanthrene in biphenyl.

we could cause the discontinuity to disappear. It cannot be stressed enough that when studying the dynamic behaviour of a photo excited triplet state at very low temperature one should work at a low level of excitation and, if necessary improve the S/N ratio by averaging techniques rather than by increasing the light flux. Many experiments reported in the literature should be regarded with caution in this respect.

In fig. 6 we have plotted the mean relaxation rate versus  $T$  for phenanthrene in biphenyl in the temperature range between about 1.2 and 15 K. The result is obtained by the analysis of the biexponential decay of the MIP signal in steady-state stimulated via a microwave sweep through the  $T_y - T_z$  resonance at 2801 MHz, see § 4.2 (i). In fig. 7 we plotted the experimental points between 1.2 and 4.2 K. Below about 5 K the relaxation rate clearly varies linearly with temperature. Above 5 K the temperature dependence seems to be quadratic, but this might in reality be a bend towards say a  $T^7$  dependence. Fig. 7 further shows that phenanthrene in fluorene behaves quite similar to the biphenyl mixed crystal.

The intriguing question that emerges from the present results, and which

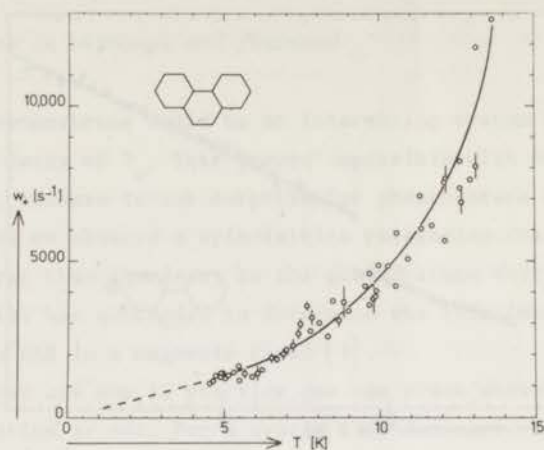


Fig. 6. Relaxation rate  $w_+ = 3 \bar{w}$  for phenanthrene in biphenyl. The experimental points in the area below 4.2 K, here represented by the dotted line, are given in fig. 7.

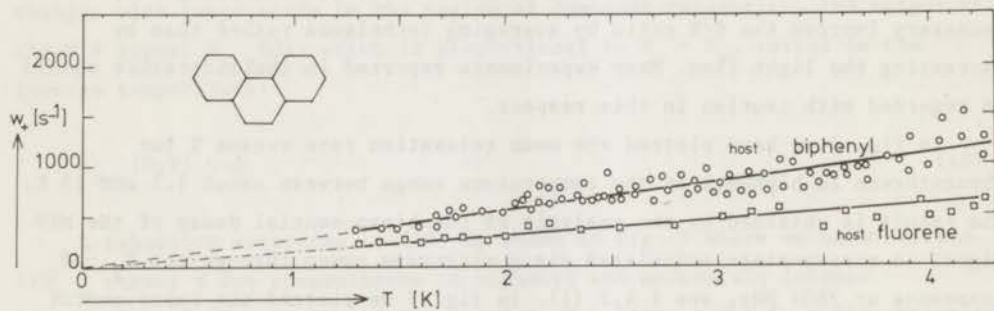


Fig. 7. Relaxation rate  $w_+$  for phenanthrene in biphenyl and fluorene against temperature below 4.2 K.

we cannot answer, is why the relaxation in phenanthrene at 1.2 K is at least a few hundred times faster than that between the zero-field levels of  $T_0$  in the three-ring aromatics of chapter IV, similarly dissolved in a biphenyl crystal. It also proves much faster than the relaxation rates observed for the phosphorescent states of benzene [10] and naphthalene [7] in isotopically mixed crystals.

Perhaps a precise knowledge of the relaxation rates for the separate pairs of zero-field states, instead of the mean relaxation  $w_+ = 3\bar{w}$  would help us to answer this question. In principle it is possible to measure the three individual relaxation rates, even in the high temperature range of dominant relaxation, by creating a quasi-two-level system via continuous saturation of one of the zero-field transitions. Then the decay of a MIP signal produced by sweeping through one of the other transitions should follow a single exponent. We have tried to do such experiments on phenanthrene in biphenyl. It turned out that it is hard to get reliable results, because of the difficulty of achieving exact saturation when relaxation is so fast. Although we have not yet succeeded the continuation of these experiments is worthwhile.

#### 4.4 Tetramethylpyrazine in durene

(i) Between about 1.8 and 4.2 K the system of the previous chapter allows for simple but unusual application of the experiments in the intermediate temperature region. It turned out that for all temperatures in this range the spin levels  $T_y$ , and  $T_z$ , carry the same population in steady-state,  $N_y = N_z$ . Let us first see how this follows from experimental observations.

In chapter VI we studied the kinetics of the triplet state for this system under the condition of isolation between the spin states. For the definition of spin axes and ordering of the levels we refer to fig. 1 of chapter VI. In table 2 of that chapter we summarized our results, which proved that the spin states  $T_y$ , and  $T_z$ , behave identically in populating and decay. This resulted in an equality of the steady-state population for these levels:  $N_z^1/N_x^1 = N_y^1/N_x^1 = 0.74$ . From fig. 5 of chapter VI we further observe that at all temperatures between 1.2 and 4.2 K

$$h_{x^1-z^1}(0;T) = h_{x^1-y^1}(0;T) . \quad (19)$$

These  $h$ 's are the signals that represent the change in phosphorescence intensity when during constant illumination of the sample the resonance  $T_{x'} - T_{z'}$ , or  $T_{x'} - T_{y'}$ , is suddenly hit by a microwave field; they are proportional to the product of a population difference and a difference in radiative rates see (1) of chapter IV:

$$h_{x'-z'}(0;T) \sim (N_{x'} - N_{z'}) (k_{z'}^r - k_{x'}^r)$$

and similar for  $h_{x'-y'}$ . But since  $k_{z'}^r = k_{y'}^r$ , this means because of (9) that for all temperatures of fig. 5 of chapter IV,  $N_{y'} = N_{z'}$ .

Thus, because of this equality, one here obtains a single equation similar to (15) - (17) derived in connection with the continuous saturation experiments on acridine. One now has

$$w_{y'-x'} + (1 + k_{x'}/k_{z'}) w_{z'-x'} = \left( \frac{h_{x'-z'}(0; \text{ISOL.})}{h_{x'-z'}(0; T)} - 1 \right) k_{x'} \quad (20)$$

Apparently for the exceptional case of TMP in durene, where at each temperature in the whole intermediate region the population of two levels is equal, one can eliminate the relaxation rate between these levels and measure the sum of the rates between the other two pairs ( $1 + k_{x'}/k_{z'} \approx 1$ ) simply from the heights of steady-state signals. The result is plotted in fig. 8.

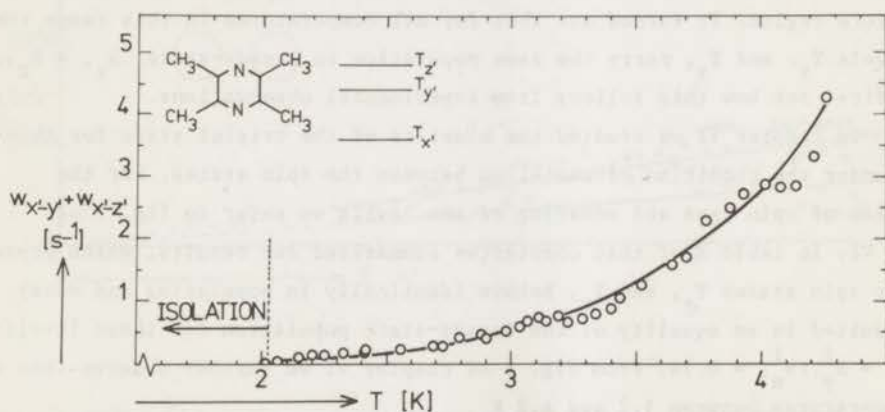


Fig. 8. The sum of the relaxation rates between the pairs of zero-field levels  $T_{x'} - T_{y'}$ , and  $T_{x'} - T_{z'}$ , for TMP in durene,  $w_{x'-y'} + w_{x'-z'}$ , against temperature.

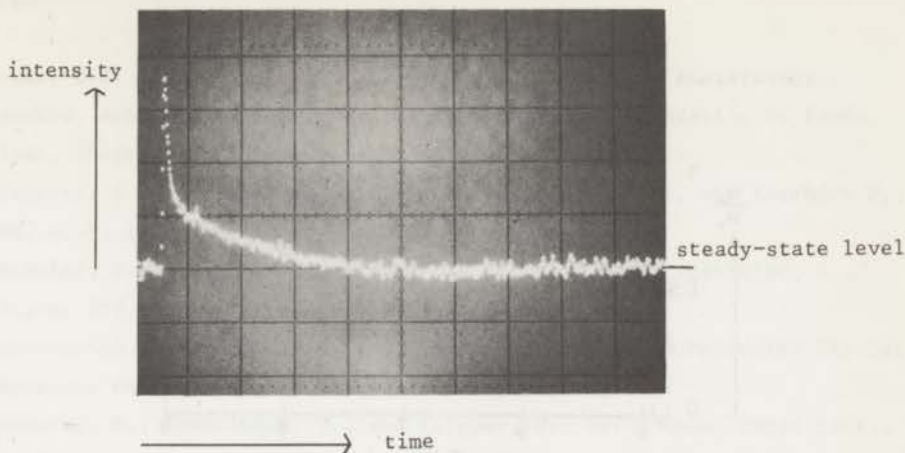


Fig. 9. Microwave induced phosphorescence signal in steady-state following on sweeping through the  $T_y$ , -  $T_x$ , resonance for TMP in durene.  $T = 7.84$  K. Horizontal 1 ms/div.

(ii) Above a temperature of about 5 K the system is to be classified in the region of dominant relaxation. We have studied it up to 9 K. In the range between 5 and 9 K the mean rate  $w_+$  approximately varies as  $T^8$ . In fig. 9 we show the MIP signal at 7.84 K on sweeping through the  $T_y$ , -  $T_x$ , transition. It is clearly seen that the decay of the signal contains two time constants according to (10). The interesting feature is that for TMP in durene the ratio of the relaxation parameters  $w_-/w_+$ , as defined in (11) - (13), shows a marked increase with temperature, see fig. 10 where  $w_-/w_+$  tends to unity at the higher temperatures. Since this ratio approaches unity so closely TMP in durene provides a nice illustration of the fact that the decay of the MIP signals in steady-state contain two time constants, viz.  $\lambda_1^{-1}$  and  $\lambda_2^{-1}$  with  $\lambda_1 = w_+ + w_-$  and  $\lambda_2 = w_+ - w_-$ . This is shown in fig. 9. The fact that  $w_- \approx w_+$  implies that one of the three rates between the spin levels must be far higher than the other two.

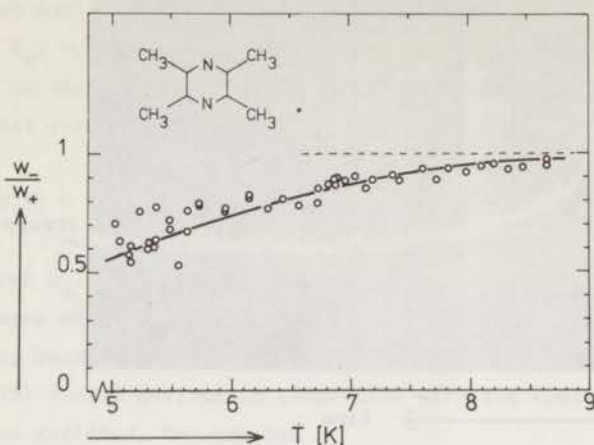


Fig. 10. The ratio of the r.m.s. deviation of the mean relaxation rate and the mean relaxation rate against temperature for TMP in durene.

Via experiments in which one of the zero-field transitions is continuously saturated by a resonant microwave field, and the system is thus reduced to a quasi-two-level system, we could decide that the rate for relaxation between the two radiative levels  $T_z$  and  $T_{y'}$ ,  $w_{z'-y'}$ , increases more rapidly with the temperature than  $w_{z'-x'}$  and  $w_{y'-x'}$ . It may well be that this remarkable finding is related to the skewness of the in-plane spin axes  $y'$  and  $z'$  in this system. Since the skewness must be imposed by the crystalline environment one would expect the precise location of the spin axes to be strongly affected by molecular and (or) crystalline vibrations. On raising the temperature higher vibrational states will become accessible and a random "scrambling" of the  $T_x$  and  $T_z$  spin states might result which could lead to fast relaxation.

## REFERENCES

- 1 Gorter, C.J., Paramagnetic Relaxation, 1947 (Elsevier: Amsterdam);  
Manenkov, A.A., and Orbach, R., 1966, Spin-lattice relaxation in ionic  
solids, (Harper and Row: New York, Evanston and London).
- 2 Geschwind, S., in Proceedings of the Colloque Ampère XV, ed. Averbuch P.,  
1968, p. 61 (North Holland: Amsterdam).
- 3 Geschwind, S., in Electron Paramagnetic Resonance, ed. Geschwind, S.,  
1972, p. 353 (Plenum Press: New York and London).
- 4 Communicated by Schwoerer, M., and Sixl, H., at the 5th Molecular Crystal  
Symposium, Philadelphia 1970;  
Schwoerer, M., Konzelmann, U., and Kilpper, D., 1972, Chem. Phys. Lett.,  
13, 272.
- 5 Wolfe, J.P., 1971, Chem. Phys. Lett., 10, 212.
- 6 Konzelmann, U., and Schwoerer, M., 1973, Chem. Phys. Lett., 18, 143.
- 7 Sixl, H., 1971, Thesis, University of Stuttgart.
- 8 Abragam, A., The principles of nuclear magnetism, 1970 (Oxford University  
Press).
- 9 Schweitzer, D., Zuclich, J., and Maki, A.H., 1973, Molec. Phys., 25, 193.
- 10 van Egmond, J., 1973, Thesis, University of Leiden.
- 11 Hall, L.H., and El-Sayed, M.A., 1971, J. chem. Phys., 54, 4958.
- 12 Zuclich, J., von Schütz, J.U., and Maki, A.H., 1974, Molec. Phys., to be  
published.

## SAMENVATTING

Dit proefschrift bevat een studie over de laagst aangeslagen triplettoestand van enkele vlakke organische molekulen met geconjugeerde bindingen. Als zo'n aromatisch molekuul vanuit zijn singulet grondtoestand  $S_0$  via absorptie van ultraviolet licht in de eerste toegestane absorptieband  $S_1 + S_0$  wordt aangeslagen, neemt men naast enige kortlevende  $S_1 \rightarrow S_0$  emissie vanuit de eerste aangeslagen singuleettoestand  $S_1$  ( $\approx 10^{-8}$  s) in het algemeen waar dat het systeem nalicht in het zichtbare gebied van het optische spectrum met een levensduur variërend van 1 ms tot 10 s. Dit nalichten noemt men *fosforescentie*. Blijkbaar wordt in de meeste molekulen een aanzienlijk deel van de elektronische aanslagenergie van de singuleettoestand  $S_1$  omgezet in trillingsenergie van de kernen via een spin-verboden stralingsloze overgang naar de elektronenconfiguratie van de laagste triplettoestand  $T_0$ . Van hieruit kunnen de molekulen terugkeren naar hun diamagnetische grondtoestand  $S_0$ , hetzij via fosforescentie emissie dan wel opnieuw via een stralingsloos proces.

In tegenstelling tot de situatie in atomen met bolsymmetrie, zijn de drie spincomponenten van de toestand  $T_0$  van een meeratomig molekuul in het algemeen niet ontaard. Door deze nulveldsplitsing bestaat de mogelijkheid elektronspinresonantie experimenten uit te voeren aan de fosforescerende toestand zonder een uitwendig veld aan te leggen. Omdat de afzonderlijke spin-niveaus van  $T_0$  meestal ongelijke kansen hebben om via fosforescentie straling naar de grondtoestand te vervallen, kan de magnetische resonantie optisch worden gedetecteerd.

Alle proeven die in deze dissertatie worden beschreven berusten dan ook op het idee van door microgolven geïnduceerde fosforescentie: met behulp van een microgolfveld dat resonant is met één van de nulveld overgangen van de triplettoestand wordt het verschil in bezetting van twee niet gelijk stralende spinniveaus van de optisch geëxciteerde molekulen verstoord, hetgeen aanleiding geeft tot *variatie* in de fosforescentie intensiteit. De experimenten werden uitgevoerd hetzij tijdens het verval van de fosforescentie na beëindiging van de optische excitatie, dan wel gedurende continue belichting. Onderzocht werden een aantal aromatische molekulen, alle verdund ( $\approx 1 : 10^3$ ) opgelost in kristallijne matrices bij temperaturen variërend van ca. 1.2 K tot 15 K.

De experimenten hadden tot doel twee verschillende aspecten van de kinetiek van de fosforescerende triplettoestand te bestuderen, t.w.:



1. Onderzoek naar de selectiviteit van de processen die de individuele spinniveaus van  $T_0$  bevolken en ontvolken.

2. Spin-roosterrelaxatie tussen de spincomponenten van de triplettoestand.

De hoofdstukken I, II en III zijn bedoeld als inleidende tekst. In het eerste hoofdstuk wordt een korte uiteenzetting gegeven over de bedoelingen van het proefschrift. Hoofdstuk II geeft een indruk van de relevante eigenschappen van en processen in fosforescerende molekulen, terwijl we in hoofdstuk III enkele experimentele zaken belichten.

In het bijzonder ging onze aandacht uit naar het bestuderen van de spin-verboden *stralingsloze* overgangen in de optische pompcyclus van aromatische molekulen, t.w. de  $S_1 \rightarrow T_0$  en  $T_0 \rightarrow S_0$  "intersystem crossing" processen. In hoofdstuk IV worden de proeven bediscussieerd die we aan een reeks iso-elektronische molekulen hebben uitgevoerd: anthraceen, acridine, phenazine en vier gedeutereerde isomeren, alle verdund opgelost in één-kristallen van biphenyl. We hebben deze molekulen op grond van drie overwegingen gekozen.

Allereerst bezitten ze een relatief kort levende triplettoestand. Het is namelijk zo, dat we het preciese gedrag van het bevolken en ontvolken van de spinniveaus van  $T_0$  alleen maar behoorlijk kunnen bestuderen als door voldoende afkoeling een situatie is te bereiken waarbij spin-roosterrelaxatie tussen de spincomponenten aanzienlijk trager verloopt dan het verval van de niveaus naar de grondtoestand  $S_0$ .

In de tweede plaats is de elektronenstructuur van deze verbindingen goed bekend en heeft de triplettoestand nagenoeg dezelfde energie en dezelfde spindichtheidsverdeling voor alle zeven molekulen uit de reeks. De vervanging van C-H door C-D of N heeft echter wel een groot effect op de snelheid van de intersystem crossing processen, die in deze serie systematisch onderzocht kunnen worden.

Het laatste en erg belangrijke argument voor onze keuze vloeit voort uit het feit dat de  $T_0 \leftrightarrow S_0$  separatie dermate klein is,  $\approx 15.000 \text{ cm}^{-1}$ , dat het verval van  $T_0$  bijna uitsluitend via stralingsloze processen verloopt. De fosforescentie emissie levert weliswaar een te verwaarlozen bijdrage aan het totale verval maar wordt toch gebruikt als "monitor" voor de bevolkingsvariaties in de triplettoestand: we kunnen nauwkeurige kwantitatieve gegevens over de stralingsloze deactivatie van  $T_0$  verkrijgen via waarneming van de uitgezonden straling.

De resultaten voor anthraceen blijken verrassend overeen te stemmen met berekeningen van Metz. Verder zijn we in staat geweest zijn argumenten te generaliseren en het effect van stikstofsubstitutie op de intersystem crossing processen voor de afzonderlijke spincomponenten uit te leggen (hoofdstuk V).

In hoofdstuk VI worden de experimenten aan de kinetiek van de fosforescerende toestand van tetramethylpyrazine (TMP) in een dureen kristal beschreven. Onze interpretatie van de resultaten ondersteunt de suggestie van de Groot, Reinders, Hesselmann en van der Waals gebaseerd op ESR experimenten, dat voor  $T_0$  van TMP in dureen de in het vlak liggende hoofdassen van de nulveldsplitsingstensor ca.  $45^\circ$  gedraaid zijn ten opzichte van de in het vlak liggende symmetrieassen van het molecuul.

In het zevende hoofdstuk geven we een overzicht van enkele methodes voor het experimentele onderzoek van spin-roosterrelaxatie in optisch aangeslagen triplettoestanden in organische molekuulkristallen bij afwezigheid van een uitwendig veld. Over dit onderwerp zijn in de afgelopen drie jaar enkele spaarzame experimentele gegevens bekend geworden. Het is, in dit geval, nog helemaal niet duidelijk hoe het fononveld van het rooster gekoppeld is aan het triplet elektronspin systeem. Het succes van de door microgolven geïnduceerde fosforescentie experimenten in het onderzoek van de dynamica van het bevolken en ontvolken van de spinniveaus van  $T_0$  bracht ons er toe om na te gaan in hoeverre deze experimenten konden worden uitgebreid en toegepast op situaties waarin de spincomponenten effectief door spin-roosterrelaxatie aan elkaar gekoppeld worden. We zijn in staat geweest om de spin-roosterrelaxatiekansen in een aantal systemen te meten alsmede hun afhankelijkheid met de temperatuur in het gebied tussen ca. 1.2 K en 15 K. Een boeiend resultaat is bijvoorbeeld dat het nu al is gebleken dat de relaxatiekansen voor de afzonderlijke spinparen van de triplettoestand aanzienlijk kan verschillen. We verwachten met dergelijk soort informatie uiteindelijk een inzicht te krijgen in de verschillende spin-roosterrelaxatiemechanismen die optreden in gelocaliseerde optisch aangeslagen triplettoestanden in organische molekuulkristallen.

## STUDIEOVERZICHT

In 1964 heb ik het H.B.S.-B diploma behaald aan het Jansenius Lyceum te Hulst. In september van dat jaar begon ik mijn studie aan de Leidse Universiteit. In oktober 1967 werd het kandidaatsexamen d', omvattende de hoofdvakken natuurkunde en wiskunde en het bijvak scheikunde, afgelegd.

Vervolgens trad ik toe tot de pas opgerichte werkgroep "Moleculen in Aangeslagen Toestand" onder leiding van prof.dr. J.H. van der Waals. Aanvankelijk heb ik meegewerkt aan ESR proeven, maar al gauw werd ik betrokken bij de nul-veld resonantie experimenten van dr. J. Schmidt. De voortzetting van dit werk heeft geleid tot de onderzoeken die aan dit proefschrift ten grondslag liggen.

Voor het bijvak theoretische organische chemie heb ik een tentamen afgelegd bij prof.dr. L.J. Oosterhoff en bij dr. R. Kaptein heb ik gedurende een half jaar NMR experimenten gedaan aan gepolariseerde protonen in de producten van fotochemische radicaal reacties.

In september 1970 legde ik het doctoraal examen experimentele natuurkunde af en in oktober begon ik met de studie waarvan de resultaten in dit proefschrift zijn beschreven.

In januari 1970 werd ik wetenschappelijk assistent in dienst van de Stichting voor Fundamenteel Onderzoek der Materie (FOM) bij de groep Vaste Stof Fysica/Leiden II en na mijn doctoraal examen wetenschappelijk medewerker.

Mijn bijdrage tot het onderwijs, gestart in 1969, heeft omvat 2 jaar assistentie bij het natuurkundig practicum voor chemici, 1 jaar assistentie op het eerste jaars practicum voor hoofdvakkers en 2 jaar assistentie bij het werkcollege dat parallel loopt aan de fysicacolleges voor chemici van dr. C.J.N. van den Meijdenberg en dr. H. van Beelen.

## NAWOORD

In alle stadia van het onderzoek hebben velen mij geholpen bij het oplossen van problemen van grote diversiteit.

Ik denk terug aan talrijke stimulerende gesprekken met mijn promotor en verscheidene andere leden van de werkgroep MAT.

Drs. B.J. Botter, drs. F.A. van der Loo, mevr. M.C. van den Berg-Vloemans, de heer E.C. Plak en drs. P.J.F. Verbeek hebben mij gedurende langere of kortere tijd geassisteerd bij de experimenten.

Zonder de technische hulp van de heren J. van den Berg en L. van As was niet één experiment ooit van de grond gekomen. De heer M. Noort heeft een aantal van de mengkristallen, waaraan de proeven zijn uitgevoerd, gemaakt. De heer J.D. Sprong heeft mij voorzien van in totaal 1500 l vloeibare helium, in kleine hoeveelheden gespreid over 176 dagen.

Dr. J. Schmidt en ir. C.A. van 't Hof hebben het volledige manuscript kritisch gelezen, terwijl drs. B.J. Botter ten nauwste betrokken was bij het ontstaan van hoofdstuk VI.

Marja Muns typte het manuscript. Haar zorg voor duidelijkheid leverde een wezenlijke bijdrage tot de leesbaarheid.

Zonder de inspirerende steun van mijn echtgenote zou mijn proefschrift met aanzienlijk minder plezier tot stand zijn gekomen.

